**US Army Corps
of Engineers**
Waterways Experiment
Station

Passaic River Tunnel Diversion Model Study

Report 5
Water Quality Modeling

by   *Carl F. Cerco, Barry Bunch*

DTIC QUALITY INSPECTED 4

Approved For Public Release; Distribution Is Unlimited

19970416 012

Prepared for   U.S. Army Engineer District, New York

Passaic River Tunnel Diversion Model Study

Report 5
Water Quality Modeling

by   Carl F. Cerco, Barry Bunch

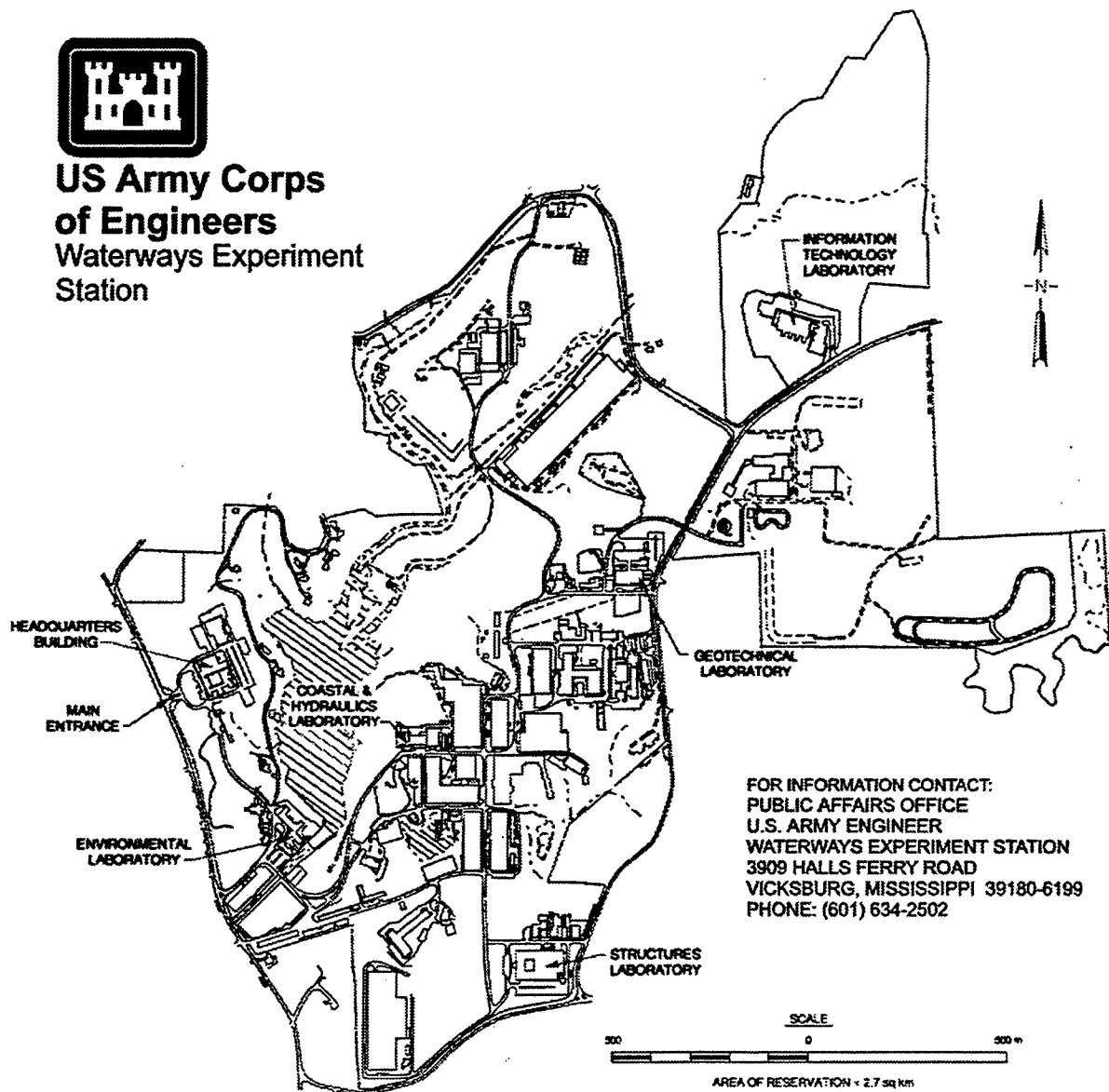U.S. Army Corps of Engineers
Waterways Experiment Station
3909 Halls Ferry Road
Vicksburg, MS   39180-6199

Report 5 of a series

US Army Corps
of Engineers
Waterways Experiment
Station

INFORMATION
TECHNOLOGY
LABORATORY

-N-

HEADQUARTERS
BUILDING

MAIN
ENTRANCE

COASTAL &
HYDRAULICS
LABORATORY

GEOTECHNICAL
LABORATORY

FOR INFORMATION CONTACT:
PUBLIC AFFAIRS OFFICE
U.S. ARMY ENGINEER
WATERWAYS EXPERIMENT STATION
3909 HALLS FERRY ROAD
VICKSBURG, MISSISSIPPI 39180-6199
PHONE: (601) 634-2502

ENVIRONMENTAL
LABORATORY

STRUCTURES
LABORATORY

SCALE
500   0   500 m

AREA OF RESERVATION = 2.7 sq km

Contents

List of Figures

List of Tables

Preface

The Passaic River Tunnel Diversion Model Study was sponsored by the U.S. Army Engineer District, New York. Project Monitors were Mr. John Bianco and Mr. Ray Schembri.

Water quality modeling activities were conducted by Drs. Carl F. Cerco and Barry Bunch, Water Quality and Contaminant Modeling Branch (WQCMB), Environmental Laboratory (EL), U.S. Army Engineer Waterways Experiment Station (WES). Direct supervision was provided by Dr. Mark Dortch, Chief, WQCMB. This report was prepared by Drs. Cerco and Bunch.

Overall supervision was provided by Dr. Richard E. Price, Chief, Environmental Processes and Effects Division, EL, and Dr. John Harrison, Director, EL.

At the time of publication of this report, WES Director was Dr. Robert W. Whalin. Commander was COL Bruce K. Howard, EN.

This report should be cited as follows:

1 Introduction

The Passaic River and Newark Bay form part of the complex New York-New Jersey harbor system (Figure 1). The major freshwater source to the system is the Hudson River, which terminates in upper New York Bay. Upper New York Bay leads to the Atlantic Ocean via two paths. The first is through the Narrows and then through lower New York Bay. The second is via the East River and then through Long Island Sound. Newark Bay is formed by the confluence of the Passaic and Hackensack rivers. At its lower end, the bay splits into the Kill van Kull and the Arthur Kill. The Kill van Kull leads to upper New York Bay. The Arthur Kill leads to Raritan Bay which joins lower New York Bay and the Atlantic Ocean. Lesser tributaries to the system include the Raritan River, the Rahway River, and the Elizabeth River.

The upper portion of the Passaic River basin is subject to destructive flooding during storm events. A diversion tunnel is proposed to alleviate the flooding. The tunnel will divert flow from the headwaters of the Passaic directly to the upper end of Newark Bay (Figure 2). The proposed tunnel is 32.3 km (20.1 miles) in length by 12.8 m (42 ft) in diameter. The profile of the tunnel is an inverted siphon that descends to a depth of 125 m (410 ft) below sea level before returning to sea level near the Newark Bay discharge. Because a portion of the tunnel is below sea level, 2.65×10^6 m^3 (700×10^6 gal) of residual floodwater may remain in the tunnel following a flood event.

The objective of the study is to provide information required to evaluate the effect of the diversion tunnel on living resources, primarily shellfish and finfish, in the vicinity of the tunnel outlet. Following consultation with the National Marine Fisheries Service (NMFS), three living-resource parameters were selected for examination: salinity, water temperature, and dissolved-oxygen concentration.
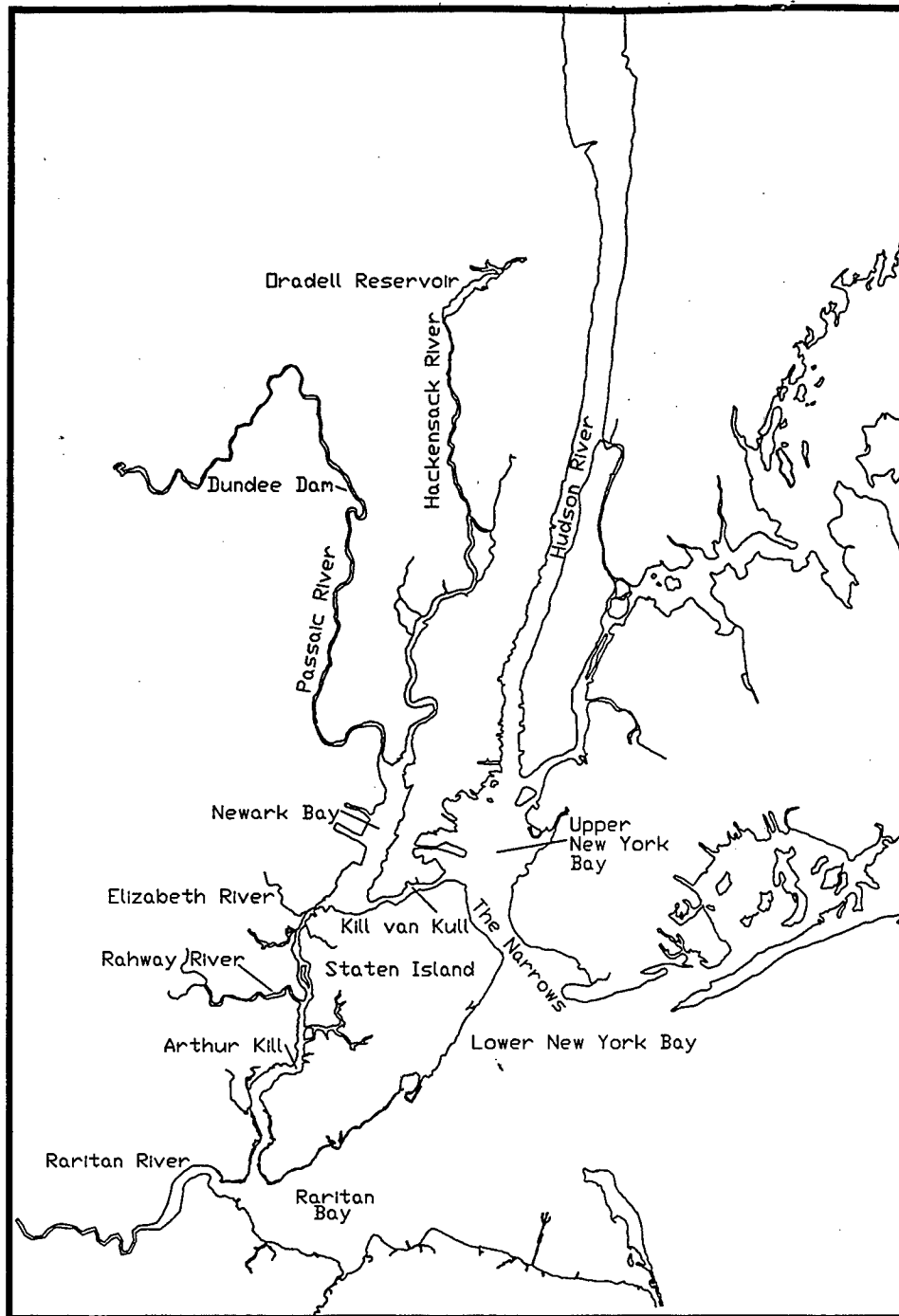
Figure 1.   New York-New Jersey harbor system
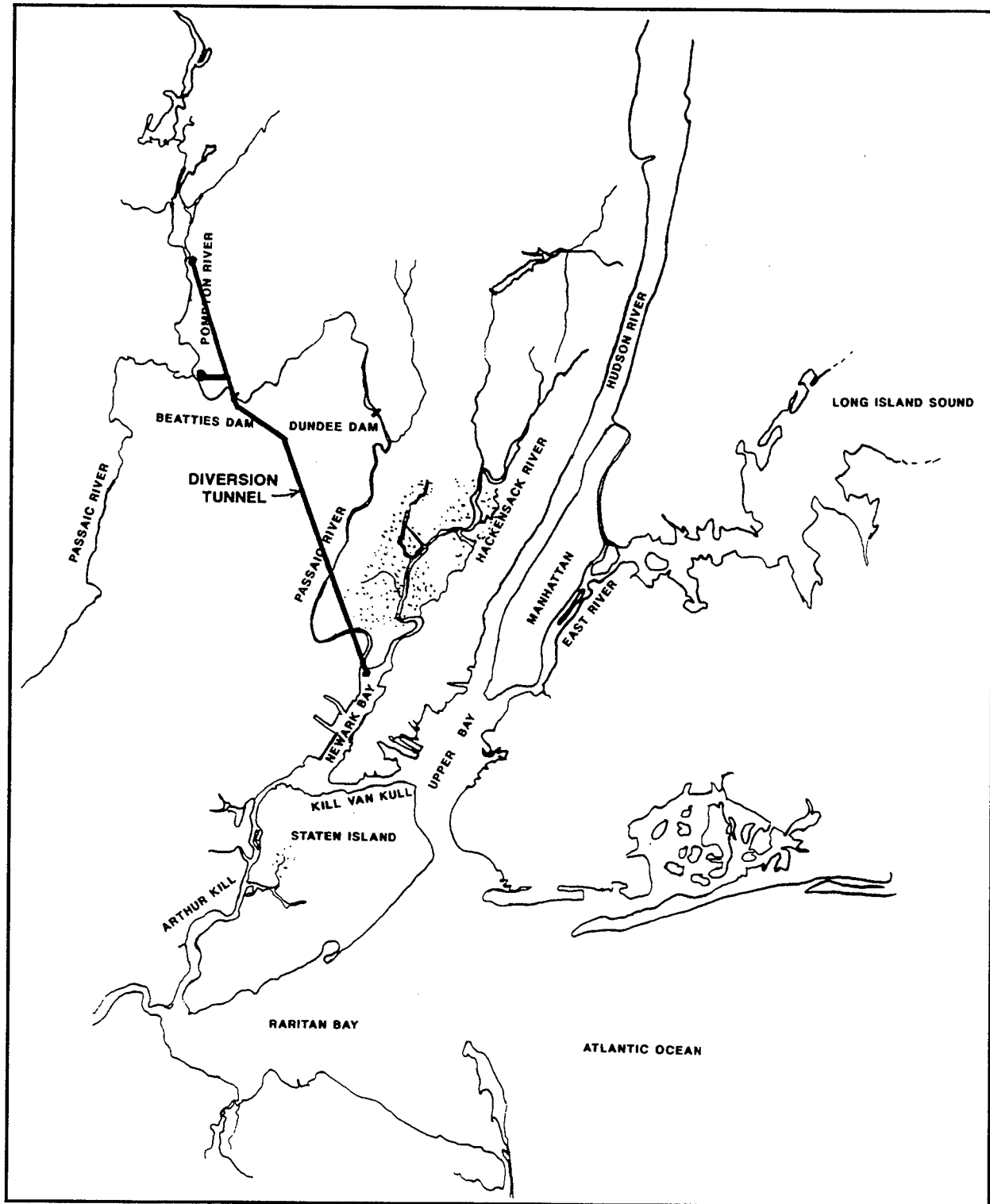
Figure 2.   Location of proposed diversion tunnel

2   Study System

The proposed tunnel discharge is at the upper end of Newark Bay. Physical features of the bay are summarized in Table 1. The bay is normally saline throughout its extent although winter and spring freshets can drive fresh water into the bay under extreme conditions (Figure 3). By Hansen and Rattray's (1966) classification scheme, the bay is a Type 2 estuary (Figure 4), which means net flow reverses at depth. Net flow is downstream at the surface and upstream near the bottom. During summer, typical salinity stratification, $\Delta S/S$, ≈ 0.1 (Figure 5). By Hansen and Rattray's (1966) classification, the bay is located near the transition from a Type 2b estuary (appreciable stratification) to a Type 2a estuary (well-mixed).

Table 1
Physical Characteristics of Newark Bay

Length	9.6 km
Volume at mean tide	$99.3 \cdot 10^6$ m³
Surface area	$14.5 \cdot 10^6$ m²
Mean depth	6.8 m
Typical cross section	8,000 m²
Mean tide range	1.6 m
Maximum tidal current	0.36 m sec⁻¹

Temperature (Figure 6) and dissolved oxygen (Figure 7) in the bay both undergo annual cycles. Maximum temperatures occur in July while annual minima, near freezing, occur in January and February. Minimum dissolved oxygen occurs in July and August, coincident with high temperatures. Maximum dissolved oxygen occurs in March, the result of cold temperature and wind-driven reaeration. Monthly minimum dissolved oxygen is ≈ 4 g m⁻³, and concentrations below 3 g m⁻³ seldom occur.
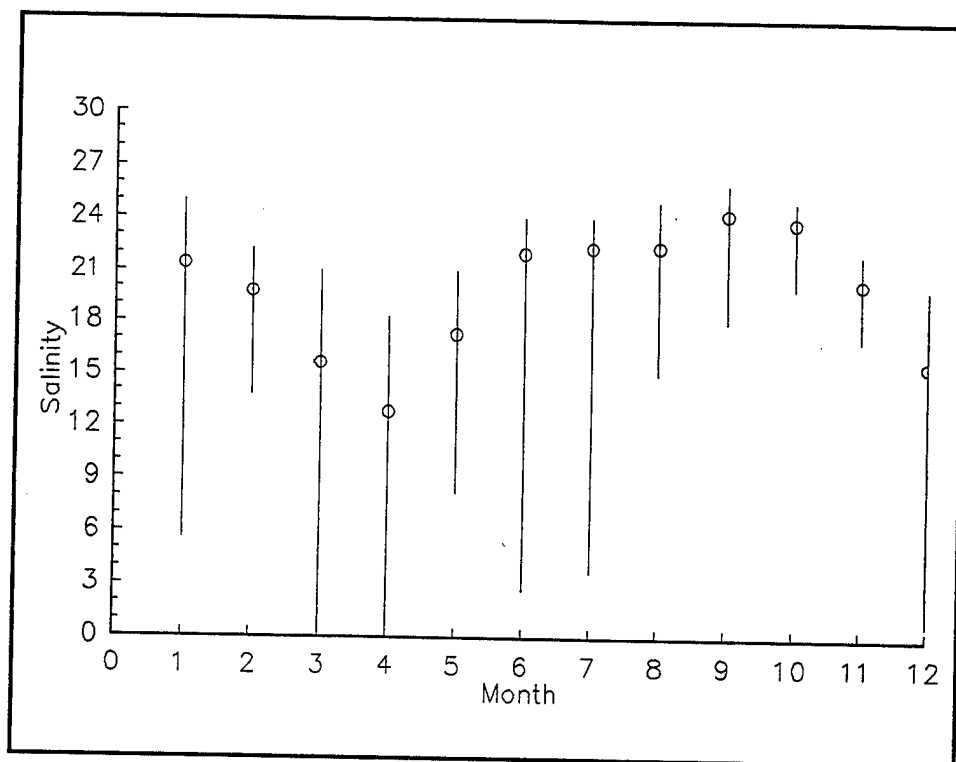
Figure 3. Salinity in Newark Bay (Monthly mean and range of data from National Marine Fisheries Service (NMFS), New York Department of the Environment (NYDEP), and Stevens Institute of Technology (SIT))
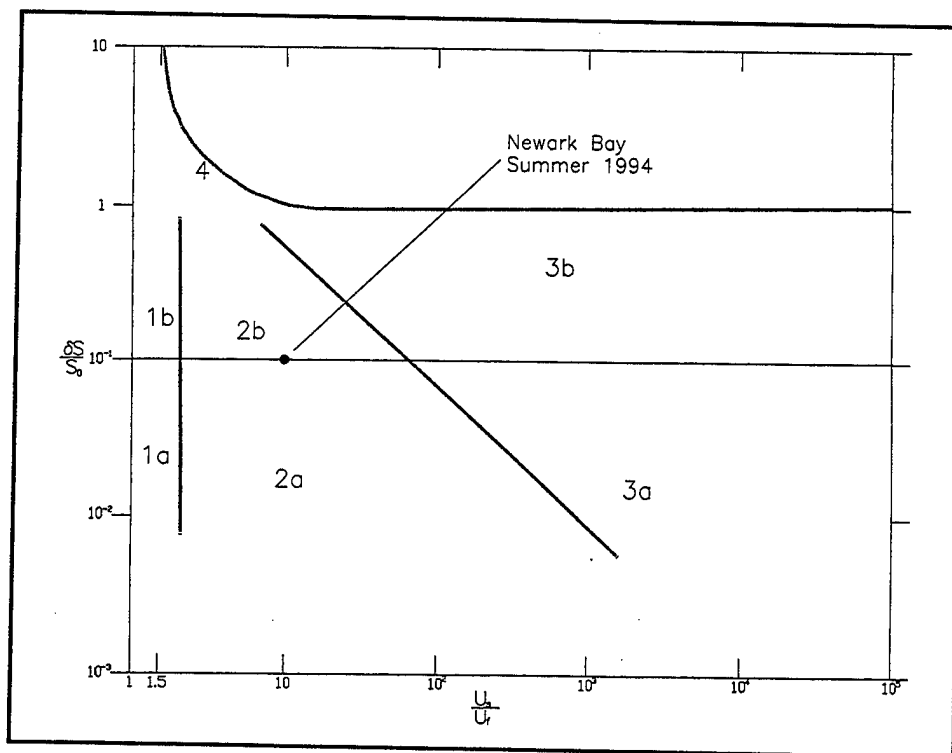
Figure 4. Classification of Newark Bay (after Hansen and Rattray 1966)

SALINITY 19 JULY 1994
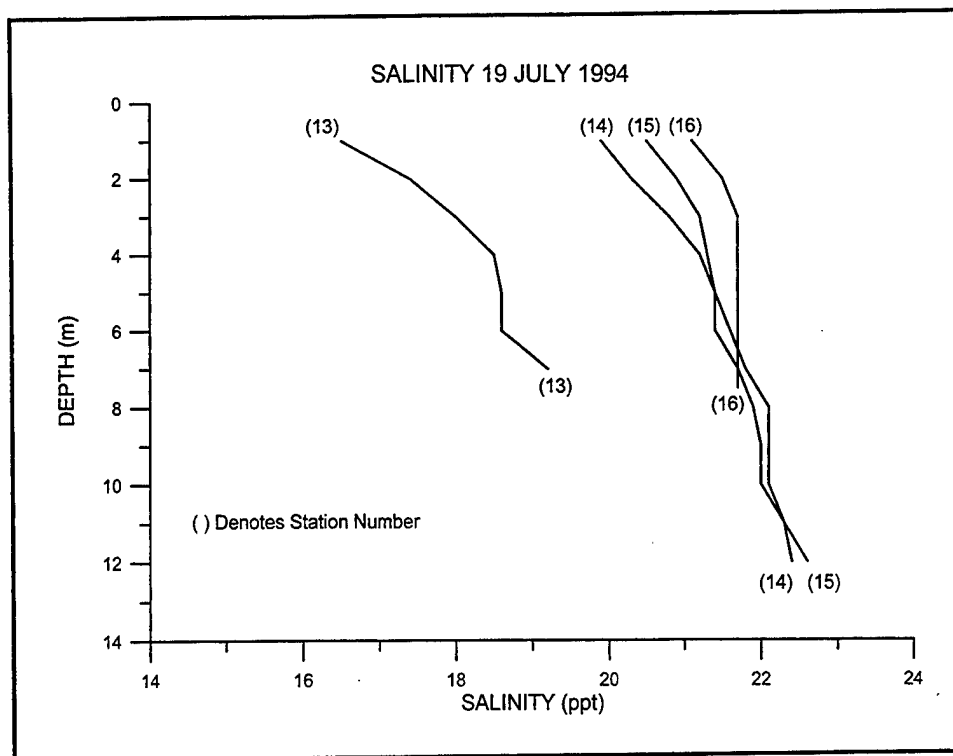
Figure 5.   Newark Bay salinity profile
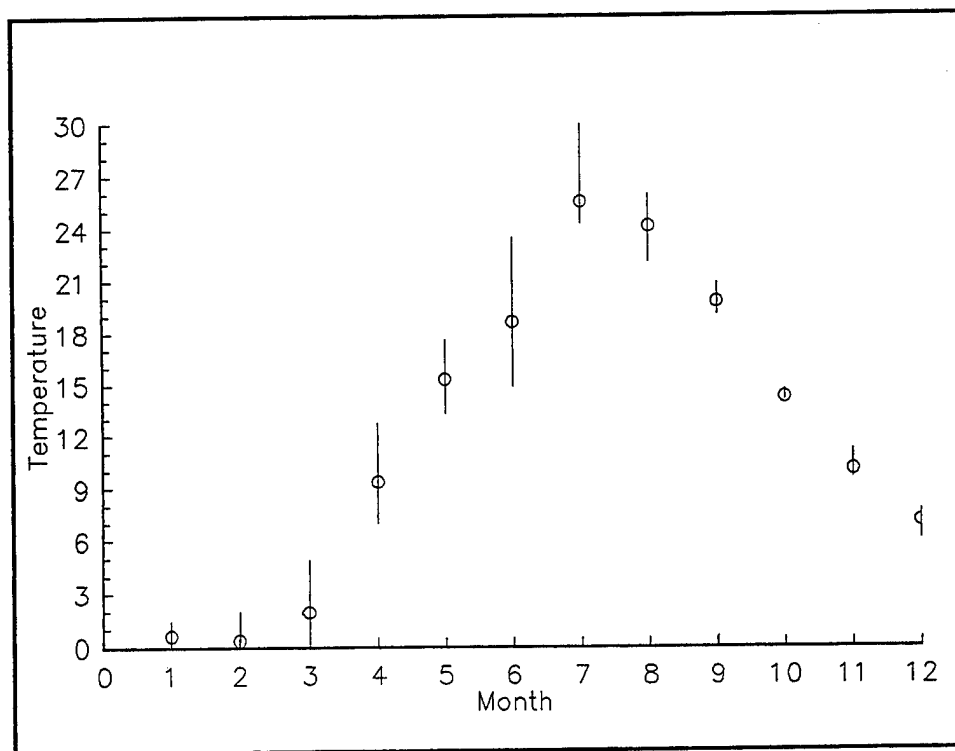
Figure 6.   Temperature in Newark Bay (Monthly mean and range of data
            from NMFS, NYDEP, and SIT)
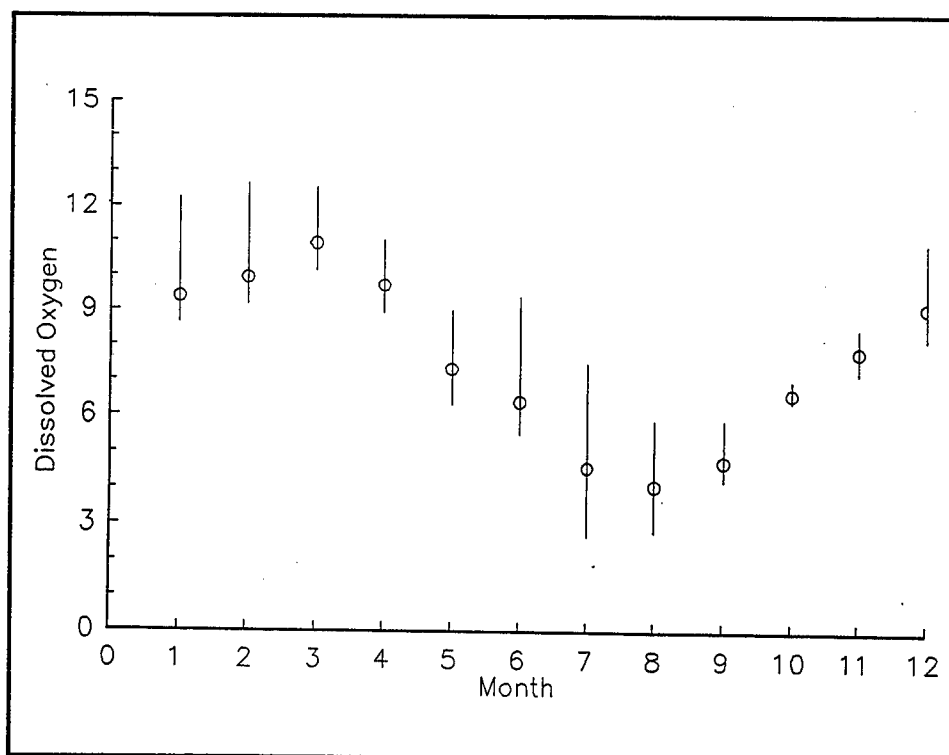
Figure 7.   Dissolved oxygen in Newark Bay (Monthly mean and range of data from NMFS, NYDEP, and SIT)

Newark Bay, its tributaries, and its distributaries form a rough "X" shape. The Passaic River comprises the upper left branch of the "X." The tidal portion of the Passaic extends from its juncture with Newark Bay at Kearny Point upstream to a dam at Dundee. Physical features of the river are summarized in Table 2. The river is saline at its junction with Newark Bay, but transitions to tidal freshwater about one-fourth the distance to the fall line.

Table 2 Physical Characteristics of Tidal Passaic River	
Length	27.2 km
Typical depth	5.8 m
Typical cross section	730 m^2
Mean flow at fall line	32.5 m^3 sec^{-1}
Drainage area above fall line	1,974 km^2
Drainage area at mouth	2,422 km^2

The Hackensack River forms the upper right branch of the "X." Physical features of the river are summarized in Table 3. The tidal portion extends from Kearny Point upstream to a dam at Oradell. Flow in the Hackensack

is regulated by discharges over the dam and by water-supply withdrawals below the dam. The river is saline at its junction with Newark Bay and transitions to tidal freshwater roughly halfway between the bay and the dam.

Table 3 Physical Characteristics of Tidal Hackensack River	
Length	34.7 km
Typical depth	5.2 m
Typical cross section	1,400 m^2
Mean flow at fall line	2.7 m^3 sec^{-1}
Drainage area above fall line	293 km^2
Drainage area at mouth	523 km^2

Temperature (Figure 8) and dissolved oxygen (Figure 9) observations within the two rivers are limited. Existing information indicates the phase of the annual temperature cycle, and the temperature extremes are comparable with Newark Bay. Minimum observed dissolved oxygen in the rivers occurs in July during which concentrations in the range 1-2 g m^{-3} occur.
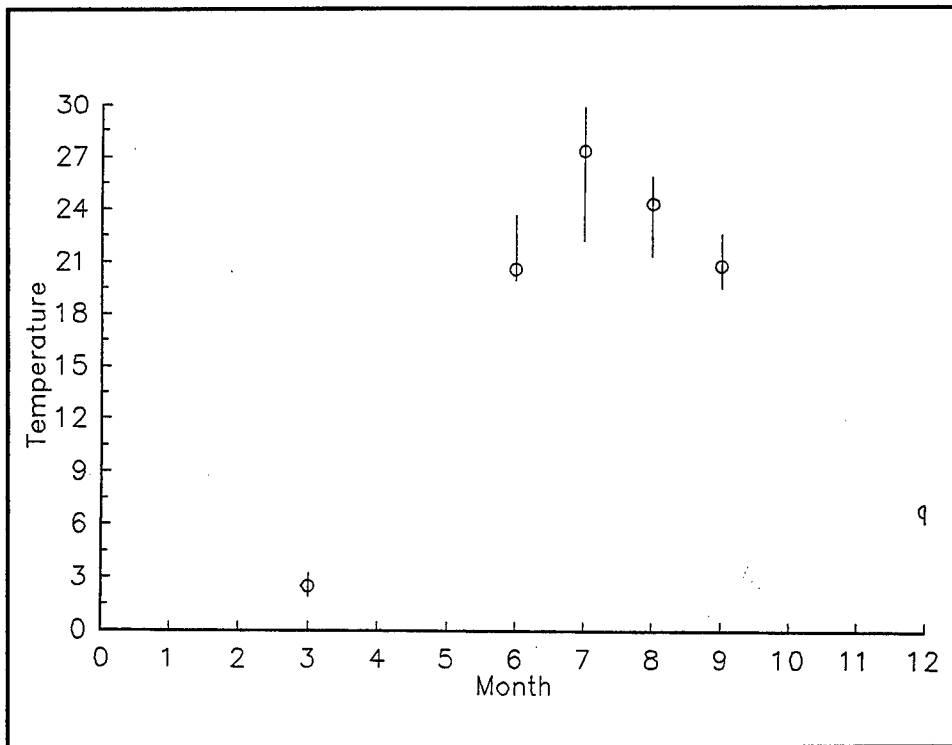
Figure 8.   Temperature in tidal Passaic and Hackensack rivers (Monthly mean and range of data from NMFS and SIT)
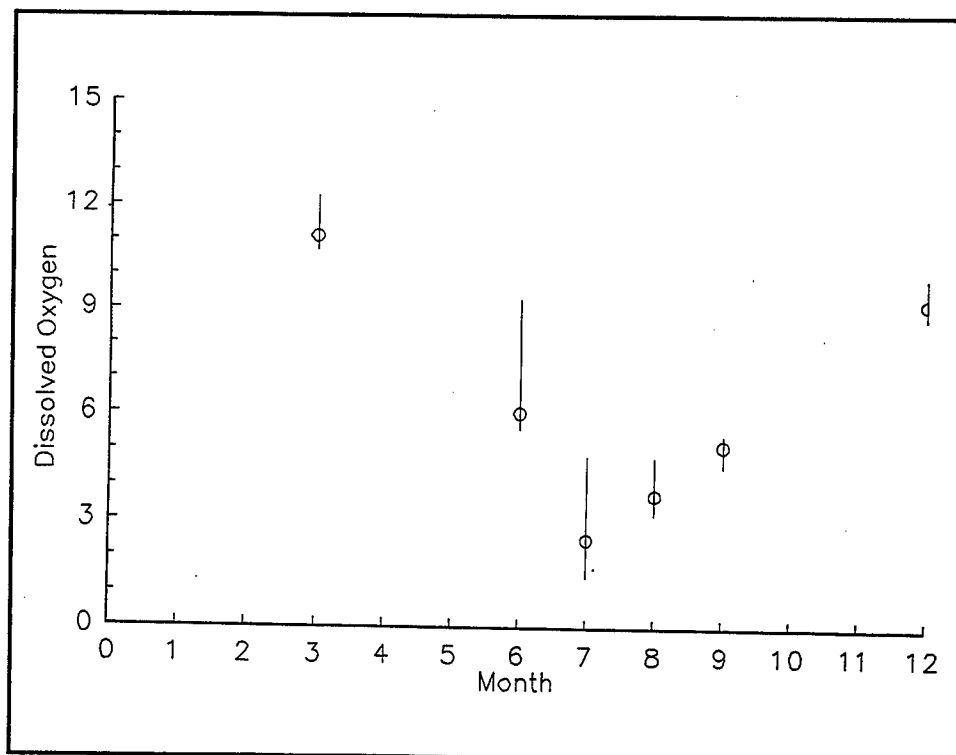
Figure 9.   Dissolved oxygen in tidal Passaic and Hackensack rivers
(Monthly mean and range of data from NMFS and SIT)

The Arthur Kill forms the lower left branch of the "X." Physical features of the Kill are summarized in Table 4. Arthur Kill joins Newark Bay with Raritan Bay and is saline throughout its extent. The Kill is subject to freshwater inflows from the Elizabeth and Rahway rivers as well as from municipal and industrial dischargers. At times, these anthropogenic flows exceed the natural flow to the system.

Table 4	
Physical Characteristics of Arthur Kill	
Length	20.2 km
Typical depth	7.7 m
Typical cross section	5,200 m^2
Mean tributary flow	2.0 m^3 sec^{-1}
Mean tide range	1.6 m
Maximum tidal current	$\approx$0.5 m sec^{-1}

The remaining branch of the "X" is formed by the Kill van Kull. Physical features of the Kill are summarized in Table 5. Kill van Kull joins Newark Bay with New York Bay and is saline throughout its extent. The only regular freshwater flow to the Kill is from a municipal waste treatment plant.

Table 5
Physical Characteristics of Kill van Kull

Length	5.0 km
Typical depth	9.2 m
Typical cross section	5,400 m^2
Mean tide range	1.4 m
Maximum tidal current	≈ 0.7 m sec^{-1}

Available observations indicate the Kills are more saline than the bay and exhibit less variation in salinity (Figure 10). At no time do runoff events push freshwater into the Kills. Minimum observed salinity is ≈ 8 ppt.

As with other portions of the system, peak temperatures in the Kills occur in July and August (Figure 11). Lowest observed temperatures occur in March rather than January or February although this finding may be skewed by lack of data. Minimum dissolved oxygen occurs in July and August (Figure 12) when concentrations as low as 2 g m^{-3} occur.
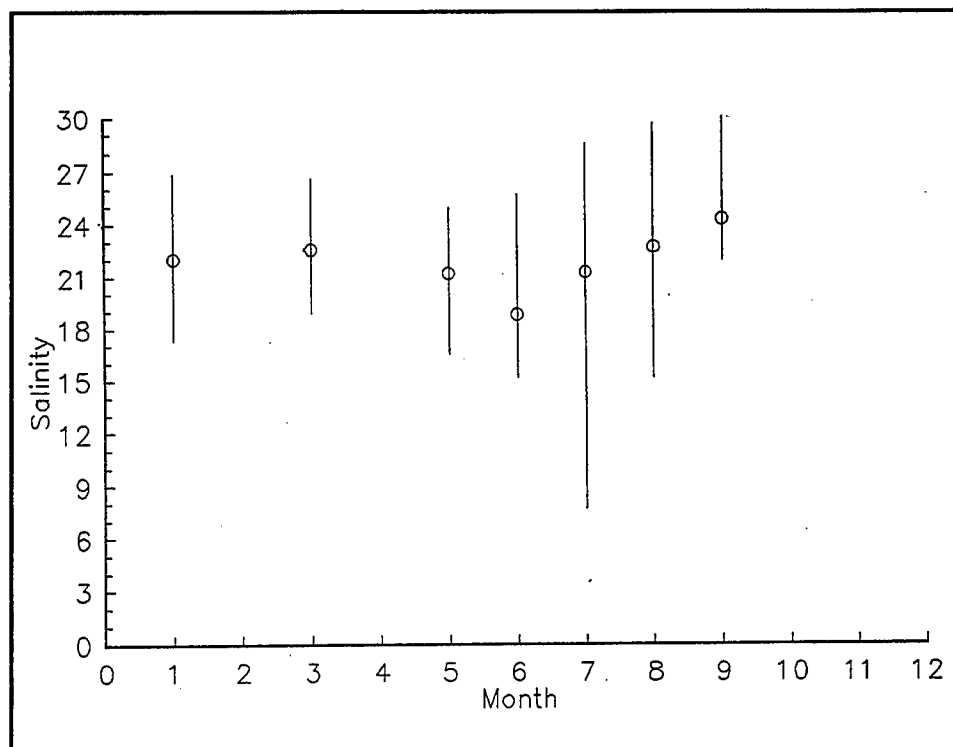
Figure 10. Salinity in Arthur Kill and Kill van Kull (Monthly mean and range of data from NYDEP and SIT)
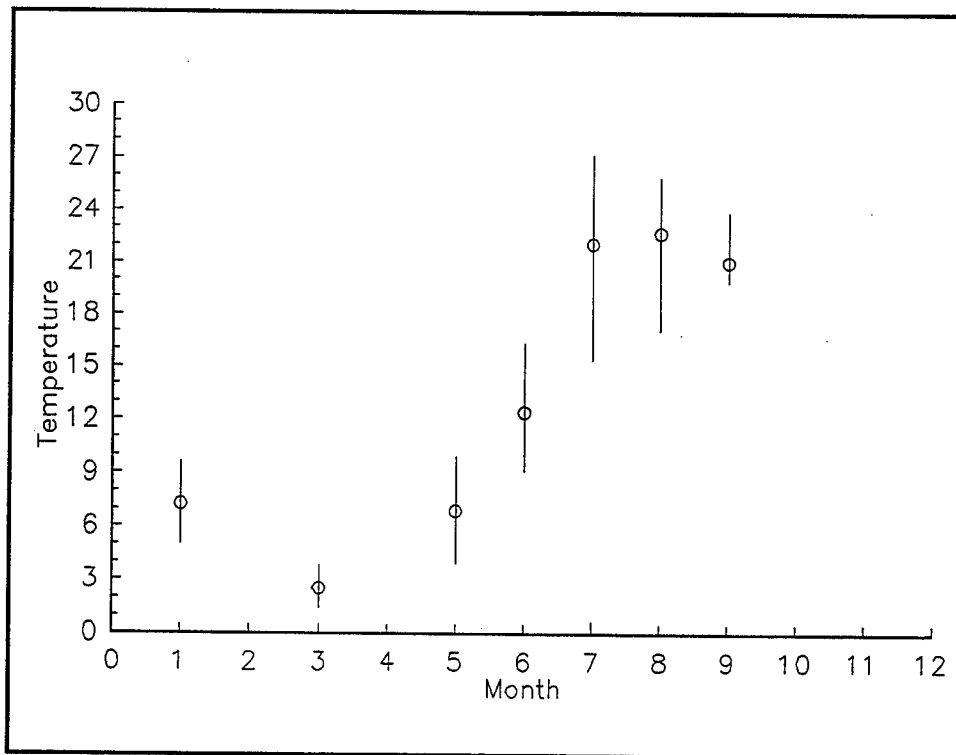
Figure 11.   Temperature in Arthur Kill and Kill van Kull (Monthly mean and range of data from NYDEP and SIT)
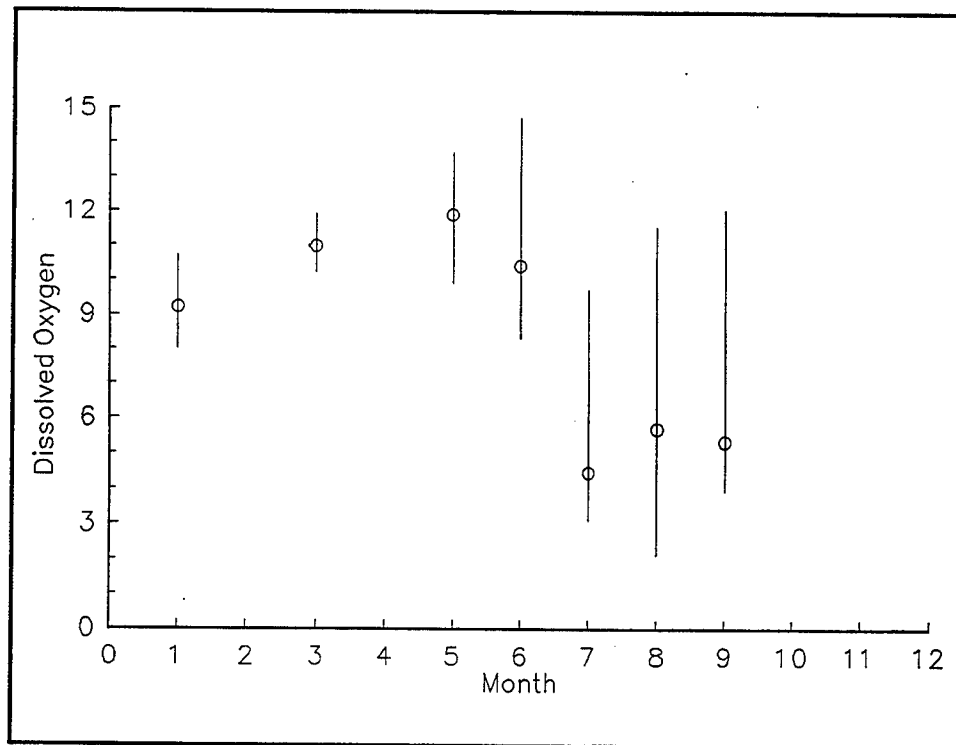
Figure 12.   Dissolved oxygen in Arthur Kill and Kill van Kull (Monthly mean and range of data from NYDEP and SIT)

3 Hydrodynamic Model and Computational Grid

Introduction

Modeling impact of the proposed tunnel required two models. Transport processes were modeled by a three-dimensional hydrodynamic model that operated independently of the water quality model. Transport information from the hydrodynamic model was processed and stored on magnetic media for subsequent use by the water quality model.

CH3D-WES

The CH3D-WES (Computational Hydrodynamics in Three Dimensions - Waterways Experiment Station) hydrodynamic model is a substantially revised version of the CH3D model originally developed by Sheng (1986). Model formulation is based on principles expressed by the equations of motion, conservation of volume, and conservation of mass. Quantities computed by the model include three-dimensional velocities, surface elevation, vertical viscosity and diffusivity, temperature, salinity, and density. Details of the model formulation and application are found in a companion report to this volume (Letter et al., in preparation).

Computational Grid

The basic equations of CH3D-WES were solved via the finite-difference method. The finite-difference solution algorithm replaced continuous derivatives in the governing differential equations with ratios of discrete quantities. Solutions to the hydrodynamics were obtained using 1-min intervals for the discrete time steps. The spatial continuum of the New York-New Jersey harbor system was divided into a grid of discrete cells. Temperature, salinity, and density were computed at the center of each cell. To achieve close conformance of the grid to the complex geometry of the prototype, cells were represented in curvilinear planar coordinates rather than rectangular coordinates. Sigma coordinates were used along

the vertical axis. Velocities were computed on the boundaries between cells.

The hydrodynamic grid (Figure 13) extended from the Hudson River fall line, near Troy, NY, through the harbor system and out onto the continental shelf. At its western extreme, the grid was bounded by the fall lines of the Passaic River, the Hackensack River, and the Raritan River. The eastern extreme of the grid encompassed half of Long Island Sound. The enormous extent of the grid was created to facilitate specification of tidal and salinity boundary conditions. The grid contained 3,006 cells in the surface plane and 5 cells in the vertical for a total of 15,030.

50 MILES
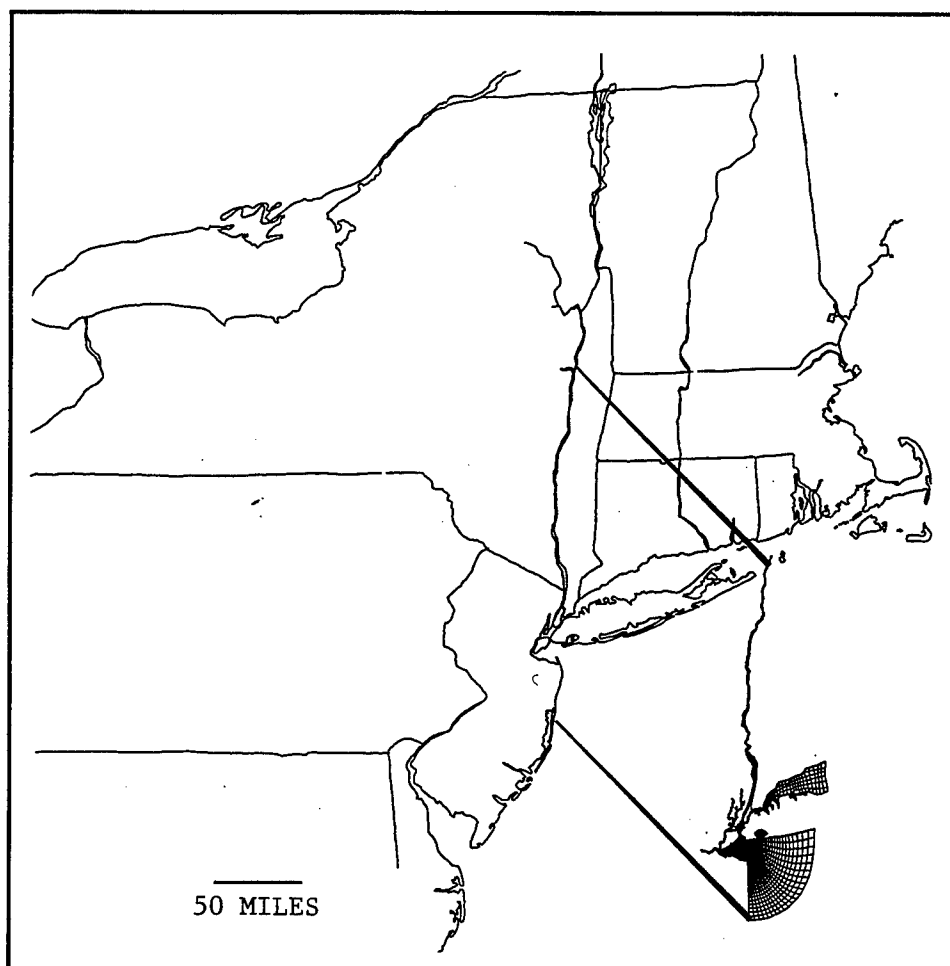
Figure 13. Plan view of hydrodynamic computational grid

Linkage to Water Quality Model

Hydrodynamics for employment in the water quality model were produced in three production runs of approximately 30 days duration: July 1-August 2; August 3-August 31; September 1-September 30. A processor imbedded in the CH3D-WES code transformed velocities, surface elevations,

and vertical diffusivities computed on a 1-min basis into values output every 30 min. Hydrodynamics from the three production runs were concatenated to produce a single continuous intratidal hydrodynamics set for use in the water quality model.

4 Water Quality Model

Model Formulation

The CE-QUAL-ICM model applied in the Passaic River study is a modified version of a model developed for Chesapeake Bay (Cerco and Cole 1994). Modifications consisted of reducing the number of state variables to a suite appropriate for the problem of interest. The suite consisted of five state variables: salinity, temperature, dissolved oxygen (DO), ultimate biochemical oxygen demand (BODu), and chemical oxygen demand (COD).

Salinity

Salinity was included largely because ambient salinity and short-term deviations from the ambient conditions are important to the viability of living resources. For impact on living resources alone, salinity as computed in the hydrodynamic model is sufficient. Salinity is independently computed in the water quality model to verify that transport is correctly routed from the hydrodynamic model. When the two models are correctly linked, computed salinity is identical in both of them. Salinity is also computed since it influences the dissolved-oxygen saturation concentration.

Temperature

Temperature was included largely because ambient temperature and short-term deviations from ambient conditions are important to the viability of living resources. For impact on living resources alone, temperature as computed in the hydrodynamic model is sufficient. Temperature is independently computed in the water quality model since it is a primary determinant of the rate of biochemical reactions. Temperature also influences the dissolved-oxygen saturation concentration.

Dissolved oxygen

DO is required for the existence of higher life forms. Oxygen availability determines the distribution of organisms and the flows of energy and

nutrients in an ecosystem. DO is a central component of the water quality model.

Ultimate biochemical oxygen demand

BODu is a quantity that indicates the amount of oxygen required to completely decay, by biological processes, the organic matter contained in a water sample. BODu, in itself, has no impact on living resources. Computation of the BODu concentration and rate of exertion are required for the subsequent computation of dissolved oxygen.

Chemical oxygen demand

In the context of this study, COD is the concentration of reduced substances that are oxidizable by inorganic means. The concentration is specified in oxygen-equivalent units (that is, the amount of oxygen required to satisfy the chemical demand). COD was included largely to allow for potential discharge of reduced substances such as iron, sulfide, and methane from the flood diversion tunnel. A second potential source of COD is sulfide released from benthic sediments when dissolved oxygen in the water column is insufficient to satisfy sediment oxygen demand.

Conservation of Mass Equation

The foundation of CE-QUAL-ICM is the solution to the three-dimensional mass-conservation equation for a control volume. Control volumes in CE-QUAL-ICM correspond to cells in x-y-z space on the CH3D grid. CE-QUAL-ICM solves, for each volume and for each state variable, the conservation of mass equation:

$$\frac{\delta V_i C_i}{\delta t} = \sum_{j=1}^{n} Q_j C_j^* + \sum_{j=1}^{n} A_j D_j \frac{\delta C}{\delta x_j} + \sum S_i \qquad (1)$$

where

V_i = volume of ith control volume, m^3

C_i = concentration in i^{th} control volume, $g\ m^{-3}$

t, x = temporal and spatial coordinates

n = number of flow faces attached to i^{th} control volume

Q_j = volumetric flow across flow face j of ith control volume, $m^3\ sec^{-1}$

C_j^* = concentration in flow across flow face j, $g\ m^{-3}$

A_j = area of flow face j, m^2

16

D_j = diffusion coefficient at flow face j, $m^2 sec^{-1}$

S_i = external loads and kinetic sources and sinks in i^{th} control volume, $g sec^{-1}$

Solution to the mass-conservation equation is via the finite-difference method using the QUICKEST algorithm in the horizontal directions and a Crank-Nicolson scheme in the vertical direction. The kinetics portion of the conservation of mass equation for four state variables is described below. Salinity is omitted since no internal sources or sinks of salinity exist.

Temperature

Formal computation of temperature requires formulation of a conservation of internal energy equation analogous to the conservation of mass equation. For practical purposes, the internal-energy equation can be written as a conservation of temperature equation. The only source or sink of internal energy considered is exchange between the atmosphere and the surface model layer.

Change of temperature due to atmospheric exchange is considered proportional to the temperature difference between the water surface and a theoretical equilibrium temperature (Edinger, Brady, and Geyer 1974):

$$\frac{\delta}{\delta t} T = \frac{KT}{\rho \, Cp \, \Delta z} (Te - T) \qquad (2)$$

where

T = temperature, $^{\circ}C$

KT = heat exchange coefficient, watt $m^{-2} \, ^{\circ}C^{-1}$

ρ = density of water, $1,000 \, kg \, m^{-3}$

Cp = specific heat of water, $4,200 \, watt \, sec \, kg^{-1} \, ^{\circ}C^{-1}$

Δz = thickness of surface layer, m

Te = equilibrium temperature, $^{\circ}C$

Ultimate biochemical oxygen demand

In the modeled system, BODu originates in external loads including industrial and municipal discharges, combined-sewer overflows, and tributary inflows. Sinks of BODu are limited to oxidation in the water column and settling into bottom sediments. Oxidation occurs as a first-order decay process. The decay rate is a function of ambient temperature and dissolved oxygen concentration. As temperature increases, decay rate increases. Decay rate is diminished as oxygen availability becomes limited in the water column. The complete representation of all modeled sources and sinks in the water column is:

$$\frac{\delta}{\delta t} BODu = -KBOD \, f(T) \, \frac{DO}{KHDOB + DO} \, BODu - WBOD \, \frac{\delta}{\delta z} BODu \qquad (3)$$

where

$$BODu = \text{ultimate biochemical oxygen demand, g m}^{-3}$$

$$KBOD = \text{BOD decay rate at specified reference temperature, day}^{-1}$$

$$f(T) = \text{function that describes effect of temperature on BOD decay rate}$$

$$DO = \text{dissolved oxygen concentration, g m}^{-3}$$

$$KHDOB = \text{dissolved oxygen concentration at which BOD decay rate is halved, g m}^{-3}$$

$$WBOD = \text{settling velocity of BODu, m day}^{-1}$$

$$z = \text{vertical coordinate, m}$$

The effect of temperature on BOD decay is described by an exponential function:

$$f(T) = e^{KTBOD\ (T-TRBOD)} \tag{4}$$

where

$$KTBOD = \text{constant that expresses effect of temperature on BOD decay rate, } {}^{\circ}C^{-1}$$

$$TRBOD = \text{reference temperature for specification of BOD decay rate, } {}^{\circ}C$$

Chemical oxygen demand

In this study, chemical oxygen demand is the concentration of reduced substances that are oxidizable through inorganic means. Potential sources of COD include discharge from the diversion tunnel and release from benthic sediments. COD may exist as reduced iron and manganese, as sulfide, or as methane. For model purposes, these are represented as a single state variable quantified in units of oxygen demand. Kinetics in the water column are represented:

$$\frac{\delta}{\delta t}COD = -KCOD\,f(T)\,\frac{DO}{KHDOC+DO}\,COD \tag{5}$$

where

$$COD = \text{chemical oxygen demand concentration, g } O_2\text{-equivalents m}^{-3}$$

$$KCOD = \text{oxidation rate of chemical oxygen demand, day}^{-1}$$

$$KHDOC = \text{half-saturation concentration of dissolved oxygen required for exertion of chemical oxygen demand, g } O_2 \text{ m}^{-3}$$

18

An exponential function (Equation 4) describes the effect of temperature, $f(T)$, on exertion of chemical oxygen demand.

Dissolved oxygen

The sole source of dissolved oxygen to the water column is atmospheric reaeration. Sinks include exertion of BOD within the water column and oxygen demand exerted by benthic sediments.

Reaeration

The rate of reaeration is proportional to the dissolved oxygen deficit in model segments that form the air-water interface:

$$\frac{\delta}{\delta t} DO = \frac{KR}{\Delta z} (DOs - DO) \tag{6}$$

where

KR = reaeration coefficient, m day^{-1}

DOs = dissolved oxygen saturation concentration, g O_2 m^{-3}

Reaeration is influenced by a host of factors including temperature (ASCE 1961), wind (O'Connor 1983), and salinity (Wen et al. 1984). No single theory that unites all these factors into a formulation of reaeration in an estuary is available. In the model, reaeration is treated as a constant that may vary spatially within the system.

Saturation dissolved oxygen concentration diminishes as temperature and salinity increase. An empirical formula that describes these effects (Genet, Smith, and Sonnen 1974) is:

$$DOs = 14.5532 - 0.38217\ T + 0.0054258\ T^2$$
$$-CL\ (1.665 \times 10^{-4} - 5.866 \times 10^{-6}\ T + 9.796 \times 10^{-8}\ T^2) \tag{7}$$

where CL is the chloride concentration (= salinity/1.80655).

The complete kinetics for dissolved oxygen in the water column are:

$$\frac{\delta}{\delta t} DO =$$
$$- KBOD\ f(T)\ \frac{DO}{KHDOB + DO}\ BODu - KCOD\ f(T)\ \frac{DO}{KHDOC + DO}\ COD \tag{8}$$
$$+ \frac{KR}{\Delta z}\ (DOs + DO)$$

Sediment-water interactions

Conditions in the water column are influenced, in part, by materials exchanges with the benthic sediments. Sediment-water interactions occur only in the bottom layer of cells on the three-dimensional grid. For these cells, the mass-conservation equation is modified:

$$\frac{\delta C}{\delta t} = [\text{transport}] + [\text{kinetics}] \pm \frac{BEN}{\Delta z} \qquad (9)$$

where

$\qquad$ BEN $\quad = \quad$ sediment-water material flux, $g\ m^{-2}\ day^{-1}$

$\qquad \Delta z \quad = \quad$ thickness of bottom layer, m

By convention BEN is positive when flux is from sediment to water.

The primary exchange in the model is forced by sediment oxygen demand (SOD). In the event dissolved oxygen in the water column is insufficient to satisfy the demand, reduced substances are released to the water column as chemical oxygen demand.

Sediment oxygen consumption

Oxygen consumption in the sediments depends upon water column temperature and oxygen availability. As temperature increases, respiration in the sediment increases. Sediment oxygen consumption is reduced as oxygen concentration in the overlying water decreases. The model accounts for these influences through the relationship:

$$BENDO = \frac{DO}{KHSO + DO}\ BENDOb\ e^{KSO\ (T-TRSO)} \qquad (10)$$

where

$\qquad$ BENDO $\quad = \quad$ sediment oxygen consumption, $g\ m^{-2}\ day^{-1}$

$\qquad$ KHSO $\quad = \quad$ dissolved oxygen concentration at which sediment oxygen consumption is halved, $g\ m^{-3}$

$\qquad$ BENDOb $\quad = \quad$ sediment oxygen consumption under conditions of unlimited oxygen availability, specified at temperature TRSO, $g\ m^{-2}\ day^{-1}$

$\qquad$ KSO $\quad = \quad$ effect of temperature on sediment oxygen consumption, $^{o}C^{-1}$

$\qquad$ TRSO $\quad = \quad$ reference temperature for specification of sediment oxygen consumption, ^{o}C

Chemical oxygen demand

The processes that create sediment oxygen demand are little affected by the concentration of oxygen in the overlying water. When oxygen is unavailable to fulfill sediment oxygen demand, the demand is exported to the water column. The exported demand may be in the form of reduced

20

iron, manganese, or sulfide, which are represented in the model as chemical oxygen demand. COD release is computed:

$$BENCOD = \frac{KHSO}{KHSO + DO} \; BENDOb \; e^{KSO\,(T-TRSO)} \tag{11}$$

where BENCOD is the sediment flux of chemical oxygen demand, g m^{-2} day^{-1}.

The computed flux is negligible when DO >> KHSO. When dissolved oxygen is absent from the water column, oxygen demand equivalent to maximum specified sediment consumption is released to the water as chemical oxygen demand.

Water Quality Model Grid

The complete hydrodynamic grid extended from the fall line of the Hudson River to the junction of lower New York Bay with the Atlantic Ocean (Figure 13). The extent of the grid was determined by the need to specify tidal boundary conditions. The entire extent of the grid was not required to compute the impact of the tunnel discharge on the quality of receiving waters. For water quality impacts, a smaller, more computationally efficient grid was feasible. As with the hydrodynamic model, the extent of the water quality model grid was determined by boundary condition requirements. The boundaries were located at a distance such that the boundary conditions did not influence predictions in the vicinity of the tunnel discharge.

Tracer Studies

The need to model water quality in the Passaic River, the Hackensack River, and Newark Bay was obvious. Lack of impact of the tunnel on the extremes of the hydrodynamic grid (Hudson River fall line, Long Island Sound, Atlantic Ocean) was also obvious. The extent to which the hydrodynamic grid could be reduced was determined by a set of tracer studies employing the two models. For these tests, a special set of hydrodynamics were created. The hydrodynamic model was run for one tidal cycle using average tidal amplitude at open boundaries. River flows were specified at 100-year flood values. The hydrodynamics were "looped" to create a 30-day set of continuous hydrodynamics representing conditions in the system with flows sufficient to generate tunnel operation.

The water quality model was run on the complete hydrodynamic grid. Conservative tracer was input continuously at the tunnel discharge. Concentrations were examined at a number of potential boundaries in the Kills, the Hudson, and New York Bay (Figure 14). The extent of the reduced water quality grid was determined as the locations at which tracer concentration (Figure 15) was diluted to insignificant concentrations (less

than five percent of initial concentration). Boundaries were set in the Hudson River at Manhattan, at the entrance to the East River, at the lower end of Arthur Kill, and just outside the Narrows. The water quality model grid (Figure 16) contained 1,363 cells in each of five layers for a total of 6,815 cells.
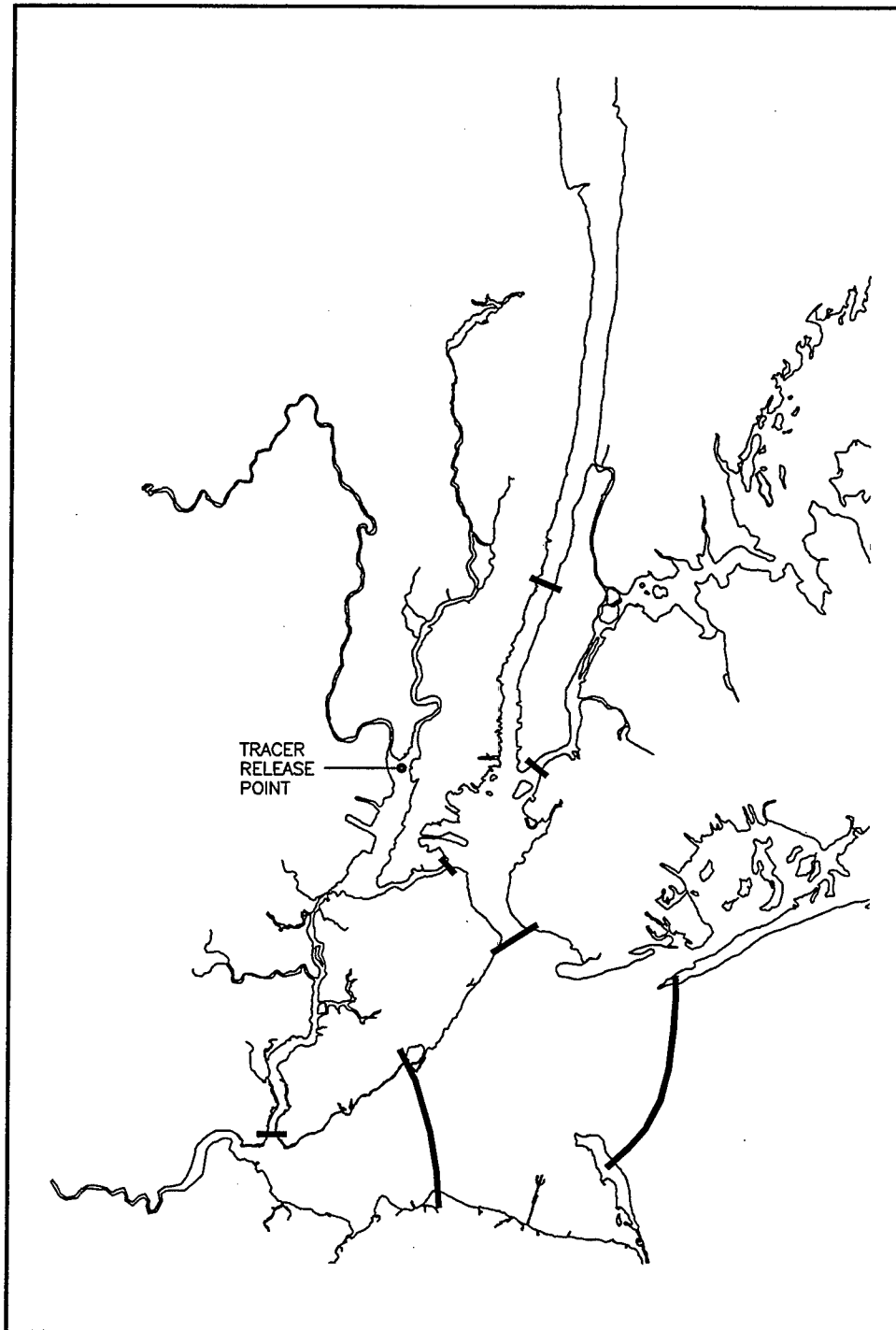
Figure 14. Location of tracer release and sites at which release was examined
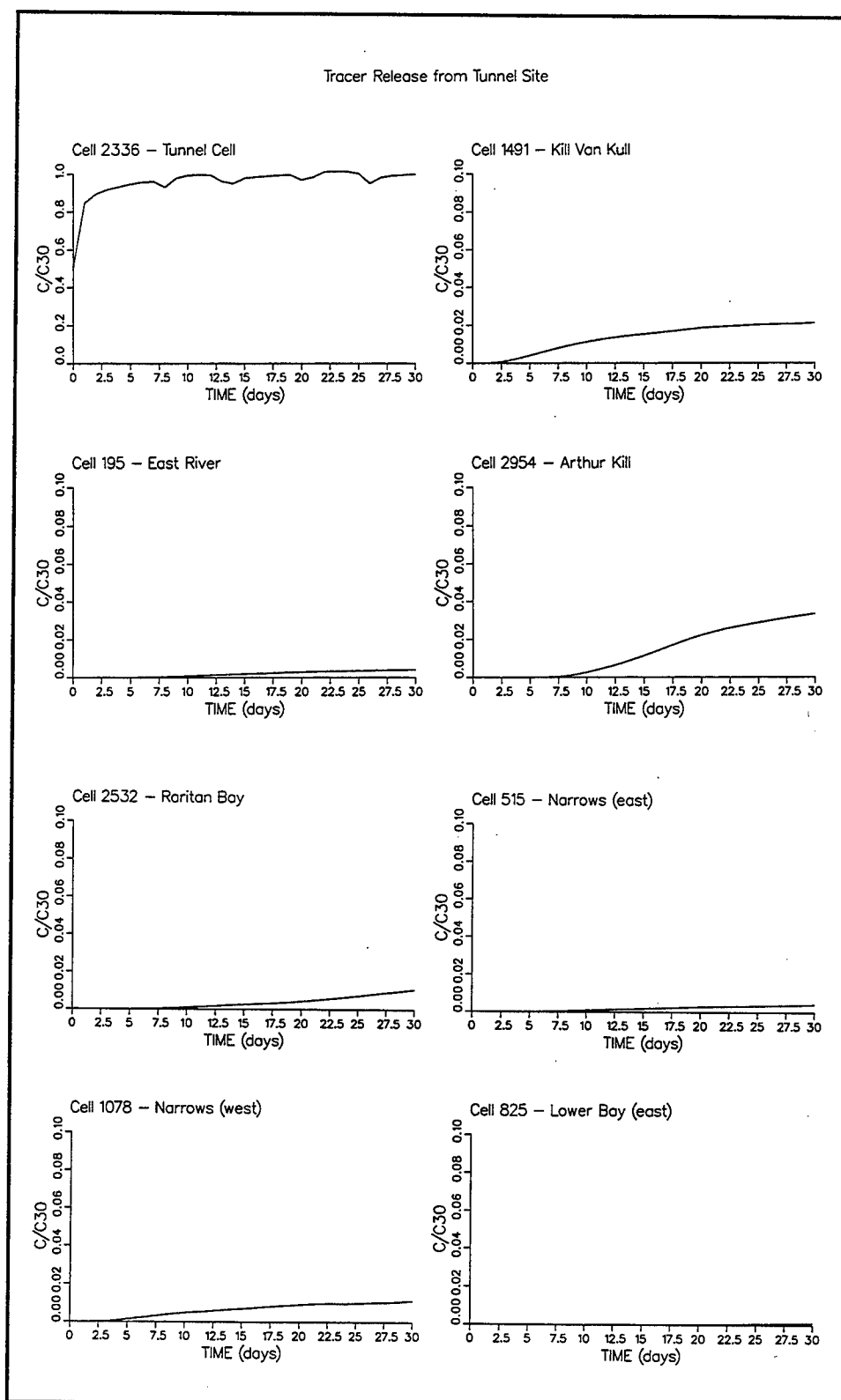
Figure 15. Time series of tracer concentration at multiple sites (Concentrations normalized by final concentration at release site: C30) (Continued)
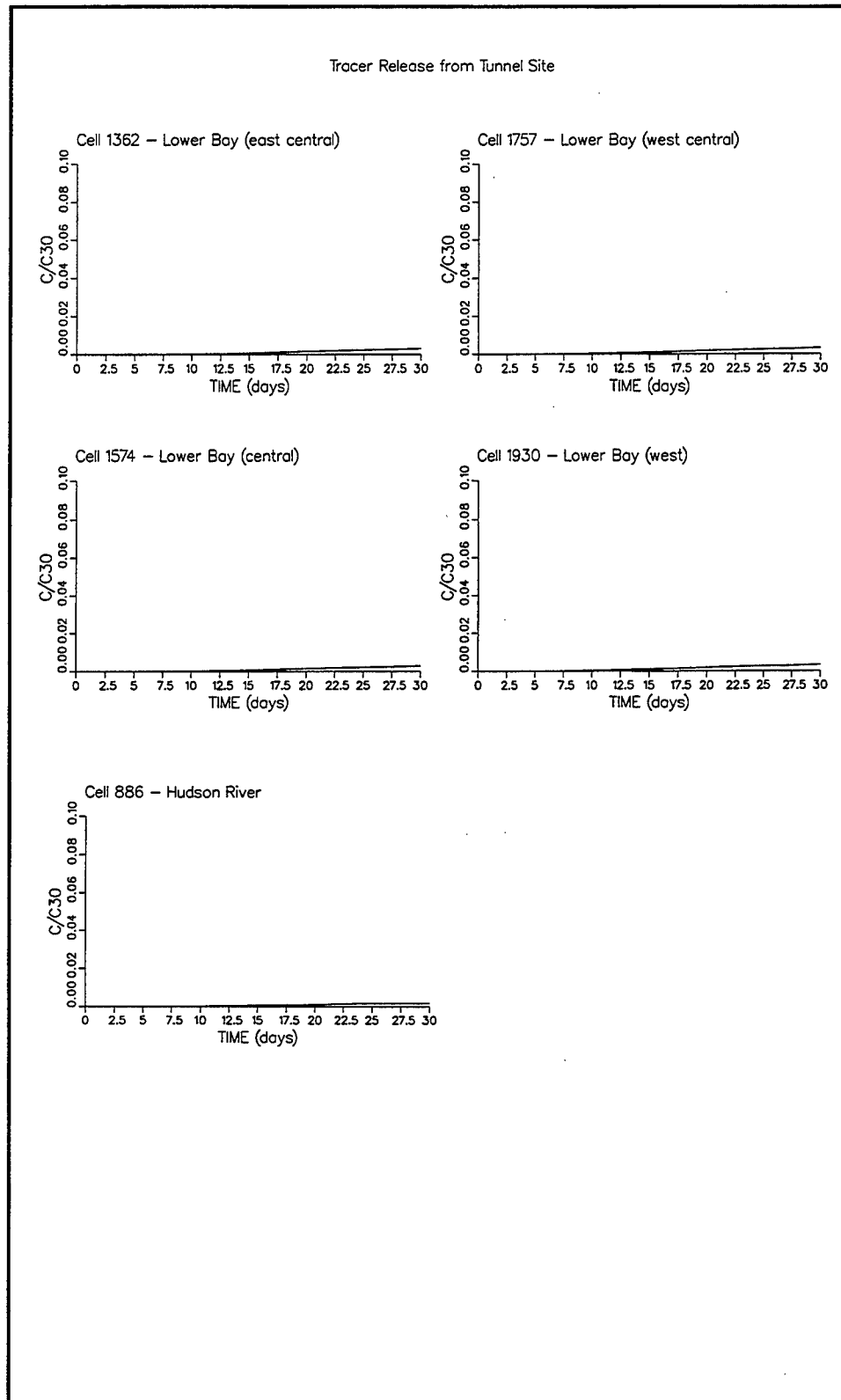
Figure 15. (Concluded)

Figure 16. Water quality model grid

5 Application of Water Quality Model

Calibration Data

Before a model can be applied in a predictive fashion, the applicability of the model must be evaluated. Evaluation usually consists of comparison of model computations with one or more sets of observations. For the Passaic River study, an observational data set including salinity, water temperature, dissolved oxygen, and BOD was required. Spatial extent of the observations had to include the entire water quality model grid. A contemporary data set was preferred. No data set was located that met the requirements. Consequently, a sample program was completed as part of the model study. Field surveys and sample analyses were conducted by the Stevens Institute of Technology, Hoboken, NJ.

Three surveys were conducted, at roughly 1-month intervals, from July 1994 to September 1994. Thirty stations were sampled (Figure 17). Complete coverage of the system required sampling over a 2-day period. Surveys were conducted during daylight close to the period of slack-before-ebb tidal current.

Water quality sampling included the following:

a. Salinity.

b. Temperature.

c. Dissolved oxygen.

d. BOD5.

e. BODu (60-day).

Salinity, temperature, and dissolved oxygen were measured in situ using a Hydrolab meter. In situ measures were collected at mid-depth for stations having a total depth less than 2 m and at 1-m intervals for deeper stations.

Water samples were collected and returned to the laboratory for BOD analyses as per Standard Methods (American Public Health Association
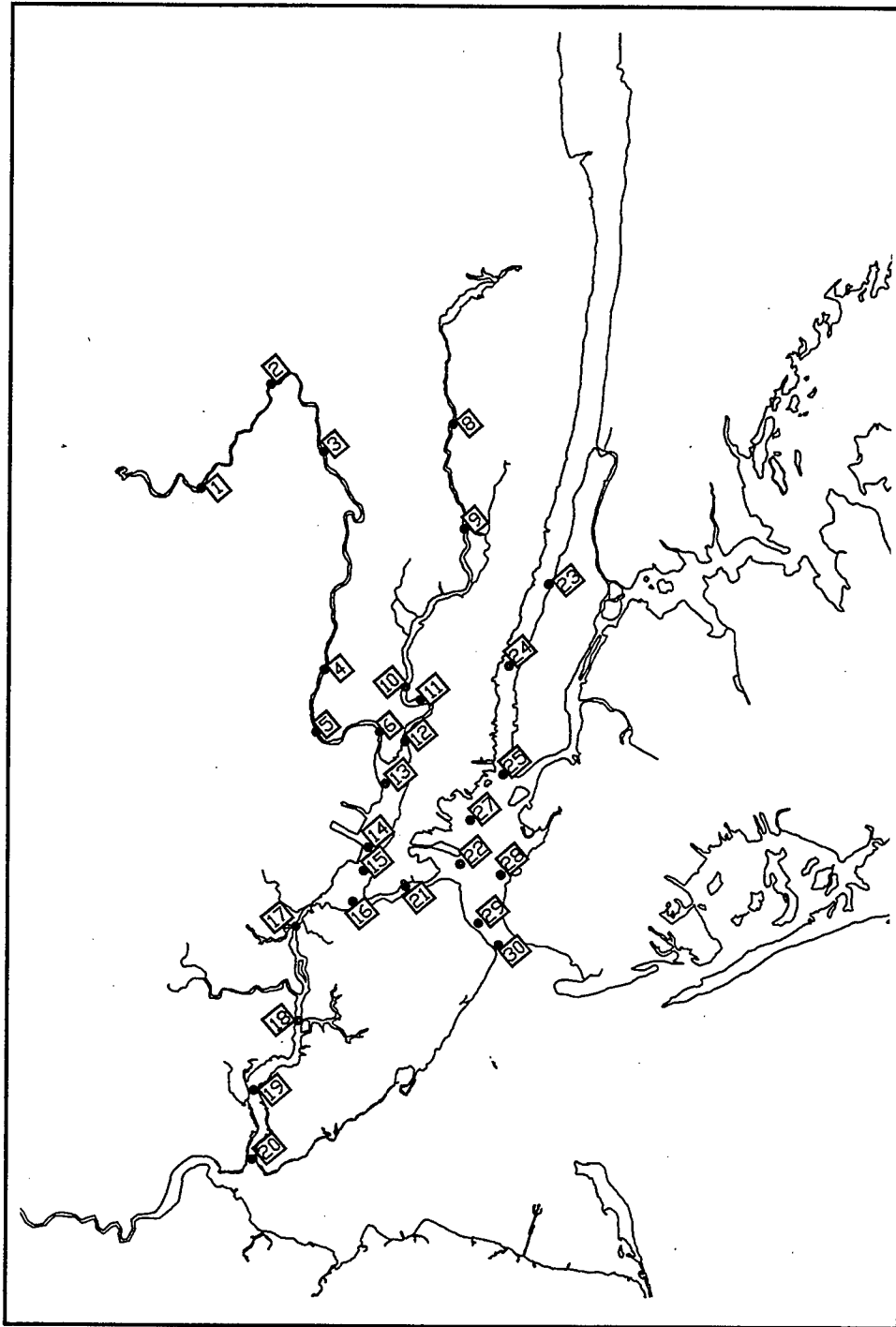
Figure 17.   Stevens Institute of Technology sample stations

1985). At stations less than 3 m depth, one sample was collected from mid-depth and analyzed for BODu. At stations greater than 3 but less than 10 m depth, samples were collected 1 m below the surface and 1 m off the bottom. The surface sample was analyzed for BODu, the bottom sample for BOD5. At stations greater than 10 m depth, samples were collected at surface, mid-depth, and bottom. The mid-depth sample was

analyzed for BODu, the remaining samples for BOD5. A median BODu to BOD5 ratio, BODu/BOD5 = 2.34, was computed and used to scale up the BOD5 measures to appropriate BODu concentrations.

Additional Databases

New York Department of Environmental Protection

The New York Department of Environmental Protection (NYDEP) conducts regular water quality monitoring in the New York harbor system. Several NYDEP stations (Figure 18) overlap with the primary area of interest in the present study. NYDEP observations of salinity, temperature, and dissolved oxygen were obtained for the 1994 summer months and merged with the data collected specifically for model calibration.

National Marine Fisheries Service

The National Marine Fisheries Service (NMFS) was retained by the project sponsors to inventory living resources in the project area and to interpret model results in terms of living-resource impacts. The NMFS conducted intensive sampling of biota and water quality in upper Newark Bay (Figure 19) from May 1993 to May 1994. Observations included salinity, temperature, and dissolved oxygen. The NMFS data were employed for system characterization and in specification of base conditions for computation of tunnel impact.

STORET database

The U.S. Environmental Protection Agency's STORET database was accessed to provide observations of temperature, dissolved oxygen, and BOD5 at the system fall lines. BOD5 was scaled up to BODu employing the ratio derived from the calibration database.

Fall-Line Flows, Loads, and Boundary Conditions

Flows

The period July 1 to September 15, 1994, was selected for model calibration. The calibration period spanned the three water quality surveys conducted July 18-19, August 22-23, and September 7-8. The calibration period commenced roughly at the peak of runoff generated by a late-June storm (Figures 20-24). By the time of the first survey, runoff had receded
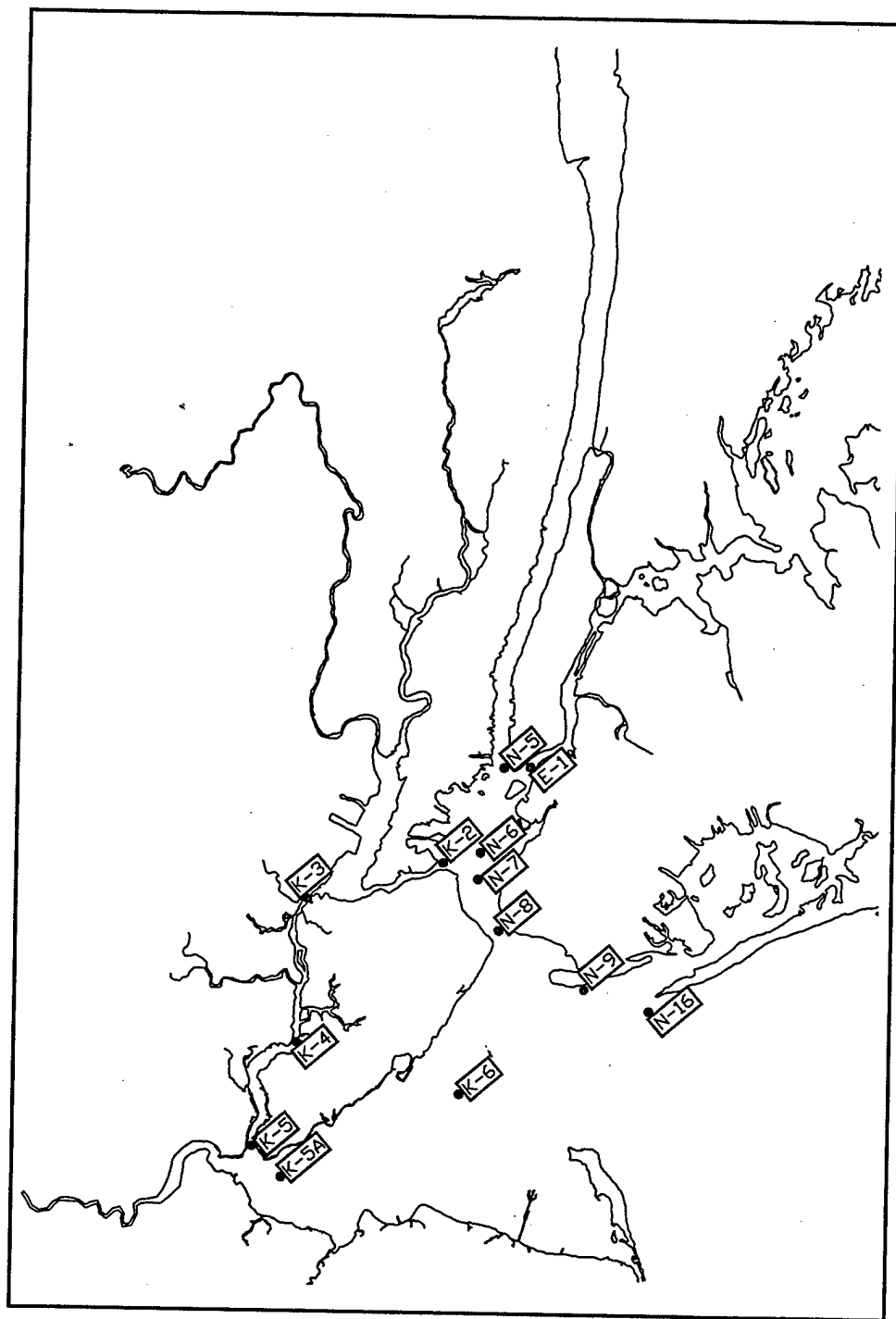
Figure 18. New York Department of Environmental Protection sample
          stations

to conditions that approximated base flow in the tributaries. Two addi-
tional storm events occurred in the calibration period. Peak runoff from
these events occurred circa July 28 and August 23. The second water
quality survey coincided with runoff from the August storm. Runoff
returned again to base flow by the final water quality survey.
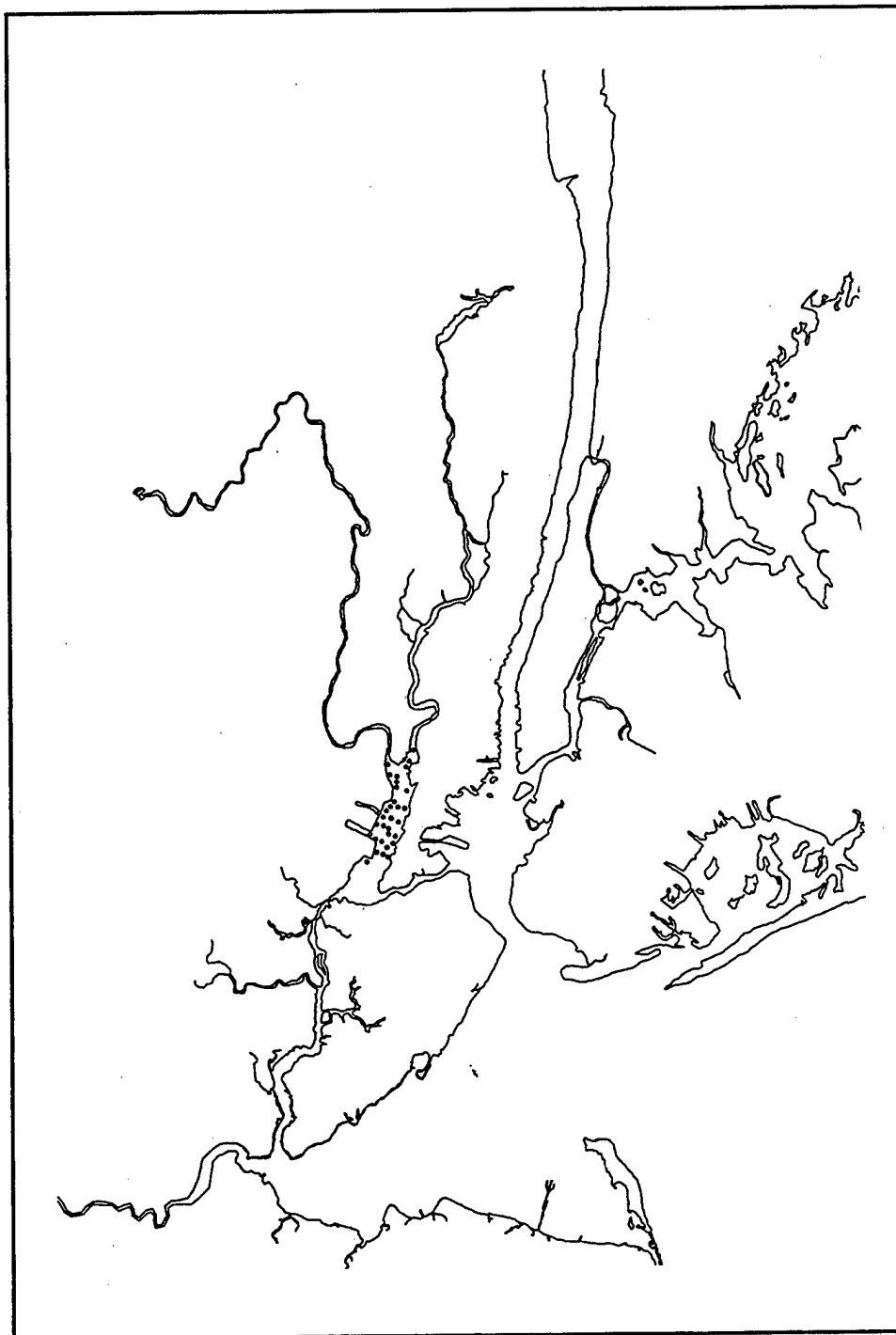
Figure 19. National Marine Fisheries Service sample stations

During the calibration period, flows in the Passaic and Hackensack were less than long-term mean values for the summer months but exceeded long-term monthly minimum flows (Table 6). Flows in the Raritan, Elizabeth, and Rahway rivers were close to mean values for the summer months. Rainfall in July and September (Table 7) was likewise less than
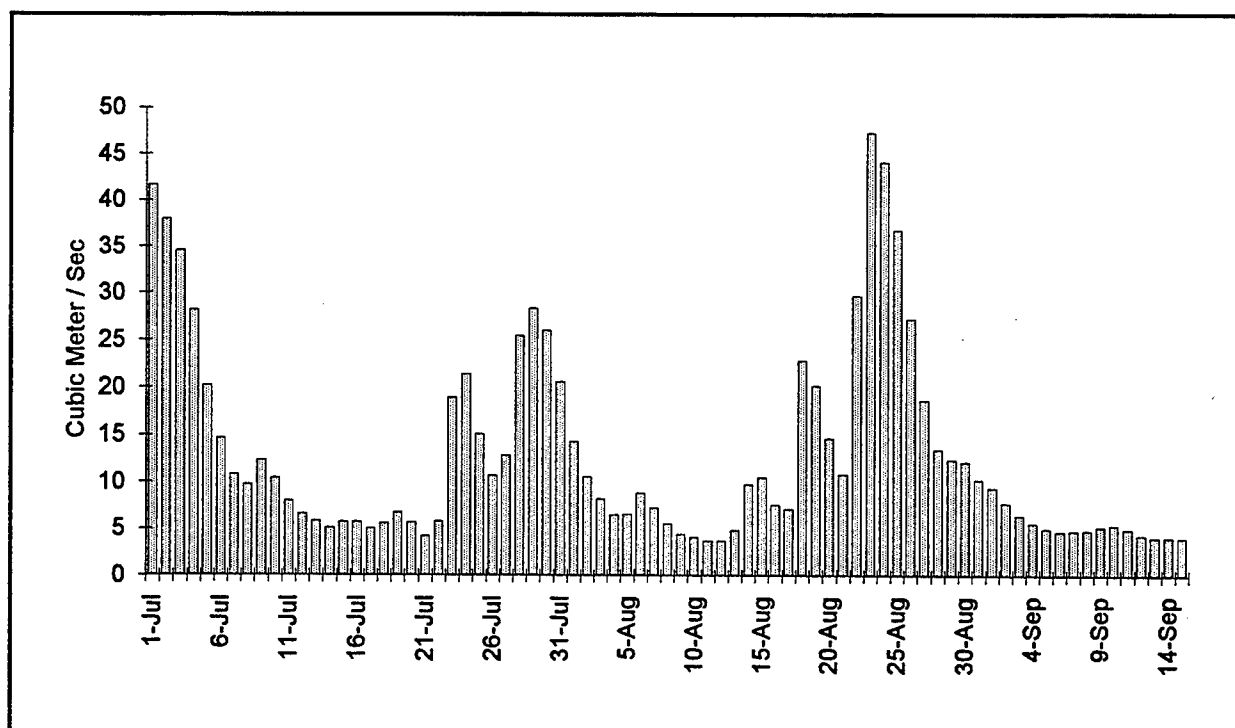
Figure 20.   Flow in Passaic River at Little Falls
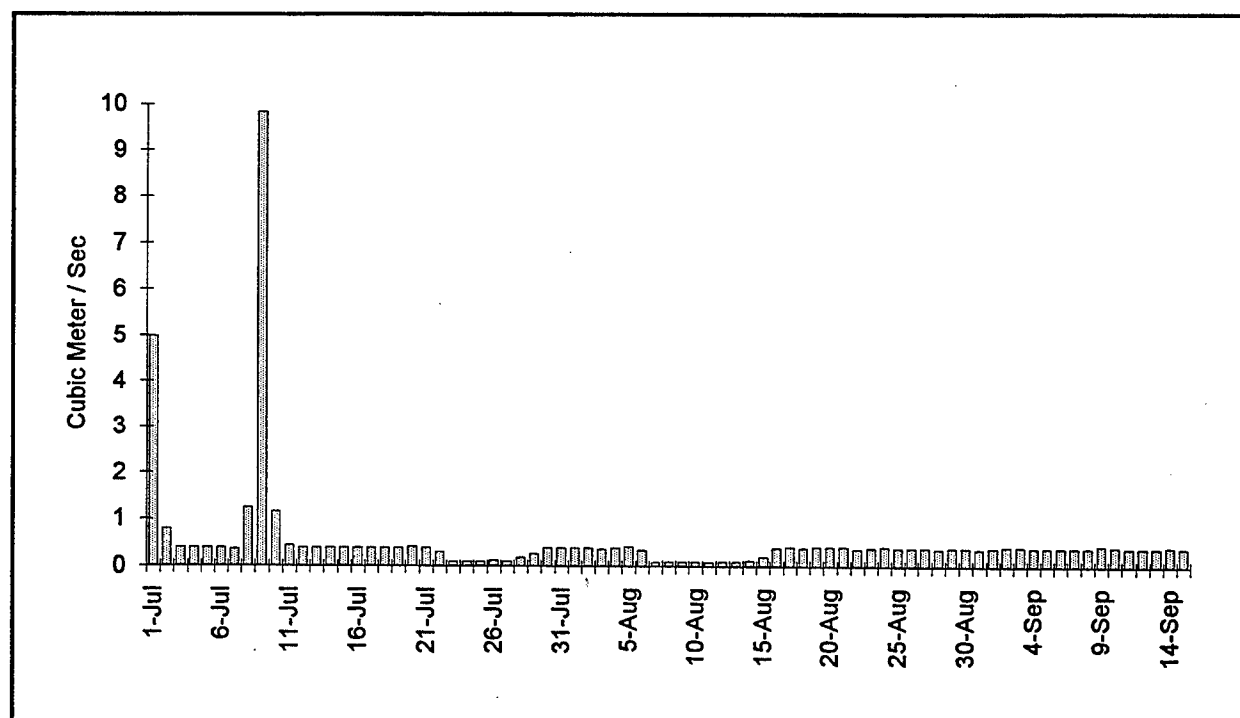
Figure 21.   Flow in Hackensack River at New Milford
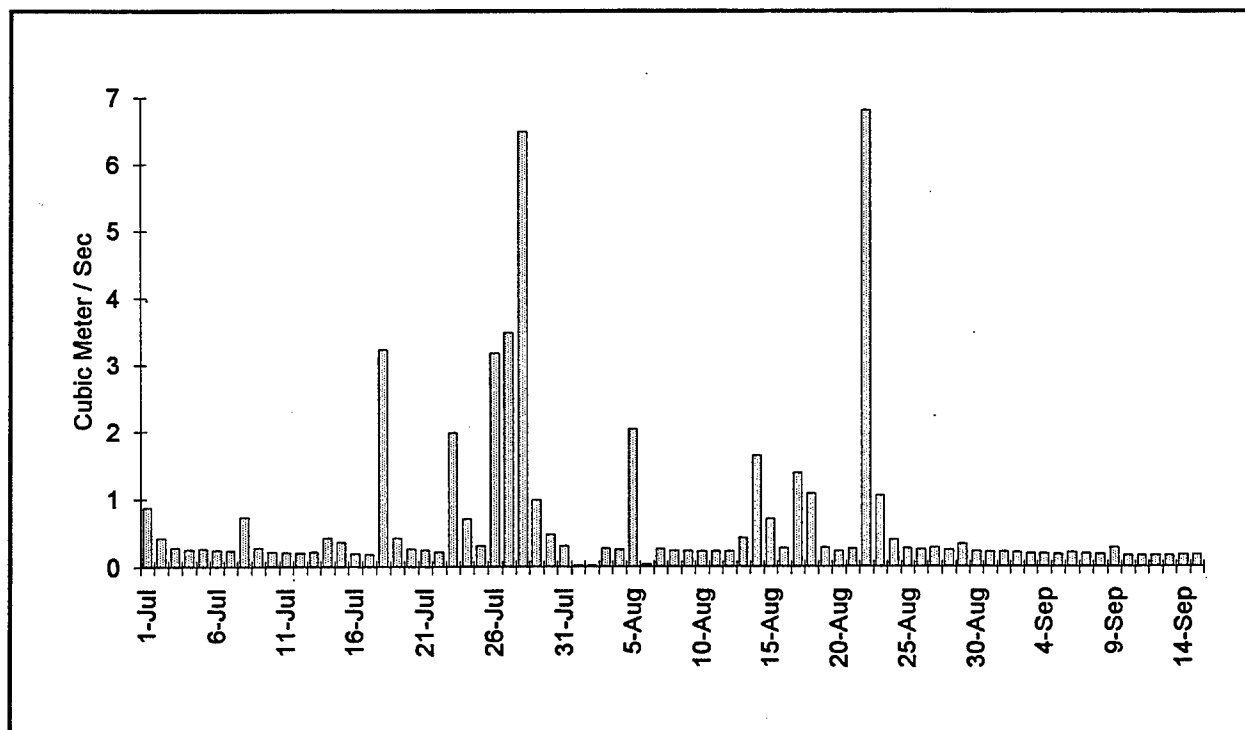
Figure 22.   Flow in Elizabeth River at Ursino
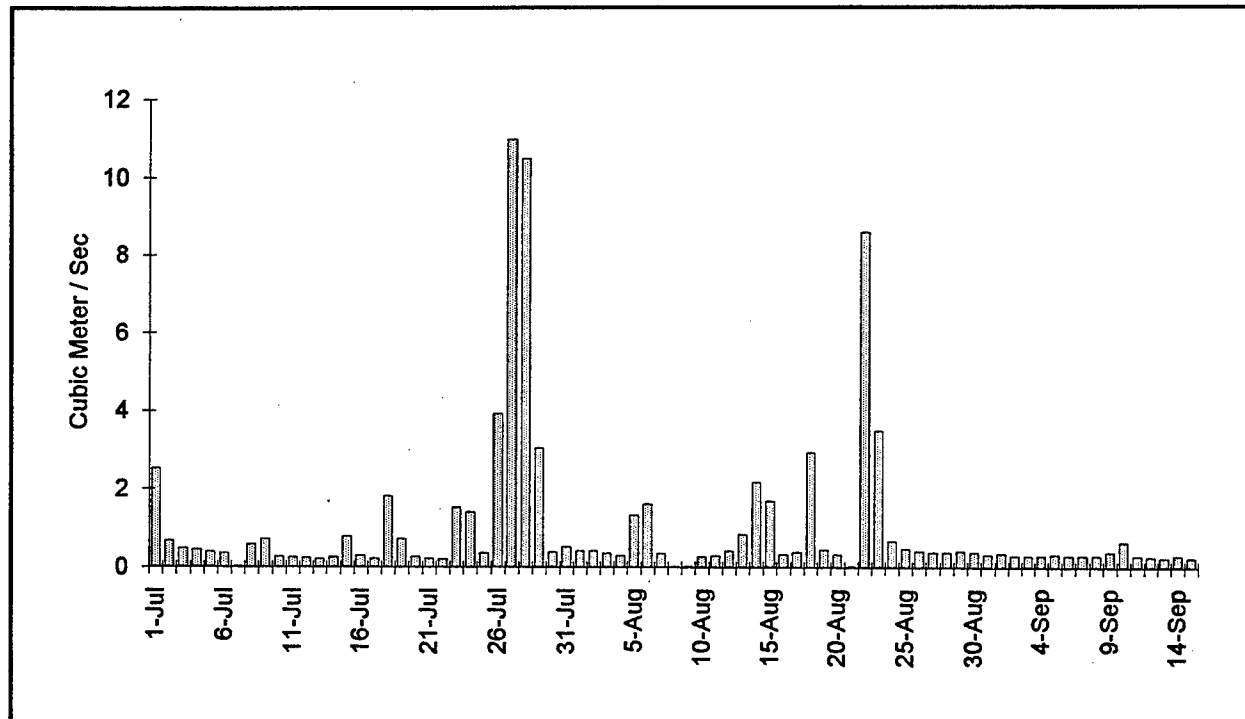
Figure 23.   Flow in Rahway River at Rahway
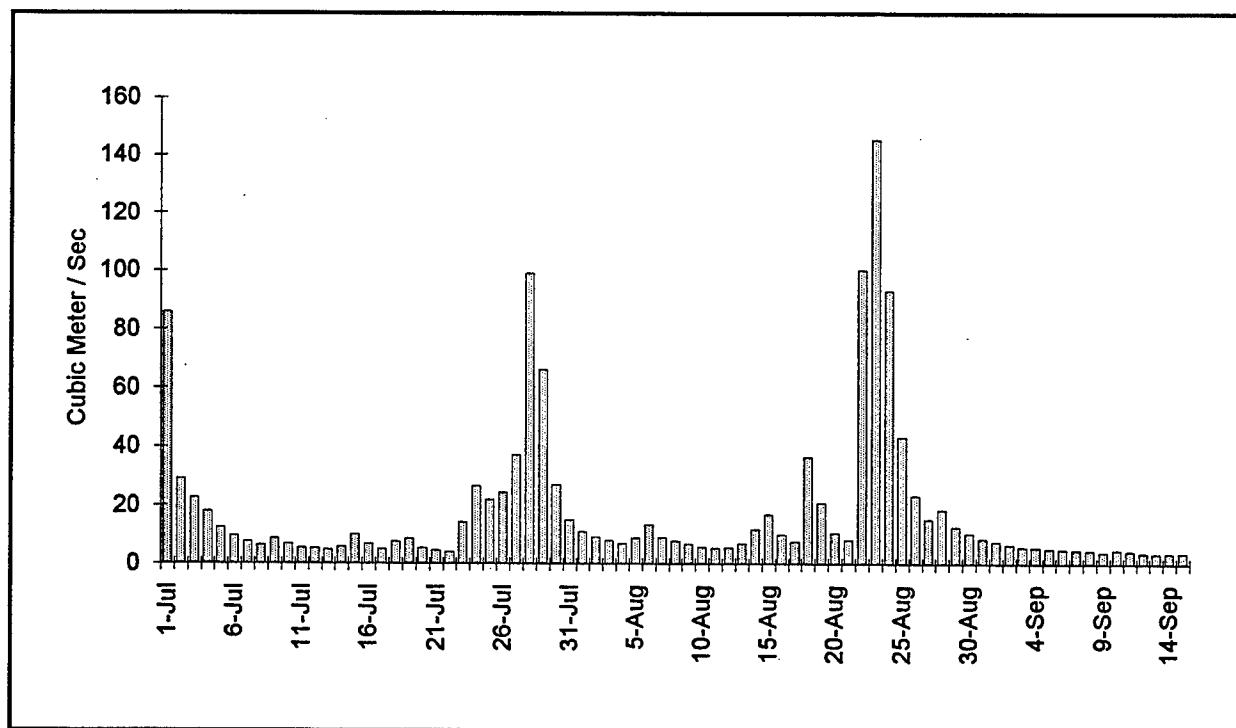
Figure 24. Flow in Raritan River at Bound Brook

**Table 6
Summer (July-September) Flows**

Fall Line	1994 $m^3\ sec^{-1}$	Long-Term Mean Flow $m^3\ sec^{-1}$	Minimum Monthly Flow $m^3\ sec^{-1}$	Maximum Monthly Flow $m^3\ sec^{-1}$
Passaic River at Little Falls	11.6	15.3	0.8	101
Hackensack River at New Milford	0.5	1.2	0.0	12.3
Raritan River at Bound Brook	16.4	17.1	2.0	101
Elizabeth River at Ursino	0.7	0.8	0.0	5.5
Rahway River at Rahway	1.0	1.1	0.1	7.6

**Table 7
Summer (July-September) Rainfall at Newark Airport**

Month	1994 cm	Long-Term Mean cm	Monthly Minimum cm	Monthly Maximum cm
July	9.1	10.7	2.3	25.3
August	12.7	10.3	1.3	30.1
September	5.7	8.7	2.4	22.9

long-term mean values. Rainfall in August exceeded the long-term mean, largely due to a storm that occurred August 21-23 (Figure 25).
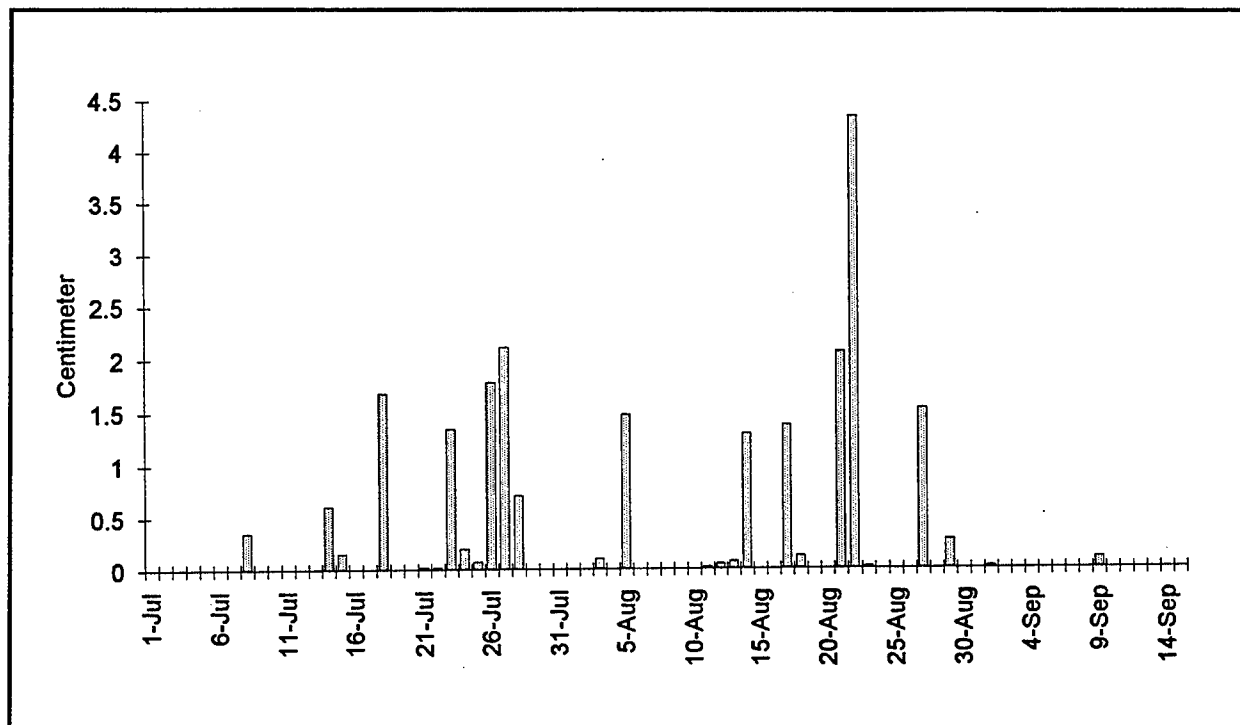
Figure 25. Rainfall at Newark Airport

Loads

Specification of BOD loading was required at the fall lines of the Passaic, Hackensack, Elizabeth, Rahway, and Raritan rivers. Observations at all fall lines were examined for relationship of BOD to flow. Only the Passaic indicated a relationship. Higher BOD concentrations were observed at lower flows, indicating a dilution effect at high flows (Figure 26). The relationship employed was:

$$BOD5 = \frac{11.5}{Q^{0.16}} \tag{12}$$

where Q is the volumetric flow, $ft^3 sec^{-1}$. Mean BOD5 concentrations were used to characterize the remaining fall lines.

Loads were computed as the product of daily flow, measured at U.S. Geological Survey (USGS) gauges, and BODu concentration. BODu (Table 8) was scaled up from BOD5 using ratios determined in the sampling program.
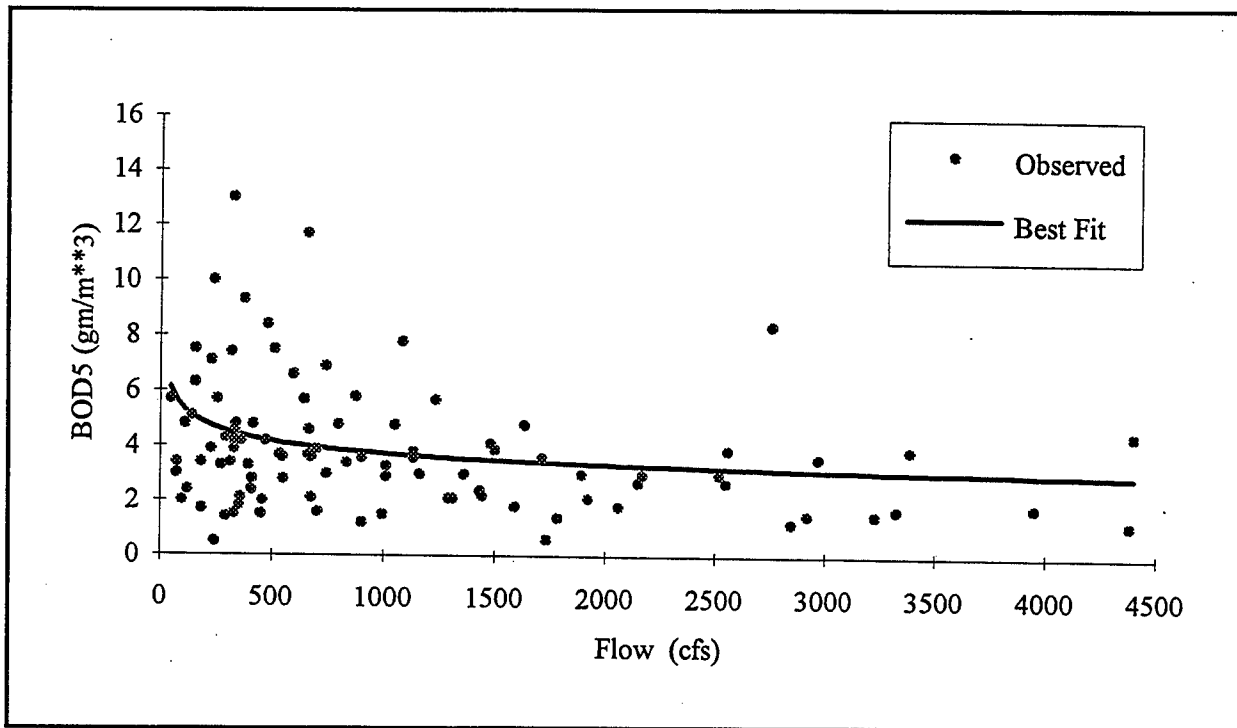
Figure 26. BOD versus flow in Passaic River at Little Falls

Table 8 Fall-Line Boundary Conditions			
River	Temperature, °C	DO, g m^{-3}	BODu, g m^{-3}
Passaic	19.9 - 25.0	8.2 - 8.8	8.1 to 17.3
Hackensack	20.6 - 24.2	6.6 - 8.0	4.6
Elizabeth	19.8 - 24.1	4.2 - 6.3	16.5
Rahway	23.1 - 23.6	7.1 - 7.2	7.9
Raritan	24.1 - 25.5	8.8	4.1

Boundary conditions

Model calibration required specification of salinity, temperature, and dissolved-oxygen concentration at the fall lines. Salinity was set to zero since the fall-line flows are freshwater sources to the system. Temperature and dissolved oxygen (Table 8) were specified based on monthly mean values in the STORET database.

Nonpoint-Source Flows and Loads

Nonpoint-source flows are distributed flows that enter the system at the edge of stream below the fall lines. Substances dissolved and suspended in the nonpoint-source flows constitute nonpoint-source loads. Nonpoint-source loads to the New York-New Jersey harbor system are characterized by the predominance of combined-sewer overflows. These overflows are from municipal sewer systems in which sanitary and storm sewers are combined. During large storms, the capacity of the treatment system is exceeded, and both runoff and sanitary effluent are washed into receiving waters.

Flows

Nonpoint-source flows and loads were determined from an areawide rainfall-runoff model created for a Section 208 study of the New York-New Jersey harbor system (Hazen and Sawyer 1978). The Section 208 study divided the system into 92 drainage basins. From these, 75 basins (Figure 27) were determined to drain into the region of interest of the present study. For each basin, flow was computed from rainfall on a daily basis:

$$NPSQ = I \, A \, CV \left(Fss + Fcs(1 - Fccs) \right) \tag{13}$$

where

$NPSQ$ = nonpoint-source flow

I = daily total rainfall

A = basin area

CV = runoff coefficient $(0 \le CV \le 1)$

Fss = fraction of basin served by separate sewers $(0 \le Fss \le 1)$

Fcs = fraction of basin served by combined sewers $(0 \le Fcs \le 1)$

$Fccs$ = fraction of flow in combined sewers captured by treatment plant $(0 \le Fccs \le 1)$

Rainfall at Newark Airport (Figure 25) was used to generate flows throughout the system. Flows from the 75 basins were aggregated into 20 distributed flows for input to the model (Figure 28). In three instances, nonpoint-source flows from basins adjacent to fall lines were combined with fall-line flows. The remainder of the distributed flows were input below the fall lines. Locations of the inputs were selected based on drainage characteristics and location of major sewage discharges.
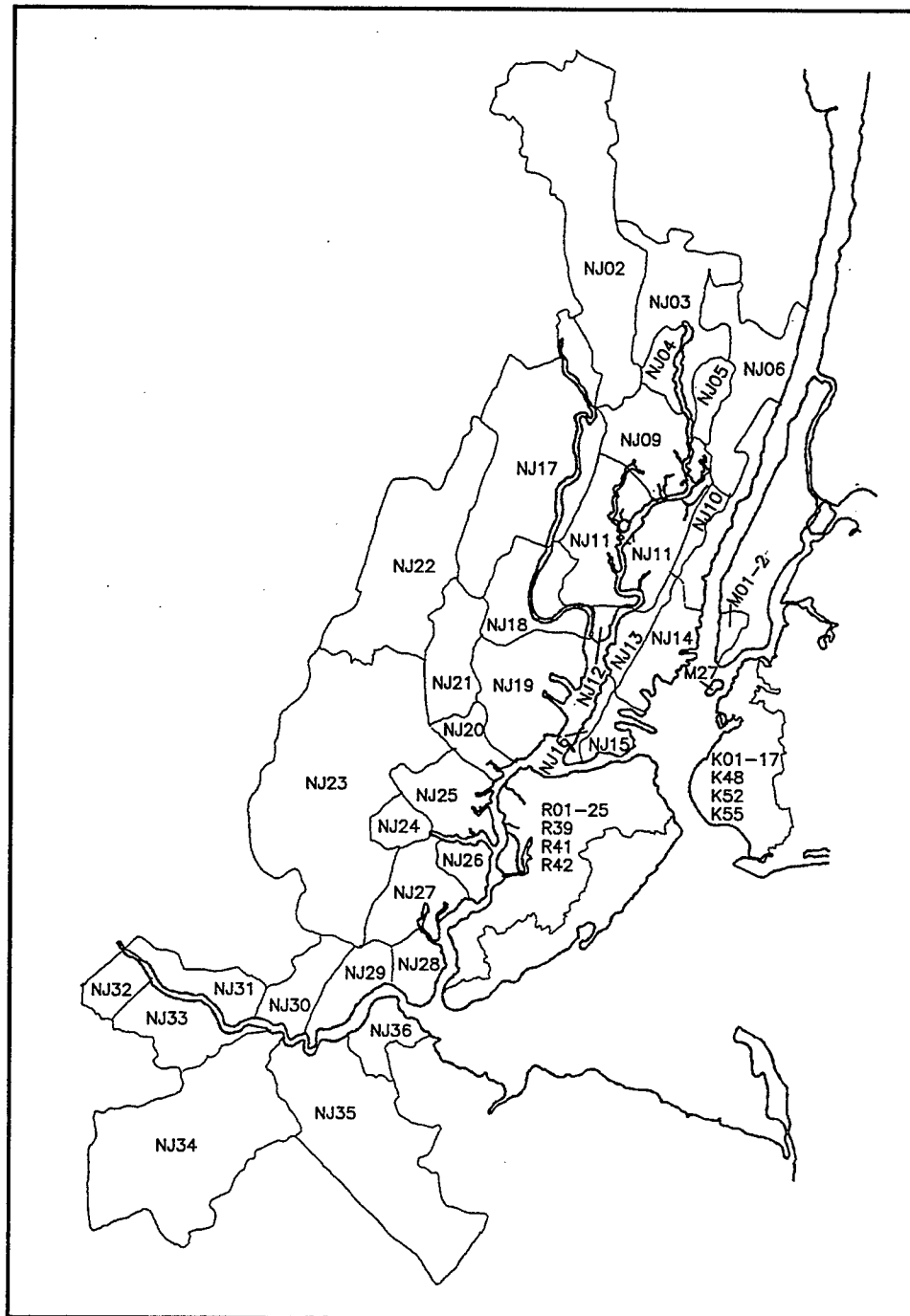
Figure 27. Drainage basins for computation of nonpoint-source flows and loads

Loads

Nonpoint-source BOD loads were computed based on flow and BOD concentration:

$$NPSBOD = I \, A \, CV \left(F_{ss} C_{ss} + F_{cs} (1 - F_{ccs}) C_{cs} \right) \tag{14}$$
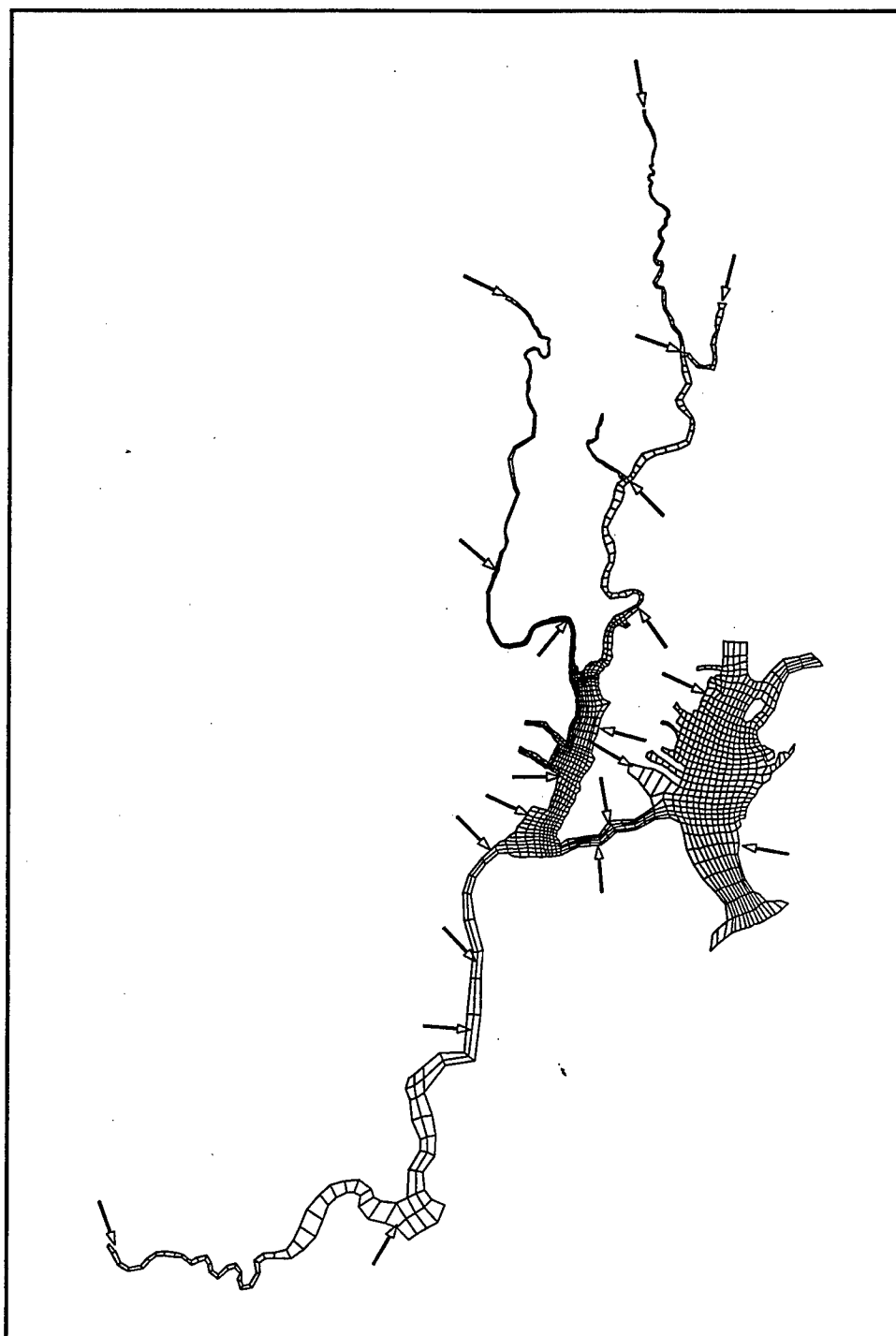
Figure 28.   Nonpoint-source flow input locations

where

NPSBOD = nonpoint-source BOD load

I = daily total rainfall

A = basin area, ha

CV = runoff coefficient ($0 \leq CV \leq 1$)

Fss = fraction of basin served by separate sewers ($0 \leq Fss \leq 1$)

Css = BOD concentration in separate sewers

Fcs = fraction of basin served by combined sewers ($0 \leq Fcs \leq 1$)

Fccs = fraction of flow in combined sewers captured by treatment plant ($0 \leq Fccs \leq 1$)

Ccs = BOD concentration in combined sewers

Characteristic BOD5 concentrations were identified from the Section 208 report as 110 g m^{-3} for combined sewers and 25 g m^{-3} for separate sewers. BODu concentration was initially approximated from BOD5 concentration using the reported COD/BOD5 ratio: COD/BOD5 = 2.5. This ratio provided an upper limit on BODu since the strong chemical oxidant employed in the COD analysis oxidizes substances that may be refractory to biological decay. The ratio was finalized as part of the model calibration process: BODu/BOD5 = 1.88.

Guidelines provided in the Section 208 report were used to route nonpoint-source BOD loads from basins into appropriate model cells. Virtually all surface shoreline cells were recipients of a nonpoint-source load.

Point-Source Flows and Loads

Point source flows and loads originate in the municipal treatment plants and industries situated along the shores of the system (Figure 29). A database of point sources was constructed from information obtained from the New Jersey Department of Environmental Protection and from HydroQual (1991). Quality of the point-source data varied widely. The best data comprised monthly flow rates and BOD5 observations. For some facilities, however, only permit flows and loads were available. Point-source flows (Table 9) comprise a significant fraction of total freshwater flow to portions of the system, especially the Kills (Thomas 1993). These flows were input to the system at appropriate locations (Figure 28). Point-source loads were computed as the product of flow and BOD concentration, when these data were available, or were taken from permits. BODu loads were scaled up from BOD5 loads using the median value, BODu/BOD5 = 7.7, determined from analyses at a number of municipal treatment plants (Weand and Grizzard 1985).

Heat Source in Hackensack River

The area surrounding Newark Bay contains numerous power generation plants and industries that discharge heated effluent to adjacent waters. Examination of data collected for this study indicated a temperature rise in the Hackensack River in the vicinity of several generation plants. Detailed
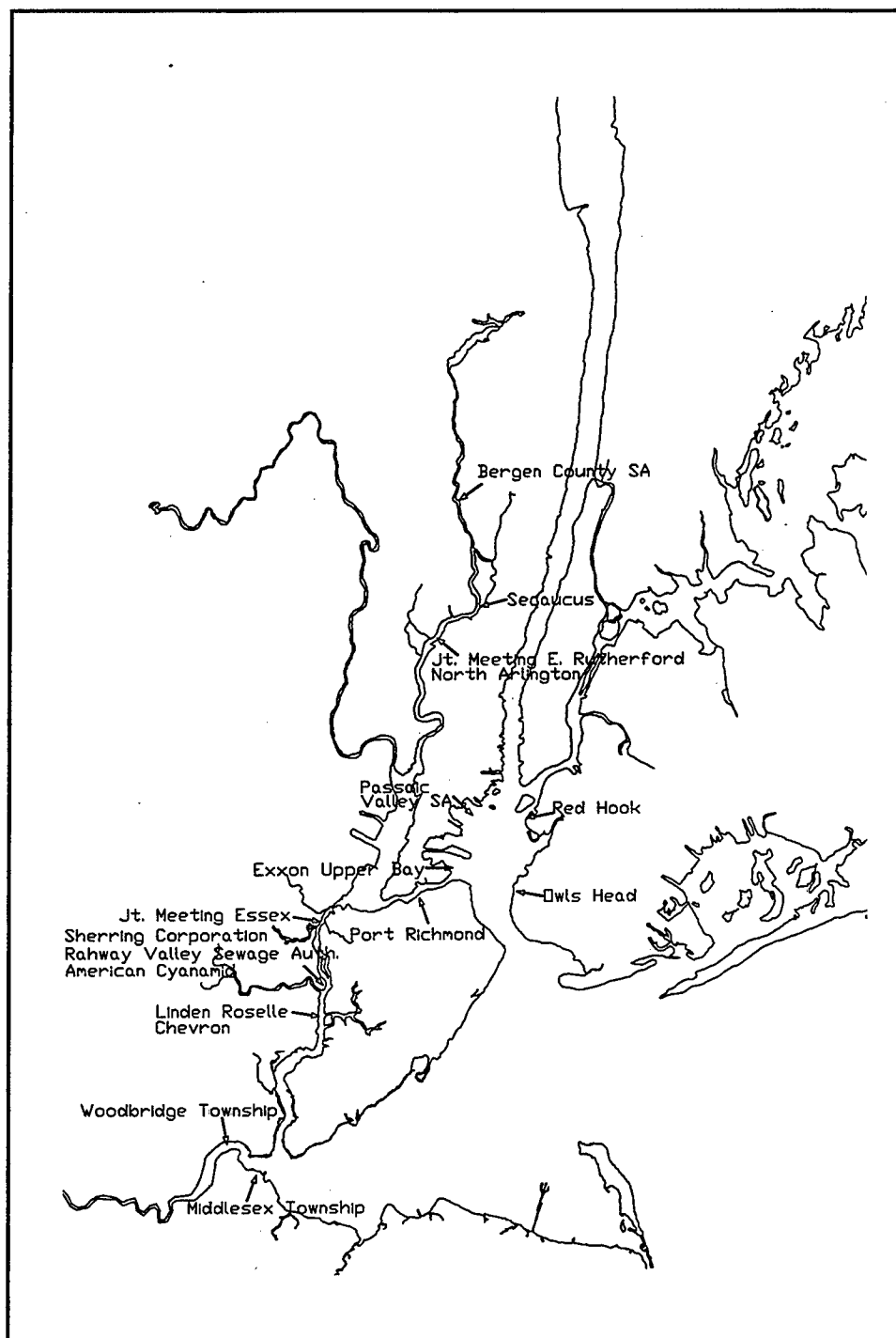
Figure 29. Location of point-source discharges

modeling of the effects of these plants on temperature was not possible.
Waste heat discharged to the river was simulated by the addition of a point
source of heat. Magnitude of the source, 608 MW, was determined during
the model calibration process by matching the observed temperature
distribution.

Table 9
Calibration Point Source Flows and Loadings

Point Source	Jul Flow m³/sec	Aug Flow m³/sec	Sep Flow m³/sec	Jul BOD5 kg/day	Aug BOD5 kg/day	Sep BOD5 kg/day	Source
Jt. Meeting Esses/Union County	2.92	2.73	2.77	5,110	6,270	6,119	NJDEP[1]
Rahway Valley Sewage Authority	1.18	1.18	1.18	2,750	2,750	2,750	HydroQual 1991
Linden Roselle	0.47	0.50	0.46	125	89	54	NJDEP
Passaic Valley Sewage Authority	11.77	11.53	12.41	18,886	19,672	18,100	NJDEP
Owls Head Wastewater Treatment Plant	5.22	5.22	5.22	29,970	29,970	29,970	HydroQual 1991
Port Richmond Treatment Plant	1.76	1.76	1.76	2,320	2,320	2,320	HydroQual 1991
Bergen County Sewage Authority	3.13	3.13	3.13	6,130	6,130	6,130	HydroQual 1991
Jt. Meeting Rutherford/East Rutherford Sewage Authority	0.11	0.11	0.11	2,590	2,590	2,590	HydroQual 1991
Red Hook Treatment Plant	2.05	2.05	2.05	2,290	2,290	2,290	HydroQual 1991
Middlesex Townships and Woodbridge and Carteret	4.22	4.22	4.22	8,320	8,320	8,320	HydroQual 1991
Woodbridge Townships	0.05	0.05	0.05	140	140	140	HydroQual 1991
Secaucus	0.13	0.13	0.13	210	210	210	HydroQual 1991
North Arlington	0.09	0.09	0.09	720	720	720	HydroQual 1991
Exxon Upper Bay	0.08	0.08	0.08	170	170	170	HydroQual 1991
Chevron USA	0.04	0.04	0.04	300	300	300	HydroQual 1991
American Cyanamid	1.10	1.10	1.10	270	270	270	HydroQual 1991
Shering Corp.	0.01	0.01	0.01	140	140	140	HydroQual 1991

[1] New Jersey Department of Environmental Protection.

Open-Boundary Conditions

Salinity, temperature, dissolved oxygen, and BOD boundary conditions were required at the open boundaries of the Hudson River, East River, Arthur Kill, and the Narrows. Boundary conditions at these locations were specified from observations collected during the water quality sampling.

Load Summary

A BOD load summary for the calibration period is presented in Table 10. Dominant loading sources vary according to location and meteorology. The Passaic River and Newark Bay receive no significant point-source discharges and are dominated by nonpoint-source loading. The remainder of the system is dominated by point-source loading under average conditions. While summer-average nonpoint-source loads are less than point-source loads, nonpoint sources are, of course, predominant under storm conditions. Overall, the largest BOD loads are discharged to upper New York Bay, Arthur Kill, and the Hackensack River.

Table 10
BODu Load Summary

	Fall Line, Summer Average kg day^{-1}	Point Source, Summer Average kg day^{-1}	Nonpoint Source, Summer Average kg day^{-1}	Total	Nonpoint Source, Aug 21-22 kg day^{-1}
Passaic River	11,208	0	17,936	29,144	125,205
Hackensack River	225	75,337	36,609	112,171	255,554
Newark Bay	0	0	9,163	9,163	63,963
Arthur Kill	1,760	72,595	39,492	113,847	275,669
Kill van Kull	0	19,439	9,458	28,897	66,051
New York Bay	0	400,974	29,182	430,156	203,702
Raritan River	6,698	66,046	20,570	93,314	143,587
Total	19,891	634,391	162,410	816,692	1,133,731

6 Water Quality Model Calibration Results

Model Parameters and Coefficients

Before the water quality model could be applied to examine tunnel impact, the numerous parameters in the governing equations (Chapter 4) required evaluation. The parameters were evaluated in a process known as calibration. Calibration is a recursive process in which parameters are selected from a range of feasible values, tested in the model, and adjusted until optimal agreement between predicted and observed variables is obtained.

Calibration was conducted primarily against data collected by Stevens Institute of Technology for the present study (Chapter 4). Comparison of computations and observations was largely visual. Experience and judgment were employed to determine optimal values of calibration parameters although a statistical comparison of computations and observations was prepared for the final calibration. Final calibration parameters are presented in Table 11.

General Circulation Patterns

Detailed hydrodynamics were produced by the CH3D hydrodynamic model (Letter et al., in preparation) and passed to the water quality model. The water quality model has the capability to derive summary information from the CH3D hydrodynamics. Especially useful are net flows (Figure 30) that aid in diagnosing water quality conditions.

Computation of long-term mean flow indicated the Passaic River provided most of the freshwater inflow to Newark Bay during the calibration period. The Hackensack was the second largest source, followed by distributed flows directly to the bay. Net flow through the Kill van Kull was from upper New York Bay into Newark Bay. Net outflow from Newark Bay was through the Arthur Kill into Raritan Bay.

The net circulation through the Kills has been the subject of field and model investigation. While field investigations provide more direct

Table 11
Water Quality Model Calibration Parameters

Parameter	Equation	Value	Units
BENDOb	10	1.0	g m^{-2} day^{-1}
KBOD	3	0.05	day^{-1}
KCOD	5	20.0	day^{-1}
KHDOB	3	0.5	g DO m^{-3}
KHDOC	5	1.5	g DO m^{-3}
KHSO	10	2.0	g DO m^{-3}
KR	6	1.0	m day^{-1}
KSO	10	0.069	°C^{-1}
KTBOD	4	0.069	°C^{-1}
TRBOD	4	20.0	°C
TRSO	10	20.0	°C
WBOD	3	1.0	m day^{-1}

evidence than simulations, direct investigations are compromised by their relatively short duration. Field investigations are applicable only to the specific conditions under which they are conducted. Model simulations can be conducted for lengthy periods and employed to investigate a variety of conditions.

Current meters placed in Arthur Kill indicate generally a two-layer circulation, from Newark Bay to Raritan Bay on the surface and from Raritan Bay to Newark Bay along the bottom (Thomas 1993). Although the magnitude and, occasionally, direction of net currents are variable, magnitude of net current along the bottom frequently exceeds net surface currents. Net transport is strongly dependent on wind forcing. Simulations conducted by Thomas (1993) indicate net flow is northward, from Raritan to Newark Bay, roughly 40 m^3 sec^{-1}, during periods of calm to light wind. Southeasterly winds increase the northward net transport to 120 m^3 sec^{-1}, while northwesterly winds can induce transport of equal or larger magnitude in the opposite direction.

The reversible net flow in Arthur Kill was exemplified in a dye study conducted in 1995 (Hires and Thomas 1996). Dye was released instantaneously in the central portion of the Kill, then monitored for a period of 9 days. The centroid of dye plume moved roughly 4 km southward in 2 days, then moved roughly 2 km northward in 7 days. Net transport was less than 2 km to the south in 9 days (Figure 31).

A second instantaneous dye release was conducted in Newark Bay (Hires and Thomas 1996) just above the confluence of the two Kills. Dye
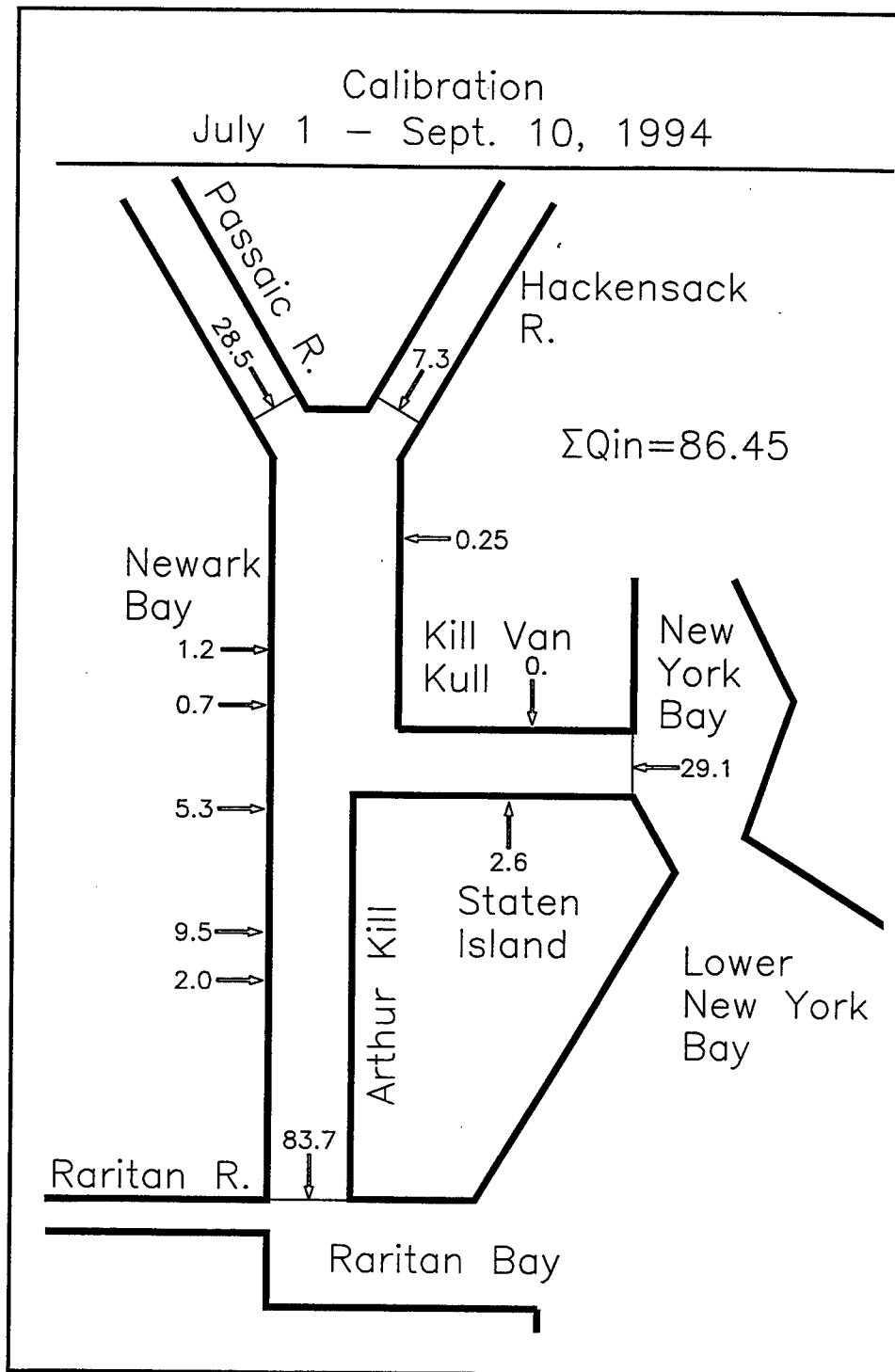
Figure 30. Computed net flows in Newark Bay and adjacent waters, summer 1994
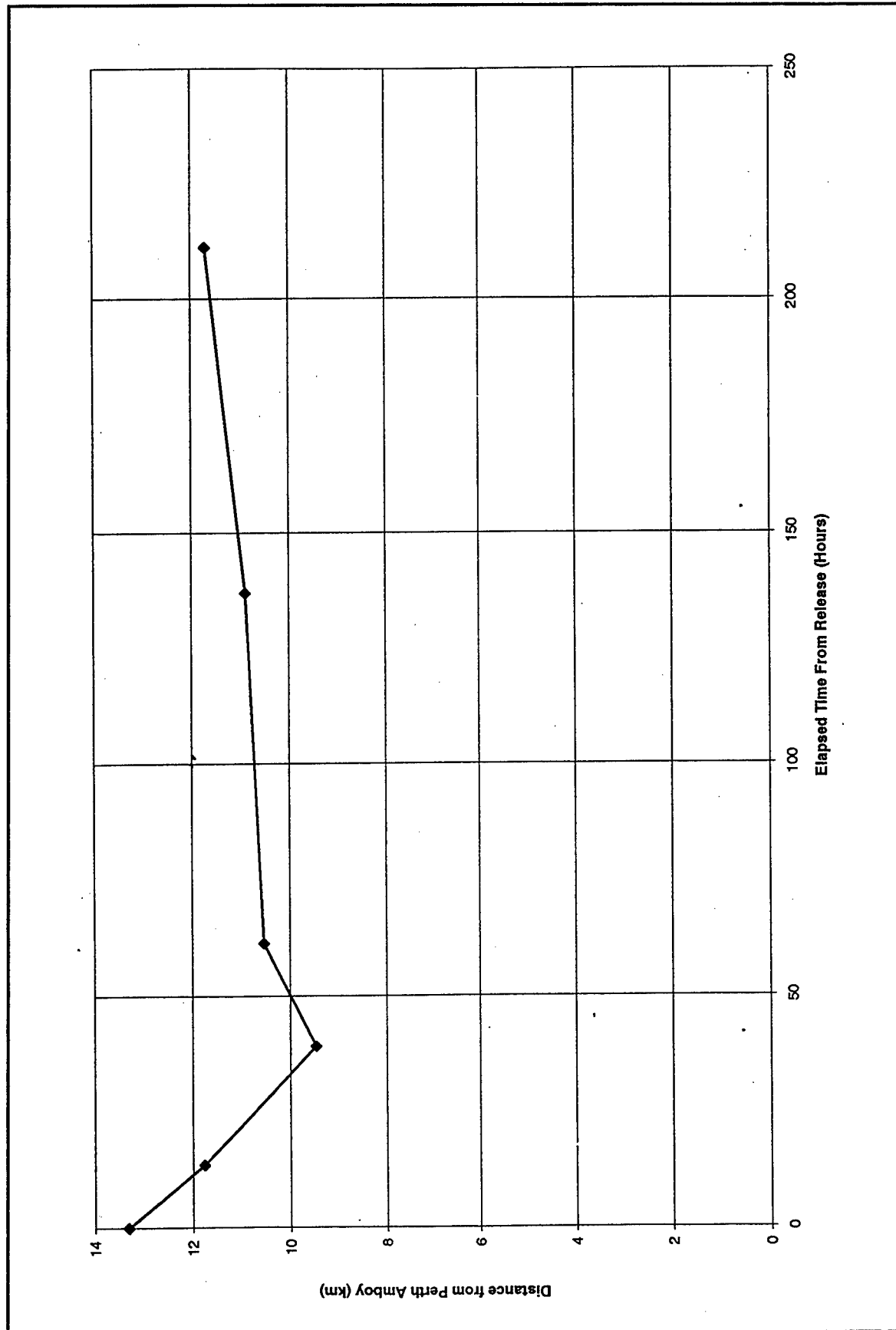
Figure 31. Location of centroid of dye plume in Arthur Kill (after Hires and Thomas 1996)

was released just prior to slack-before-ebb and monitored in the two Kills during the ebb-tide period, roughly 6 hr. Results indicated over 70 percent of the dye released passed through the Kill van Kull (Figure 32). Only 10 percent passed into the Arthur Kill (Figure 33).

The dye experiment illustrates the importance of tidal currents as well as net currents in determining transport through the two Kills. The field dye studies qualitatively verify the model tracer studies conducted to determine water quality model boundary conditions. In the model dye dump, dye appeared in the Kill van Kull prior to the Arthur Kill (Figure 15) just as dye released above the two Kills showed a tendency to move through the Kill van Kull. Over the 30-day simulation, however, predominant dye transport was through the Arthur Kill, reproducing the result of the 9-day dye study in which net dye movement was southward towards the Perth Amboy and the Raritan Bay.

Calibration Results

The calibration run simulated the period July 1 to September 15, 1994. Initial conditions were obtained by "looping" the model until equilibrium with conditions on July 1 was obtained. Model and observations were examined in a variety of formats including spatial comparisons along two longitudinal axes (Figures 34 and 35), time-series comparisons at eight locations (Figure 36), and spatial comparisons along vertical axes at eight locations (Figure 36). Since stratification in the system is normally slight, computations and observations were averaged vertically for comparison along longitudinal axes and for time-series comparisons.

Longitudinal Comparisons

The longitudinal plots are dominated by the lengthy reaches of the Passaic and Hackensack rivers. The Passaic extends from km 16 to 44 of the transect originating at the mouth of the Kill van Kull, nearly two-thirds of the axis. The Hackensack extends from km 32 to 68, more than half of the axis. Observations in these portions of the system are minimal, largely because the rivers are not navigable and access for sampling is limited.

The majority of the Passaic is tidal freshwater in both the observations and model (Figures 37 to 39). Predicted salinity upstream of the mouth of the Passaic is generally underestimated but cannot be improved through tuning of the water quality model. Examination of the limited available data indicates temperature and dissolved oxygen in the Passaic generally exceeds 4 mg/L while temperature ranges from 20 to 25 °C. The model reproduces these conditions with one exception, a dissolved oxygen sag to 2 mg/L near km 20 on July 18-19 (Figure 37). The origin of this sag is not known. It may be a transient condition due to a discharge or it may be a permanent feature due, for example, to benthal deposits.

Current Velocity vs. Time in the Kill Van Kull 9/21
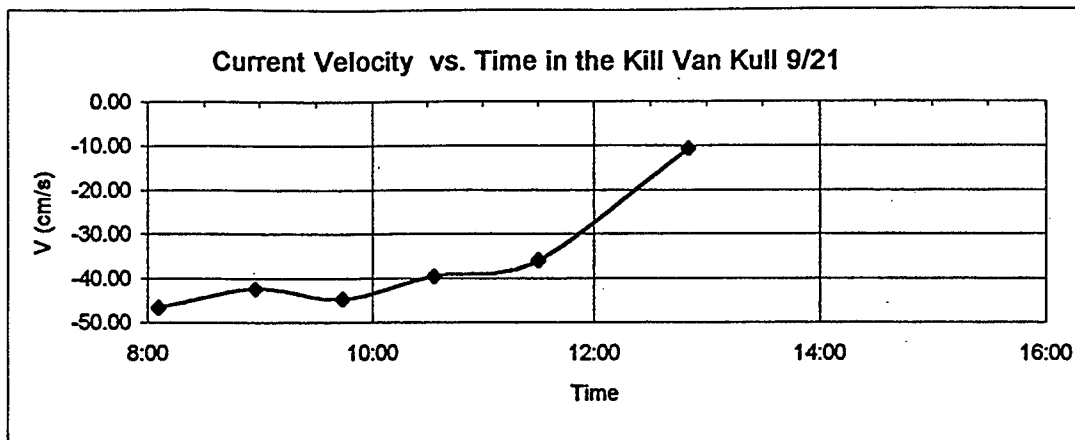
The depth-averaged velocity at station 1 in the Kill Van Kull observed on the ebb currents following the instantaneous dye release in Newark Bay on 21 September 1995.
note: ebb currents are negative

Dye Concentration in KVK 9/21
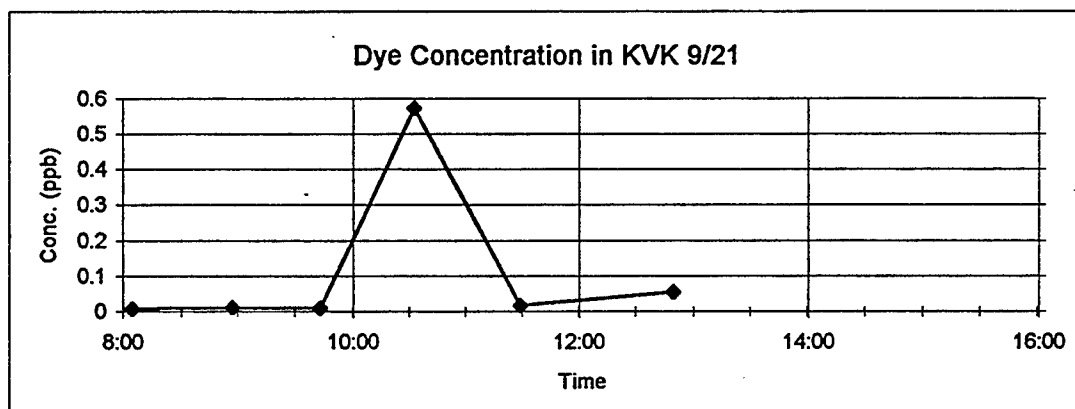
The depth-averaged dye concentration at station 1 from observation obtained simultaneous with the current observations presented in Figure 12a.

Flux of Dye in KVK 9/21
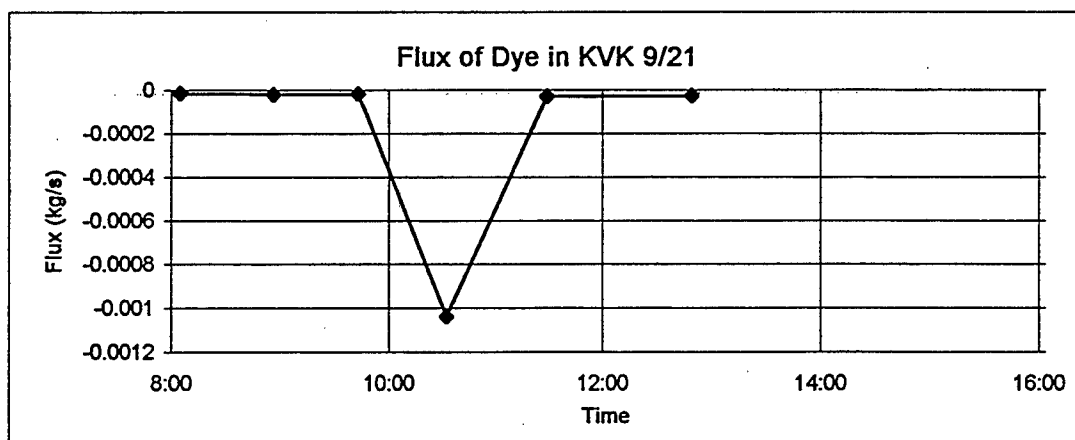
The estimated flux of dye through the Kill Van Kull based on the simultaneous observation of current velocity and dye concentration at station 1.

Figure 32. Current velocity, dye concentration, dye flux in Kill van Kull following dye release in Newark Bay (after Hires and Thomas 1996)
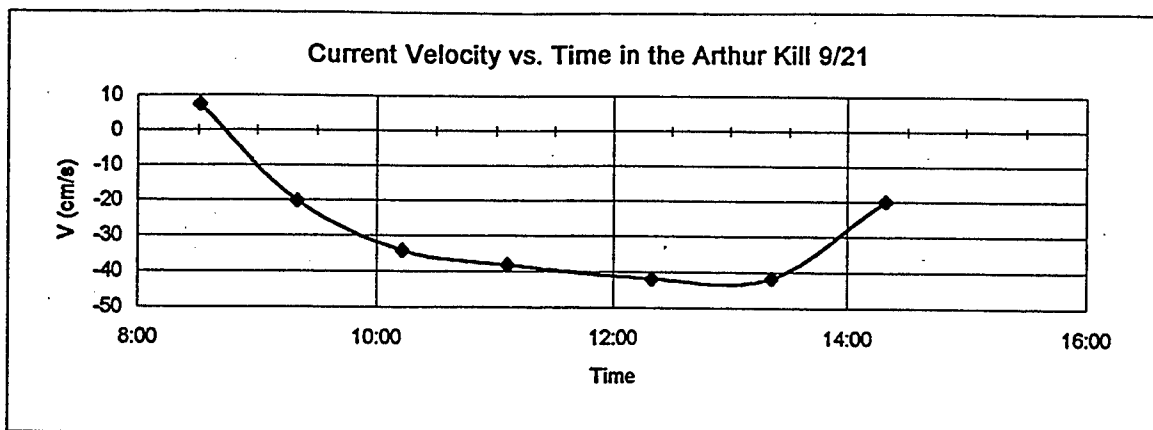
The depth-averaged velocity at station 2 in the Arthur Kill observed on the ebb currents following the instantaneous dye release in Newark Bay on 21 September 1995.
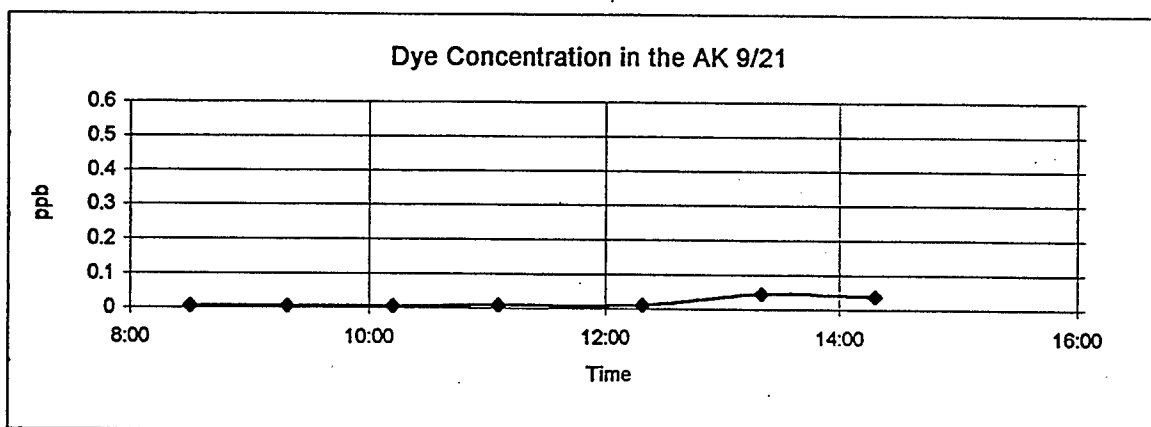
The depth-averaged dye concentration at station 2 from observations obtained simultaneously with the current observations presented in Figure 13a.
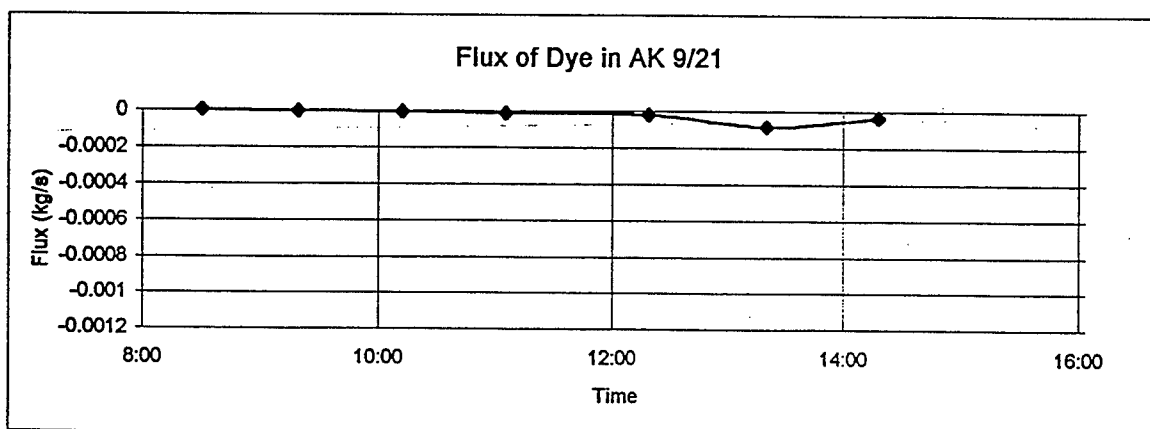
The estimated flux of dye through the Arthur Kill based on the simultaneous observation of current velocity and dye concentration at station 2.

Figure 33.   Current velocity, dye concentration, dye flux in Arthur Kill following dye release in Newark Bay (after Hires and Thomas 1996)
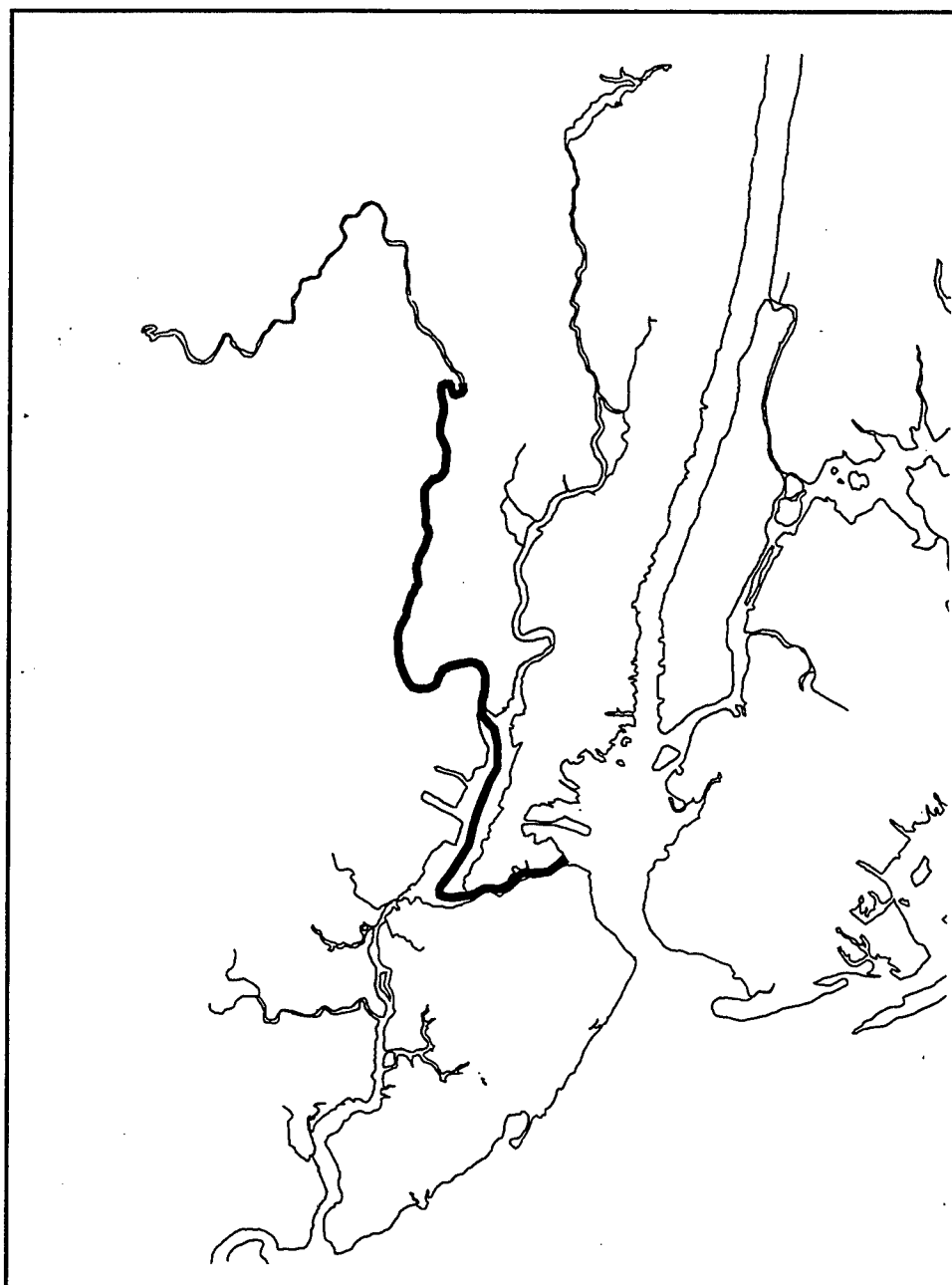
Figure 34. Axis for model-data comparisons from Passaic fall line through the Kill van Kull
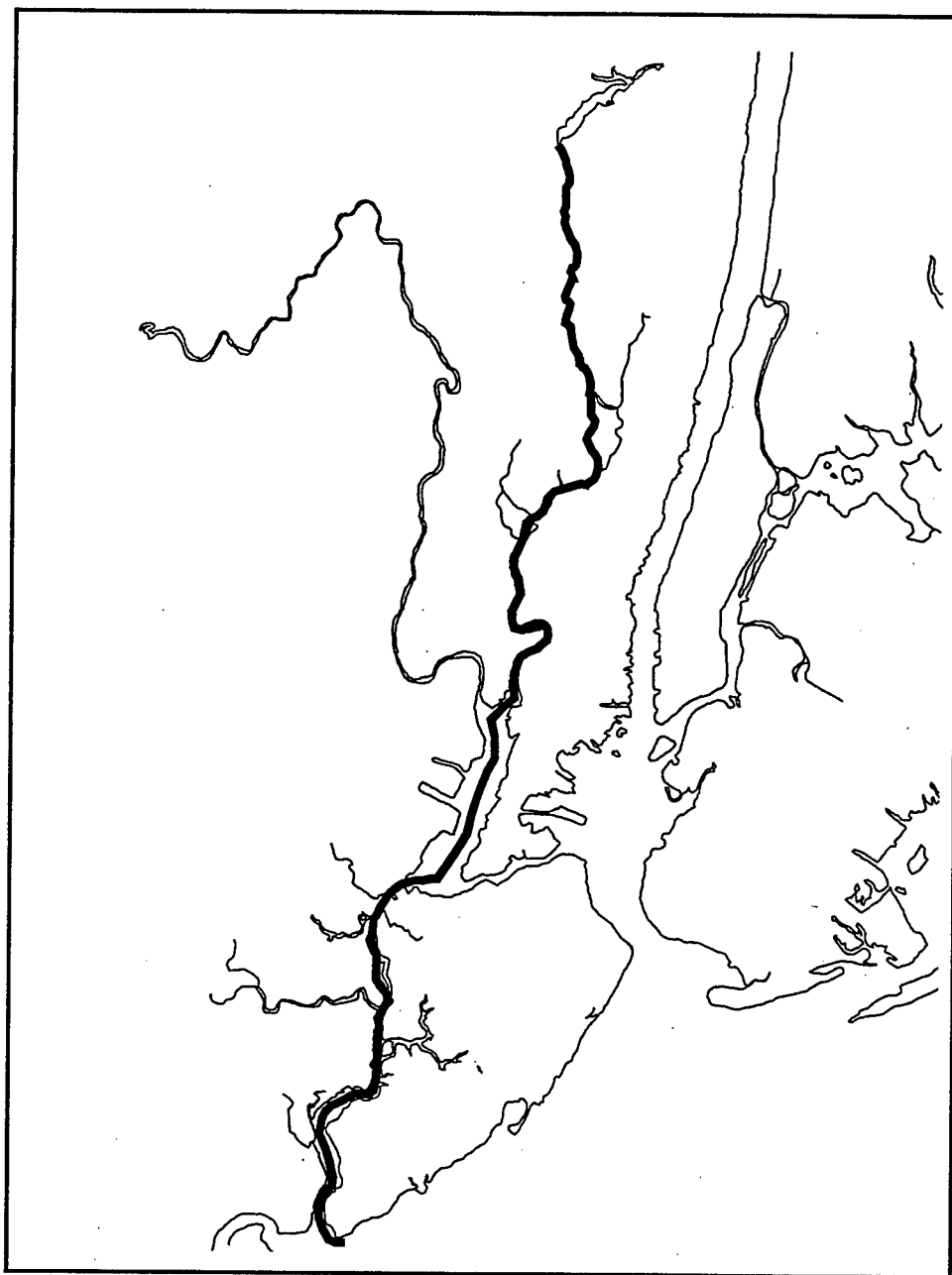
Figure 35. Axis for model-data comparisons from Hackensack fall line
through the Arthur Kill
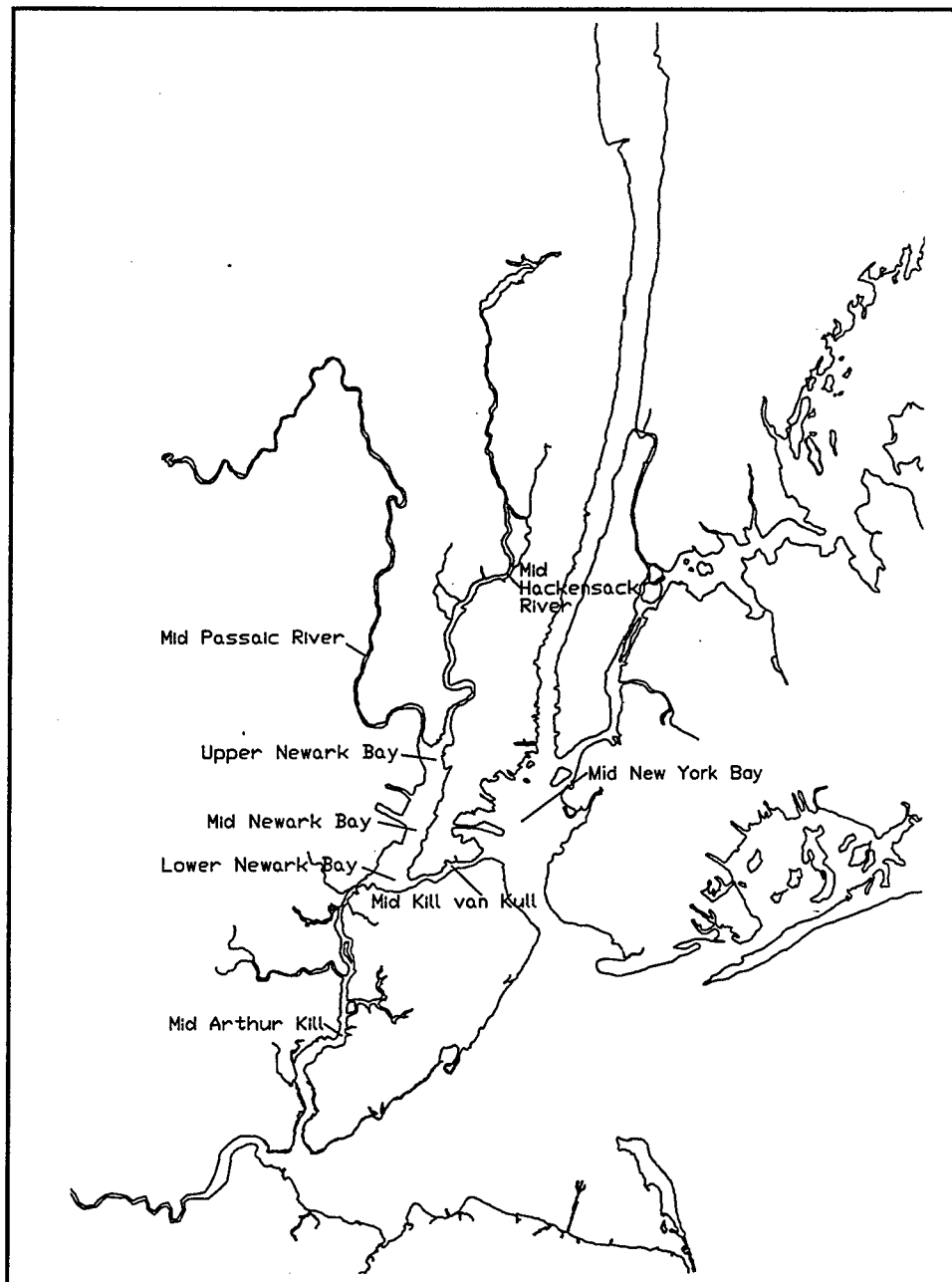
Figure 36. Location of model-data comparisons of time series and vertical profiles
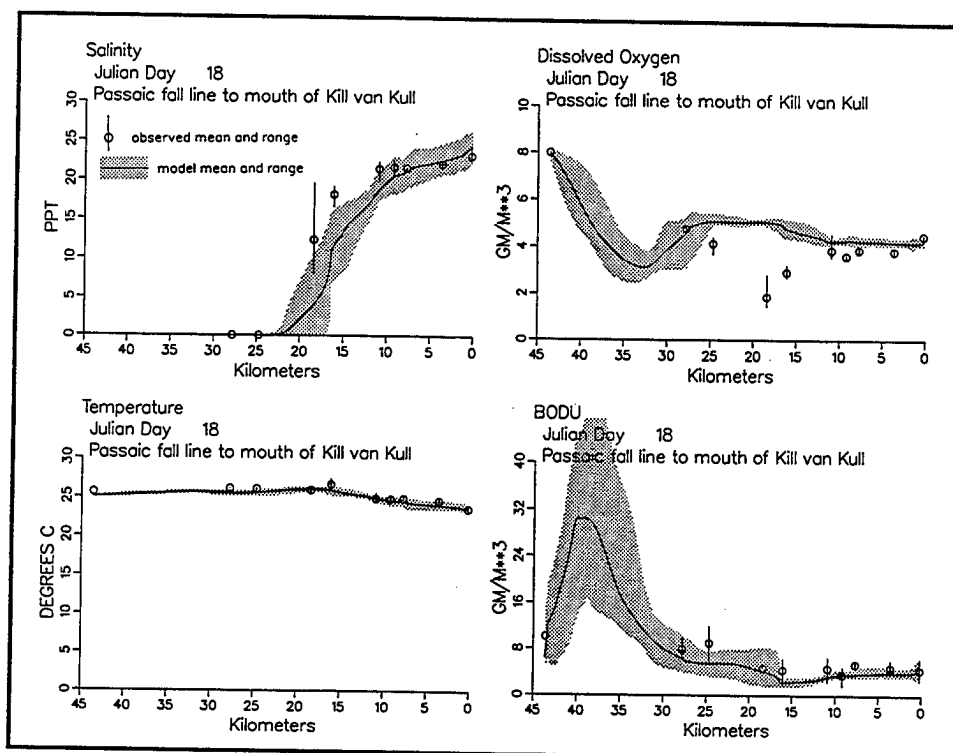
Figure 37. Computed and observed salinity, dissolved oxygen, temperature, and BOD from Passaic fall line through Kill van Kull, July 18-19, 1994
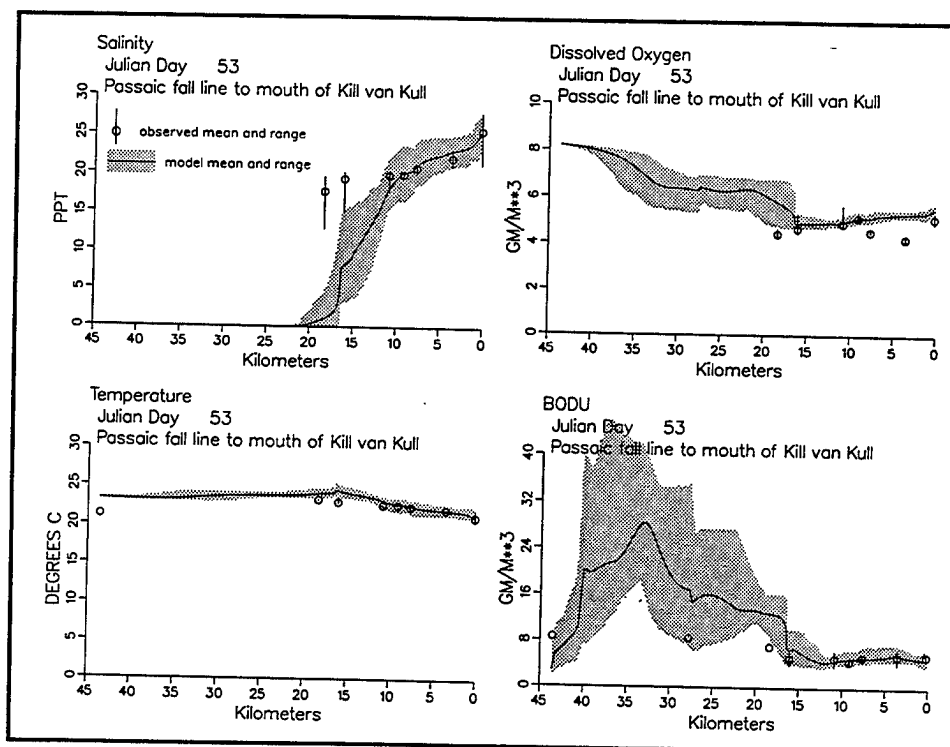
Figure 38. Computed and observed salinity, dissolved oxygen, temperature, and BOD from Passaic fall line through Kill van Kull, August 22-23, 1994
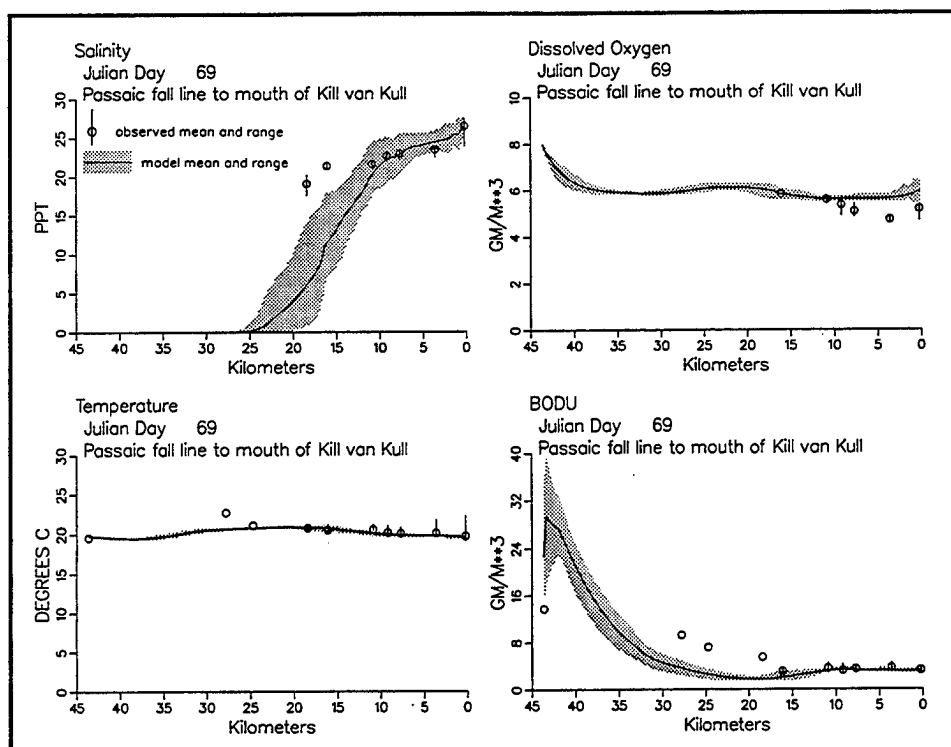
Figure 39. Computed and observed salinity, dissolved oxygen, temperature, and BOD from Passaic fall line through Kill van Kull, September 7-8, 1994

Observed conditions and model performance in the Hackensack largely mirror the Passaic (Figures 40 to 42). As with the Passaic, predicted salinity upstream of the mouth of the Hackensack is generally underestimated but cannot be improved through tuning of the water quality model. Dissolved oxygen in the Hackensack generally exceeds 4 mg/L and is reproduced well by the model except for a sag to 2 mg/L on July 18-19 (Figure 40). The sag is not apparent in the surveys of August 22-23 (Figure 41) and September 7-8 (Figure 42) and is likely due to a transient load not detailed in the point-source data. Temperature in the Hackensack exceeds adjacent waters. A temperature peak at ≈km 40 appears due to a concentration of power plants in the vicinity. Temperature is reproduced well once a heat source, to account for power plant discharge, is included in the model (Chapter 4).

Newark Bay occupies km 7 to 16 on the Passaic River axis (Figures 37-39). The same information shows in km 19 to 32 on the Hackensack axis (Figures 40 to 42). Representation of all living-resource parameters is excellent within Newark Bay, the receiving water for the tunnel discharge.

The Kill van Kull occupies km 0 to 7 on the Passaic River axis (Figures 37 to 39). Within the Kill, dissolved oxygen exceeds 4 mg/L at temperatures of 20 to 25 °C. Salinity, dissolved oxygen, and temperature are all reproduced well by the model in all surveys.

Arthur Kill stretches from km 0 to 19 on the Hackensack River axis (Figures 40 to 42). As with most of the system, dissolved oxygen in

54
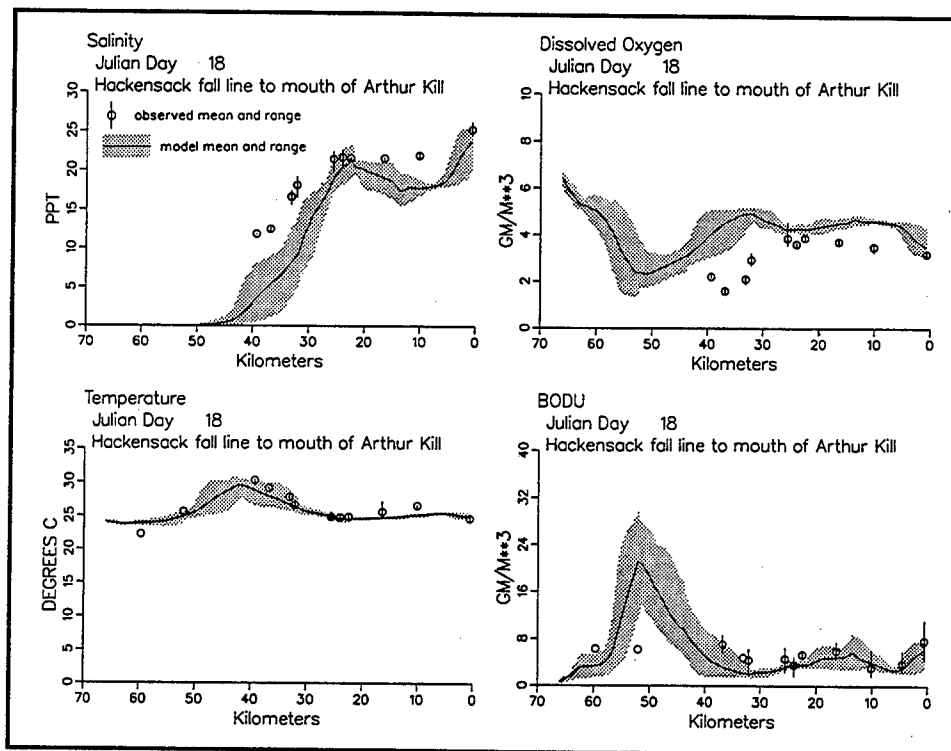
Figure 40. Computed and observed salinity, dissolved oxygen, temperature,
and BOD from Hackensack fall line through Arthur Kill, July 18-
19, 1994
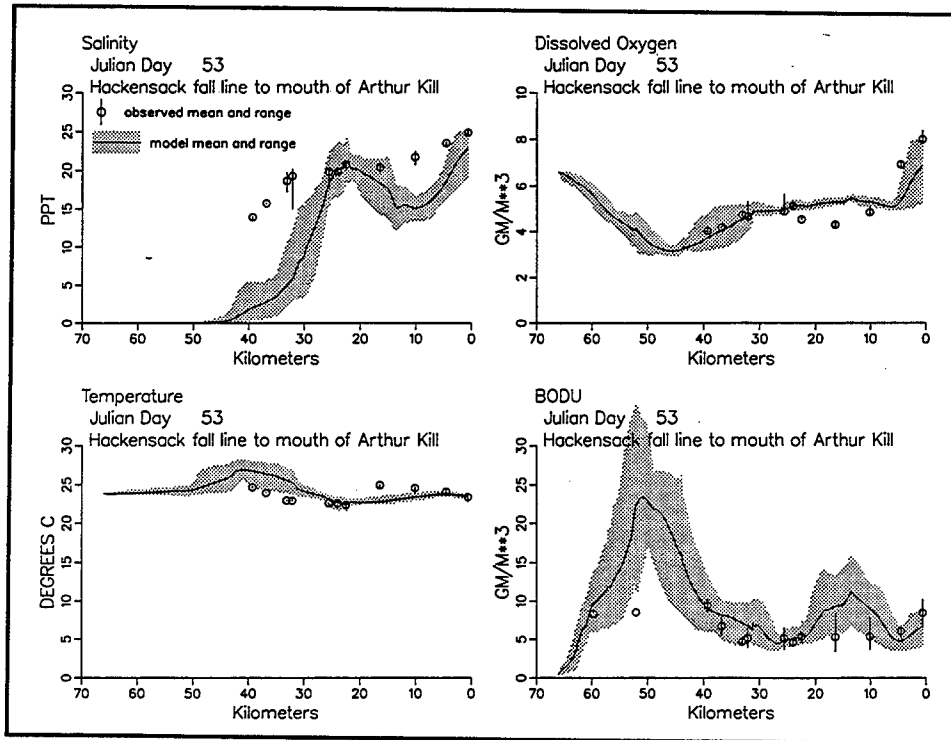
Figure 41. Computed and observed salinity, dissolved oxygen, temperature,
and BOD from Hackensack fall line through Arthur Kill, August
22-23, 1994
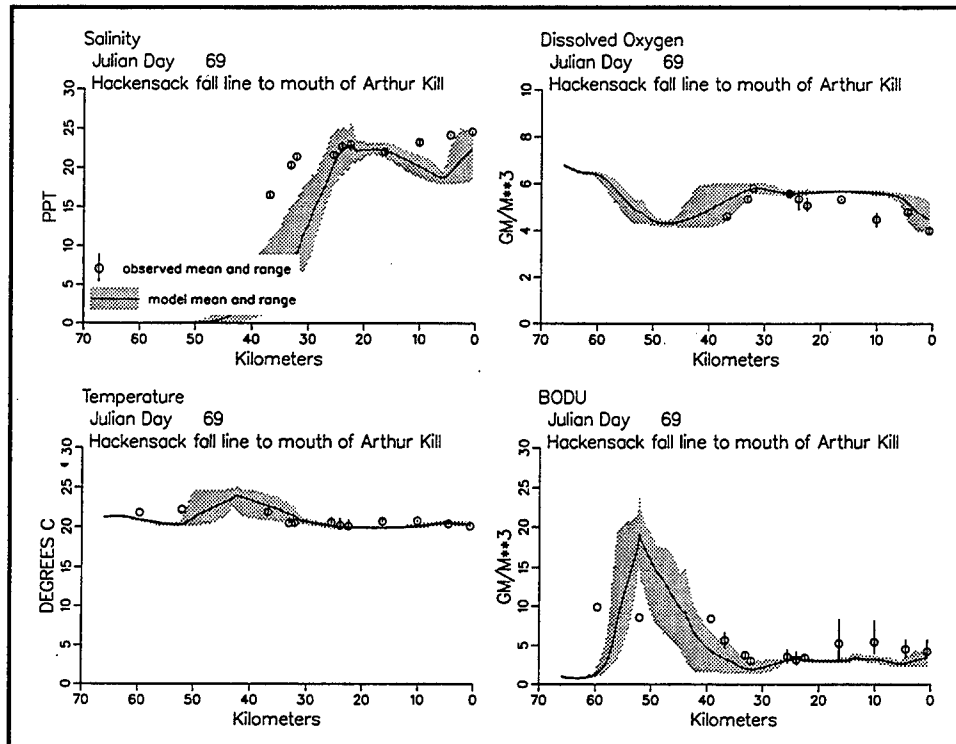
Figure 42. Computed and observed salinity, dissolved oxygen, temperature, and BOD from Hackensack fall line through Arthur Kill, September 7-8, 1994

Arthur Kill exceeds 4 mg/L at temperatures of 20 to 25 °C. Both dissolved oxygen and temperature are reproduced well by the model. The major source of fresh water to Arthur Kill is from nonpoint-source discharges. This flow is transient, depending on rainfall, and highly uncertain. Model results indicate a salinity sag in the Kill, due to dilution from inflows. The sag is only barely perceptible in the observations. The model sag indicates that nonpoint flows to the Arthur Kill are overestimated. Salinity predictions could have been improved by adjusting flows input to the hydrodynamic model. Since the Arthur Kill is well downstream of the tunnel and since adjustment would have been arbitrary, the computations were considered satisfactory as is.

Time-Series Comparisons

The time series comparisons (Figures 43 to 45) indicate that model computations of dissolved oxygen and temperature are generally excellent throughout Newark Bay. The primary feature of the data is that minimum dissolved oxygen in this portion of the bay is ≈4 mg/L at temperatures of 20 to 25 °C. Both of these key living-resource parameters are well represented in the model. Observations indicate salinity ≈20 ppt throughout the bay. Computations are in excellent agreement with observations in the mid and lower bay. Salinity is undercomputed by 5 to 10 ppt in the upper
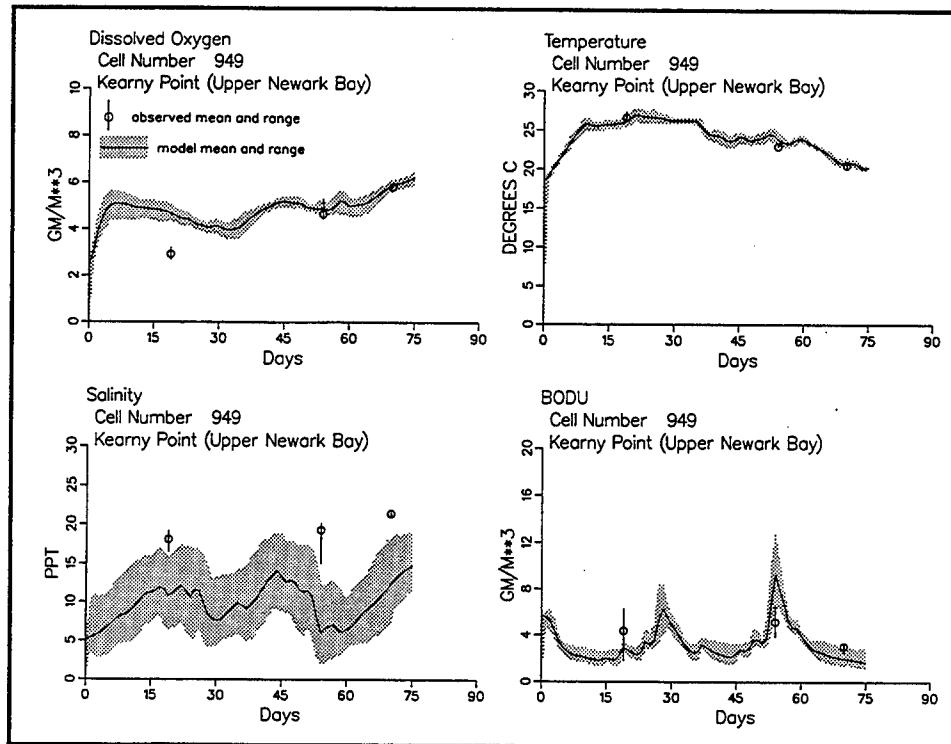
Figure 43.   Computed and observed salinity, dissolved oxygen, temperature, and BOD in upper Newark Bay, July-September 1994
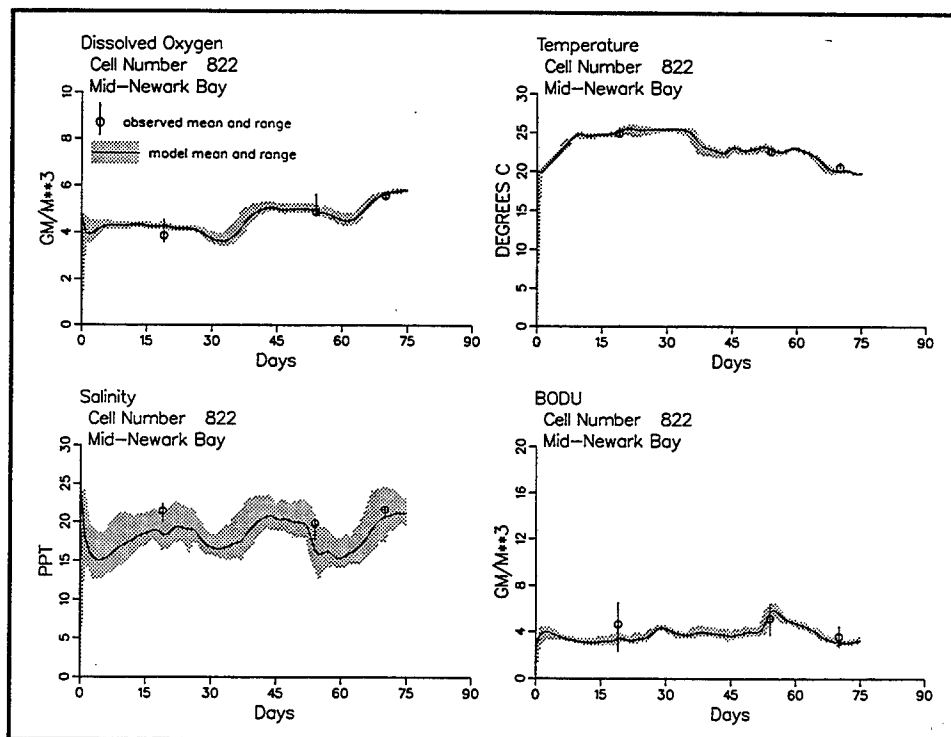
Figure 44.   Computed and observed salinity, dissolved oxygen, temperature, and BOD in mid-Newark Bay, July-September 1994
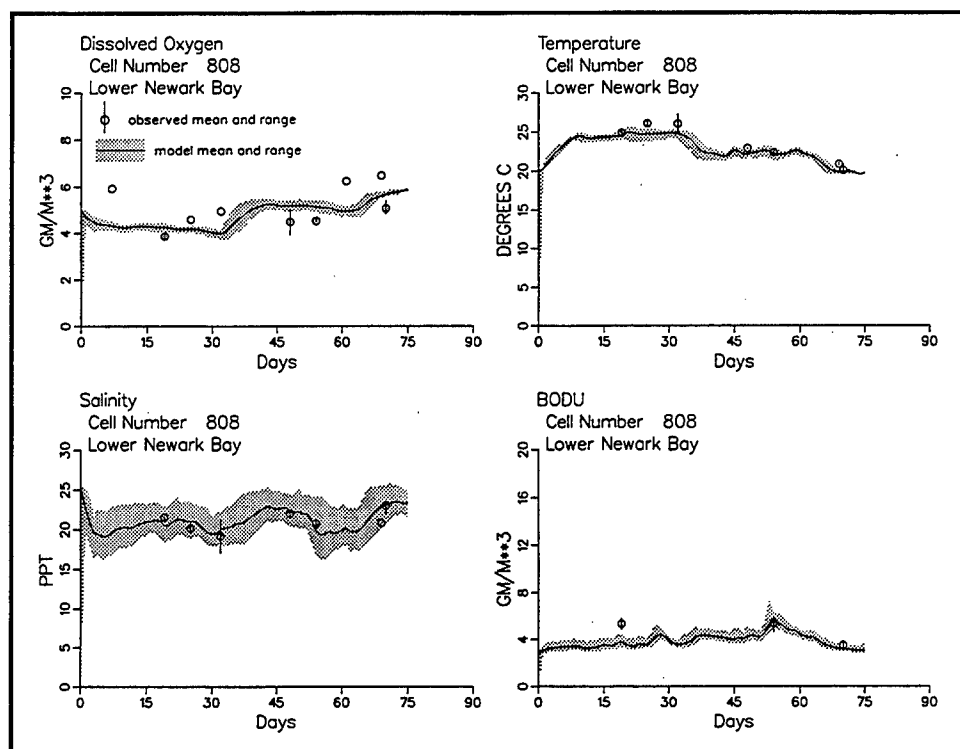
Figure 45. Computed and observed salinity, dissolved oxygen, temperature, and BOD in lower Newark Bay, July-September 1994

Bay at the juncture of the two tributaries. This behavior is consistent with salinity computations illustrated in the longitudinal comparisons.

Time-series comparisons of dissolved oxygen and temperature correspond well with the limited observations available for the central portions of the Passaic and Hackensack rivers (Figures 46-47). Observations and model indicate the central Passaic River consists of fresh water (Figure 46). Computed salinity in the central Hackensack is 8 to 10 ppt less than the observed salinity.

Time-series comparisons of computed and observed dissolved oxygen, temperature, and salinity in the mid-Kill van Kull (Figure 48) indicate nearly perfect agreement. Both model and data indicate dissolved oxygen ≈4 mg/L, temperature 20 to 25 °C, and salinity ≈20 ppt. Dissolved oxygen ≈4 mg/L is also indicated in computed and observed time series at the mid-Arthur Kill (Figure 49). Temperature in the Arthur Kill exceeded 25 °C on several occasions, greater than computed temperature and observations in the adjacent Kill van Kull. Thomas (1993) indicated the Arthur Kill receives waste heat discharges of 600 MW that were not represented in the model. The thermal discharge is likely responsible for the excess of observed overcomputed temperature. As in the Kill van Kull, observed salinity in the mid-Arthur Kill is ≈20 ppt. Observed salinity is often undercomputed by 2 to 5 ppt.

New York Bay was included in the model grid largely to ensure that downstream boundary conditions were correctly specified for computation

58
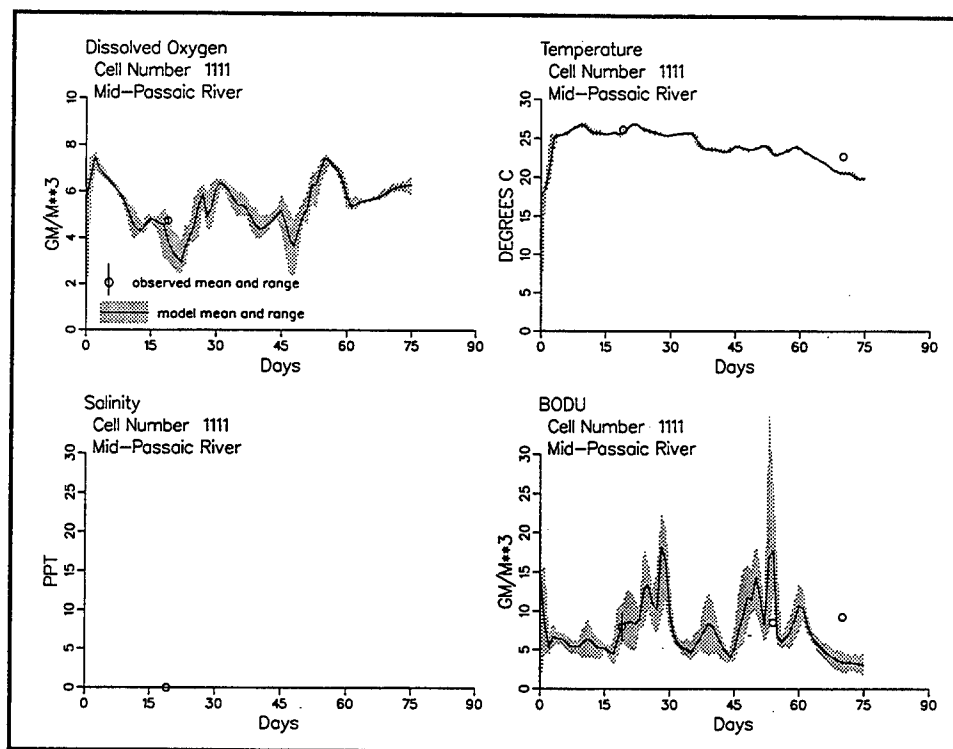
Figure 46. Computed and observed salinity, dissolved oxygen, temperature, and BOD in mid-Passaic River, July-September 1994
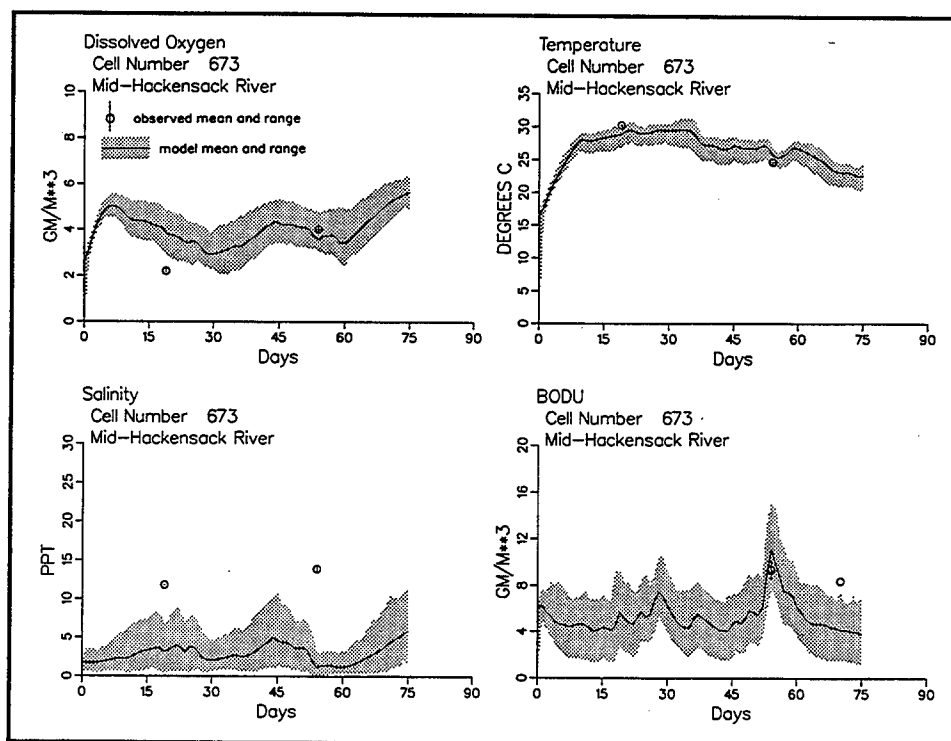
Figure 47. Computed and observed salinity, dissolved oxygen, temperature, and BOD in mid-Hackensack River, July-September 1994
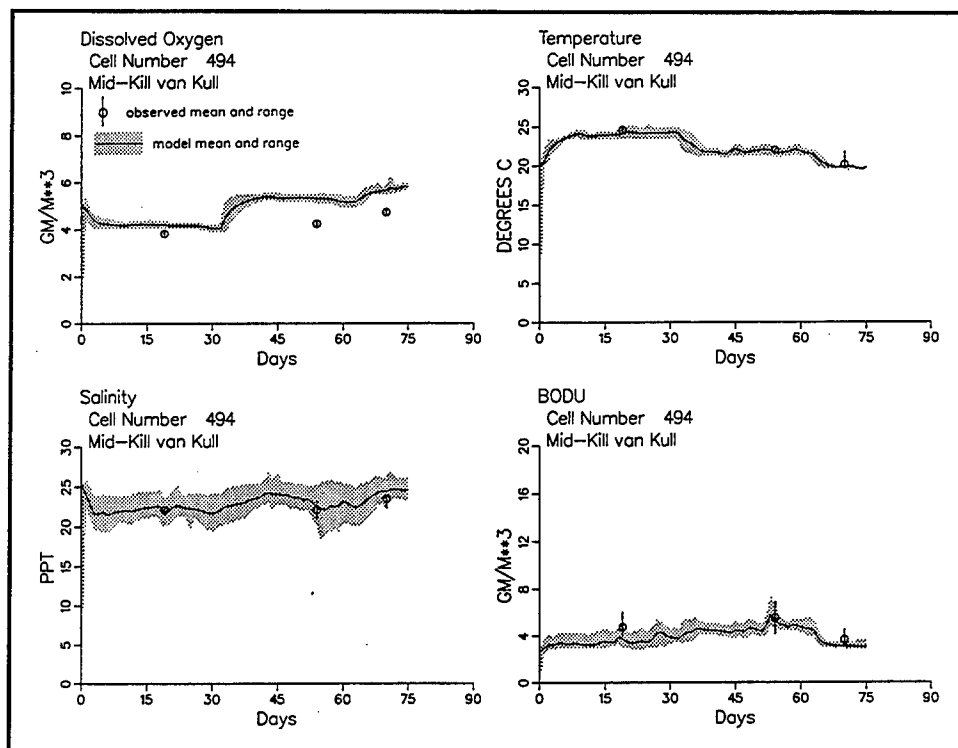
Figure 48. Computed and observed salinity, dissolved oxygen, temperature, and BOD in mid-Kill van Kull, July-September 1994
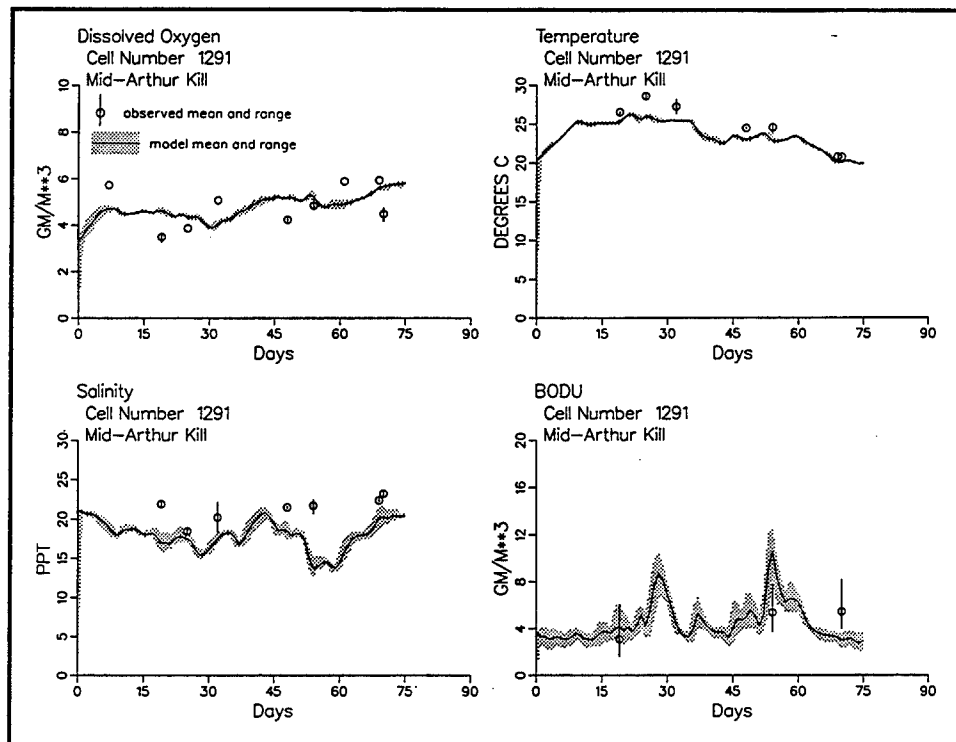
Figure 49. Computed and observed salinity, dissolved oxygen, temperature, and BOD in mid-Arthur Kill, July-September 1994

60

of tunnel impacts. Time series comparisons of computations and observa-
tions (Figure 50) indicate model performance in New York Bay is satisfac-
tory. It is worth noting that the observations collected by Stevens Institute
of Technology (Julian Days 18, 53, 69) can often be distinguished from the
NYDEP observations. Computations are usually in better agreement with
the Stevens data than the NYDEP data. The differences in the data may be
methodological, or they may represent genuine phenomenon. The Stevens
data were employed to specify boundary conditions at the upper and lower
boundaries of the bay. Conditions in the interior of the bay are strongly influ-
enced by these boundary conditions. Employment of Stevens observations at
the boundaries influences the agreement of computations with observations
collected by Stevens in the interior of the bay. The NYDEP observations
(e.g., Julian Day 32) may reflect transient phenomena not represented in the
boundary conditions based on the alternate data set.
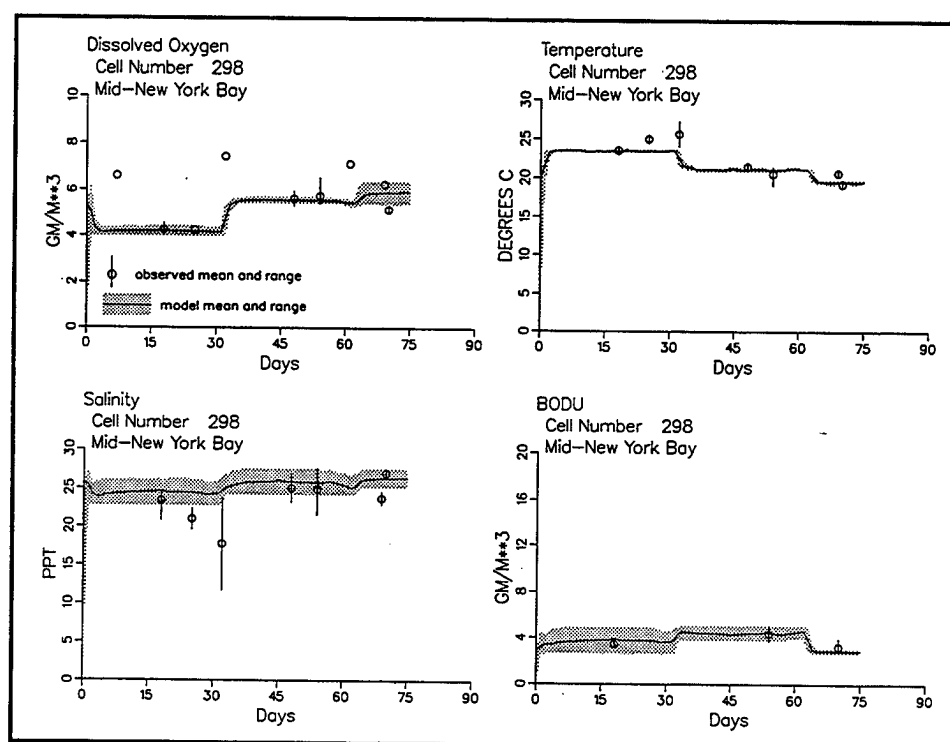
Figure 50. Computed and observed salinity, dissolved oxygen, temperature,
and BOD in mid-New York Bay, July-September 1994

Vertical Profiles

Newark Bay and adjacent waters are not strongly stratified. Water
quality problems associated with strong stratification, e.g., bottom-water
anoxia, were not indicated in the observations analyzed in the present
study. The model well represents the general absence of stratification in
the prototype system. Comparisons of computed and observed quantities
along the vertical axis (Figures 51-65) usually reflect the comparisons in
the longitudinal and time-series plots. When vertically averaged computa-
tions and observations compare well, the vertical profiles compare well
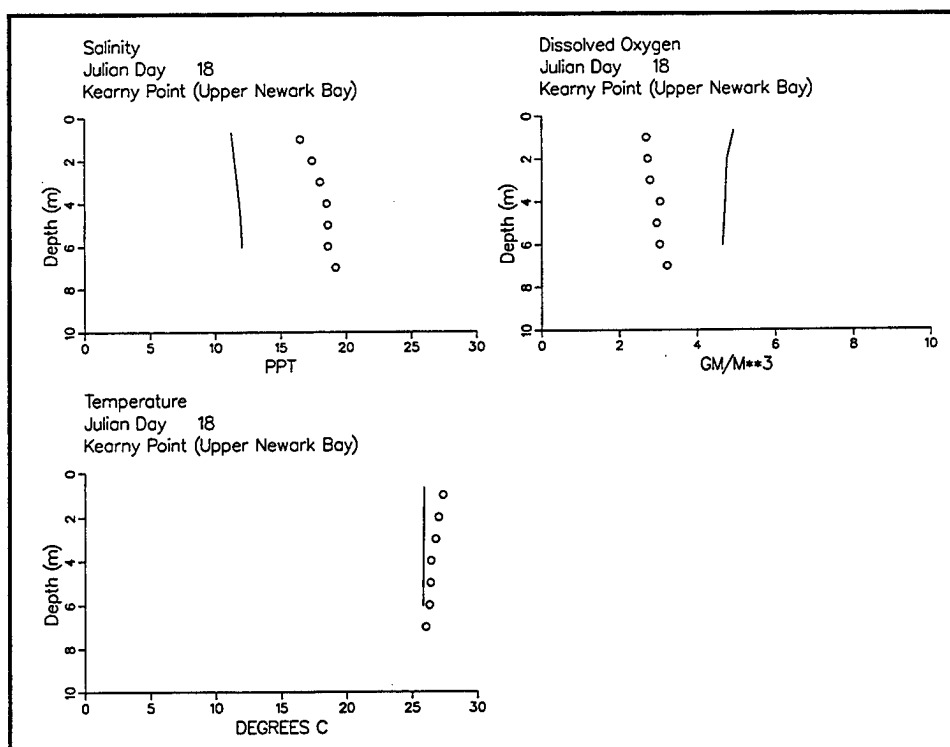
Figure 51. Computed and observed vertical profiles of salinity, dissolved oxygen, and temperature in upper Newark Bay, July 18-19, 1994
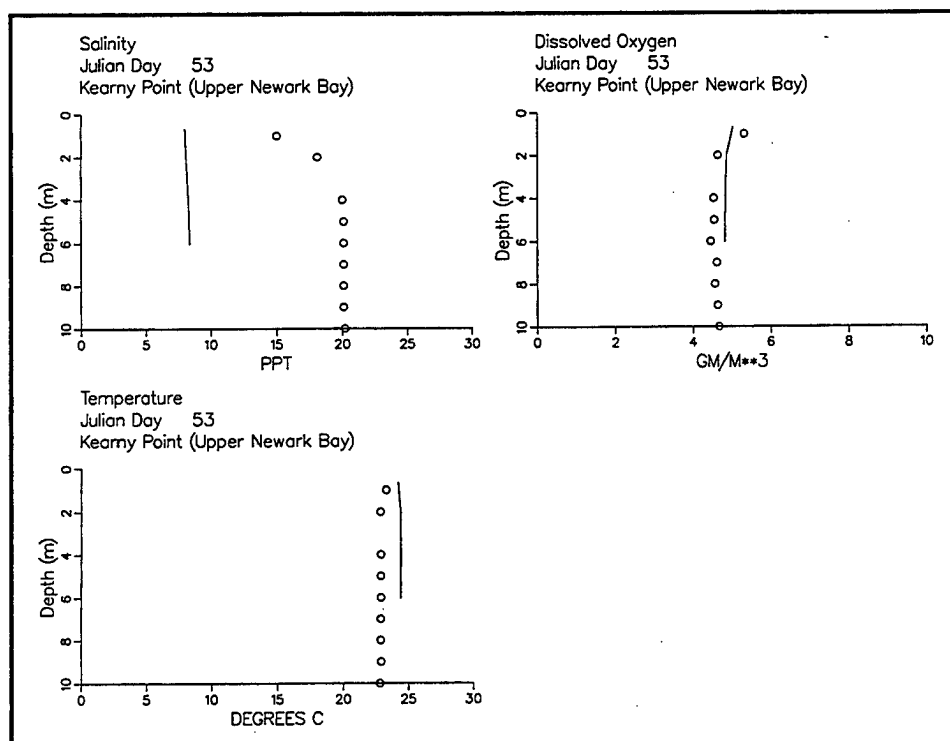
Figure 52. Computed and observed vertical profiles of salinity, dissolved oxygen, and temperature in upper Newark Bay, August 22-23, 1994
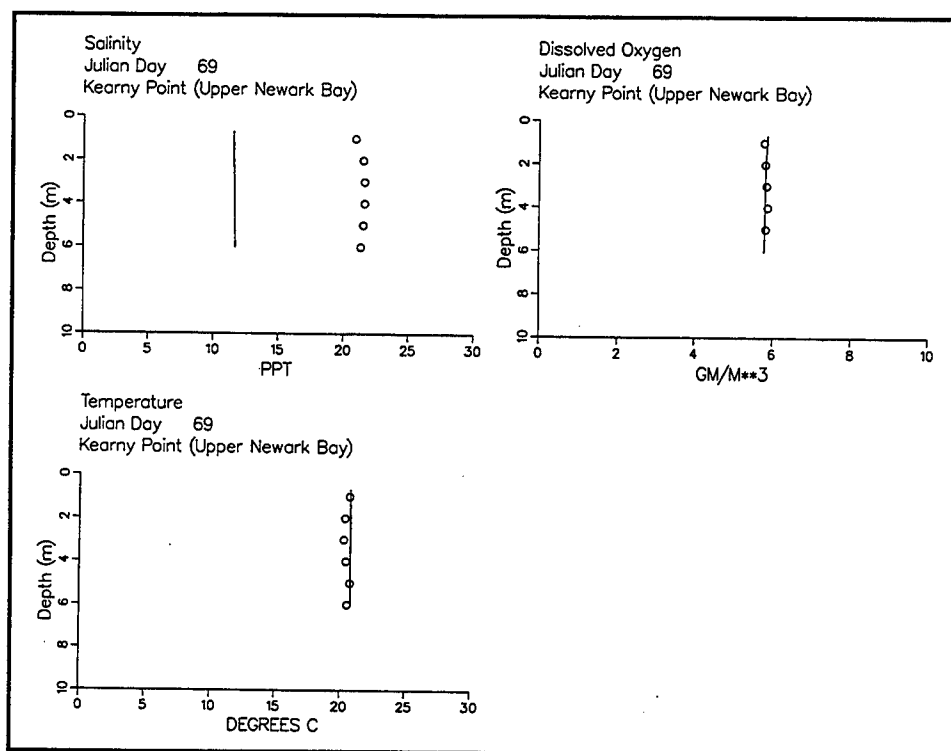
Figure 53.   Computed and observed vertical profiles of salinity, dissolved oxygen, and temperature in upper Newark Bay, September 7-8, 1994
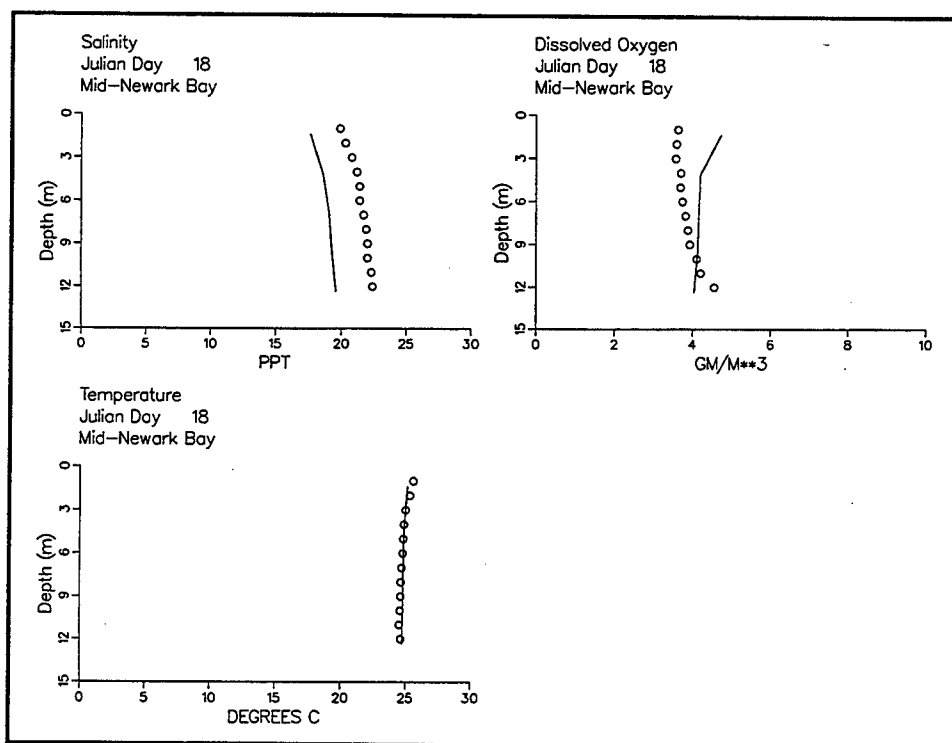
Figure 54.   Computed and observed vertical profiles of salinity, dissolved oxygen, and temperature in mid-Newark Bay, July 18-19, 1994
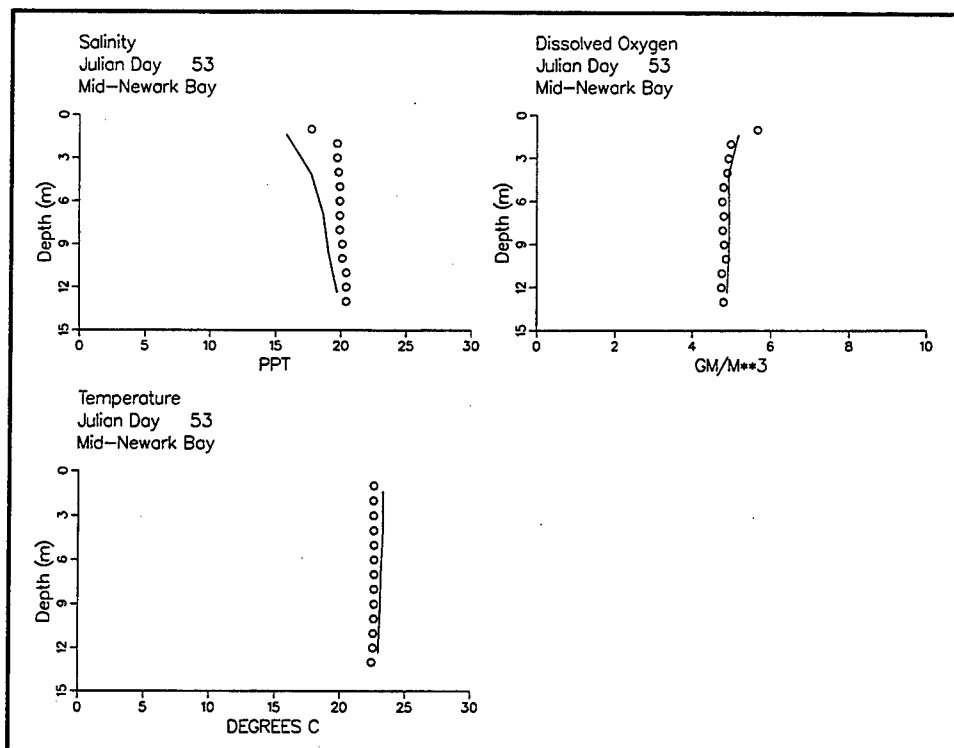
Figure 55.   Computed and observed vertical profiles of salinity, dissolved
             oxygen, and temperature in mid-Newark Bay, August 22-23,
             1994
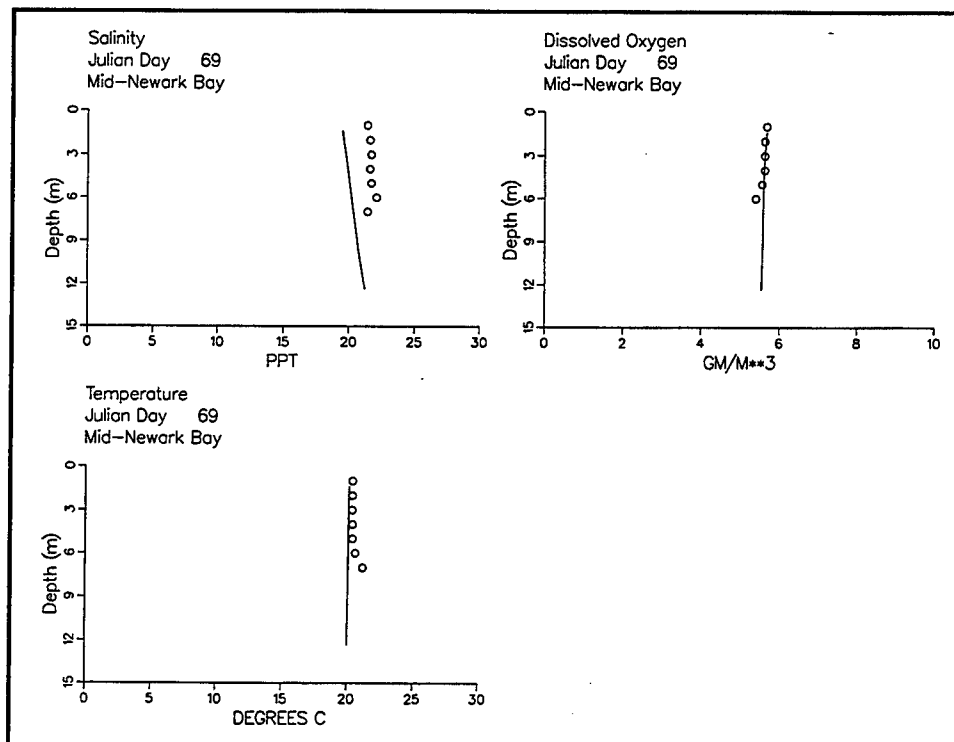
Figure 56.   Computed and observed vertical profiles of salinity, dissolved
             oxygen, and temperature in mid-Newark Bay, September 7-8,
             1994
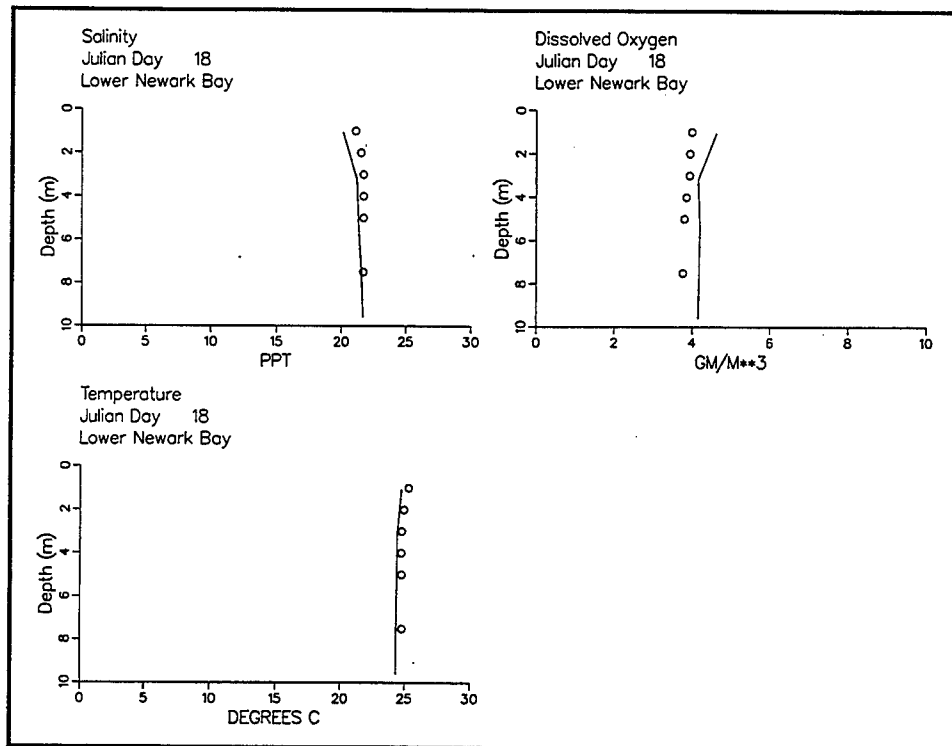
Figure 57. Computed and observed vertical profiles of salinity, dissolved oxygen, and temperature in lower Newark Bay, July 18-19, 1994
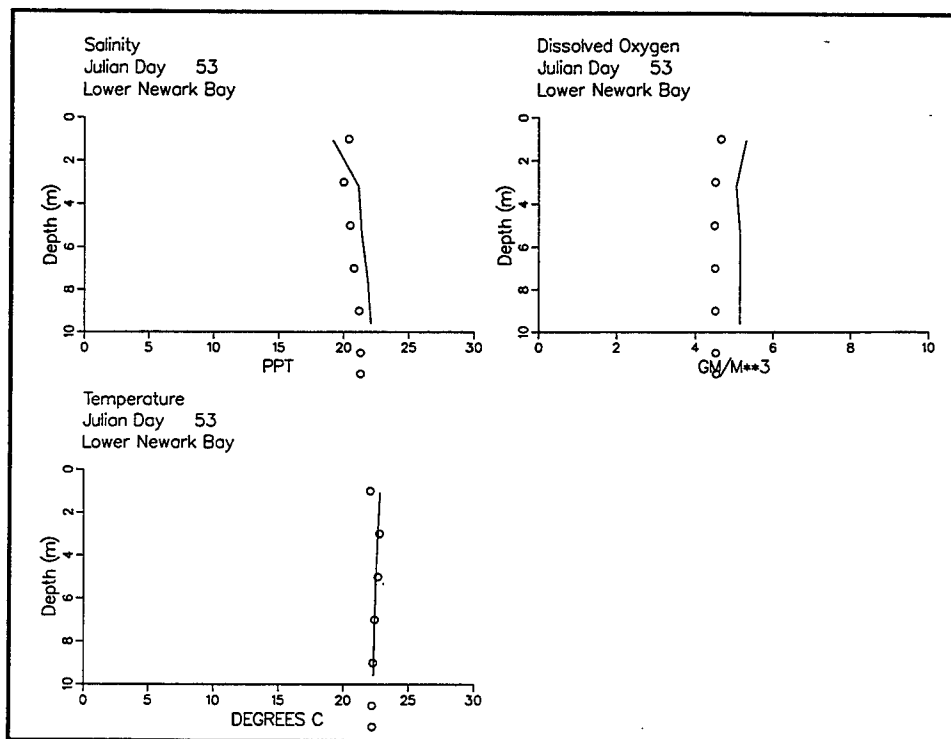
Figure 58. Computed and observed vertical profiles of salinity, dissolved oxygen, and temperature in lower Newark Bay, August 22-23, 1994
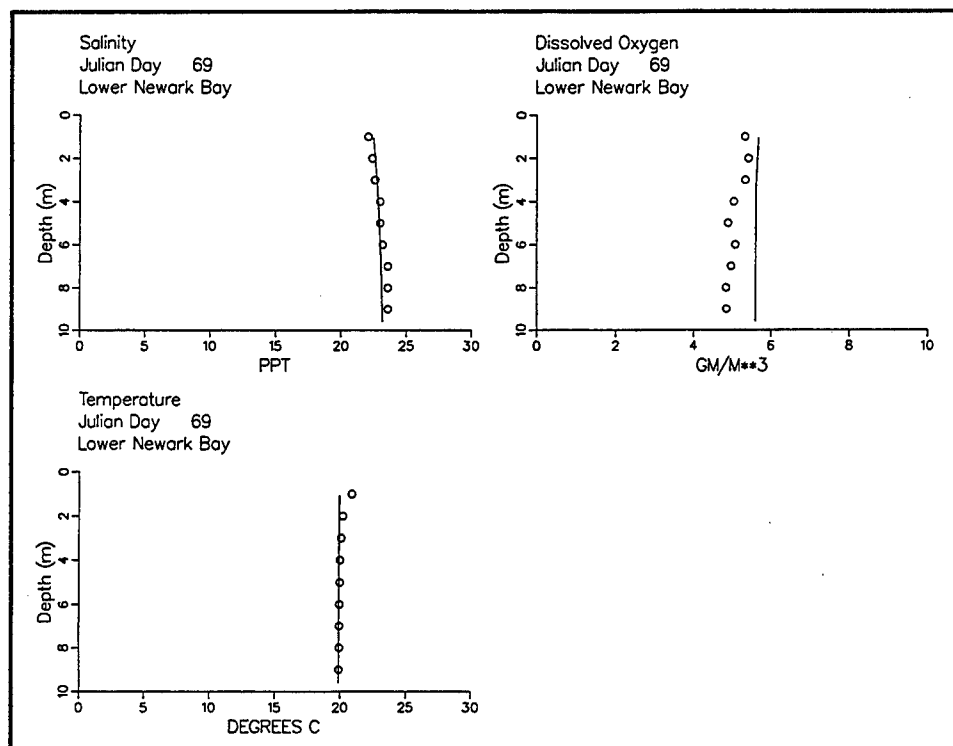
Figure 59. Computed and observed vertical profiles of salinity, dissolved oxygen, and temperature in lower Newark Bay, September 7-8, 1994
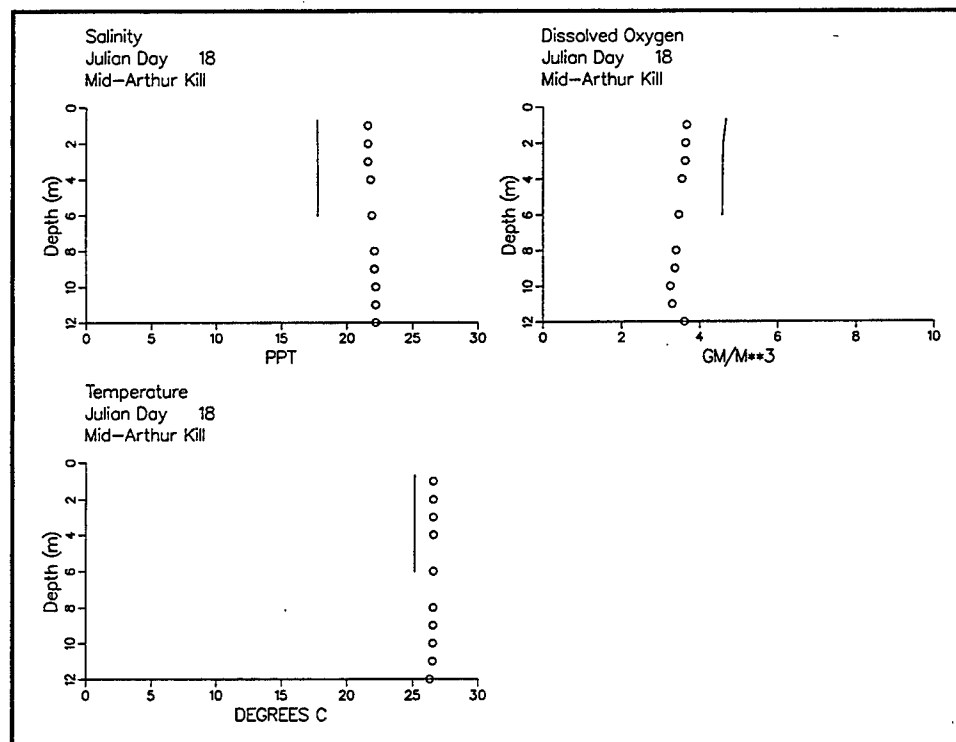
Figure 60. Computed and observed vertical profiles of salinity, dissolved oxygen, and temperature in mid-Arthur Kill, July 18-19, 1994
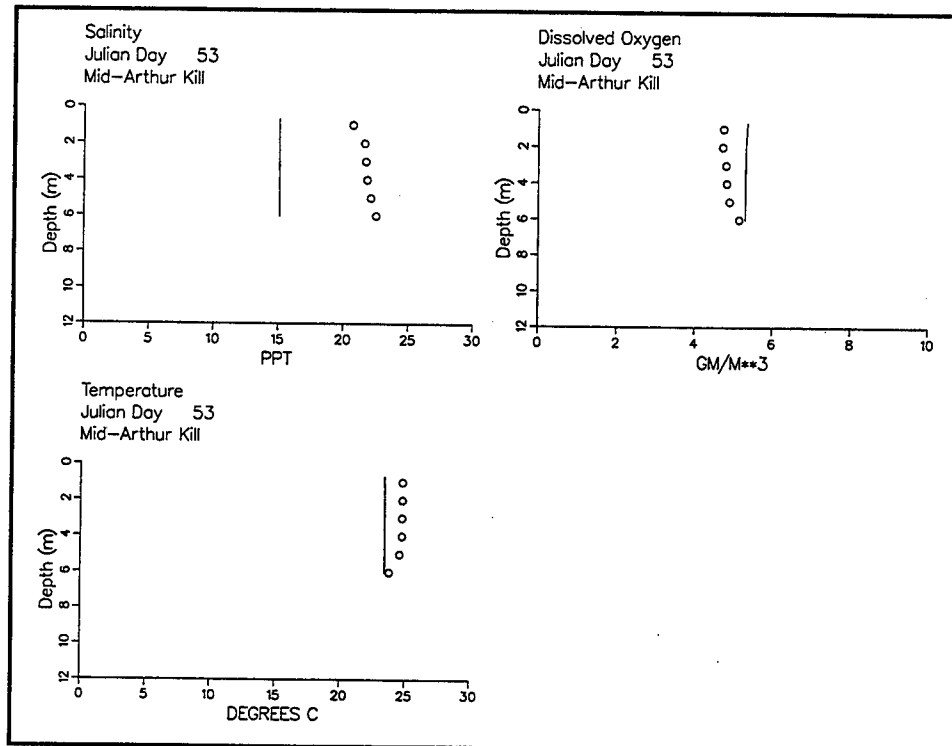
Figure 61. Computed and observed vertical profiles of salinity, dissolved oxygen, and temperature in mid-Arthur Kill, August 22-23, 1994
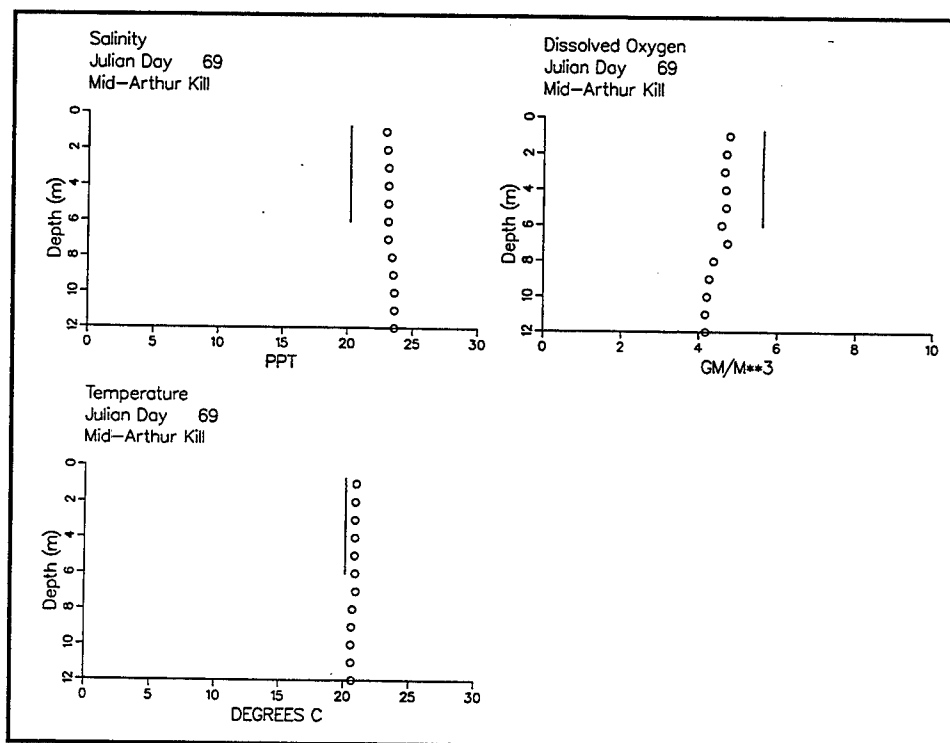
Figure 62. Computed and observed vertical profiles of salinity, dissolved oxygen, and temperature in mid-Arthur Kill, September 7-8, 1994
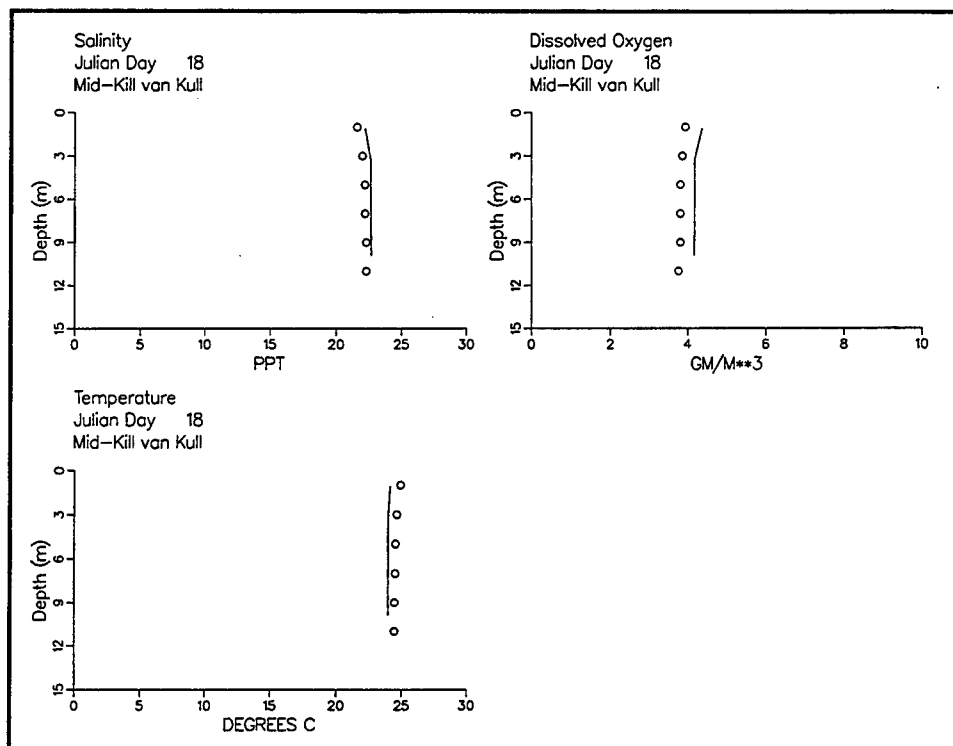
Figure 63. Computed and observed vertical profiles of salinity, dissolved oxygen, and temperature in mid-Kill van Kull, July 18-19, 1994
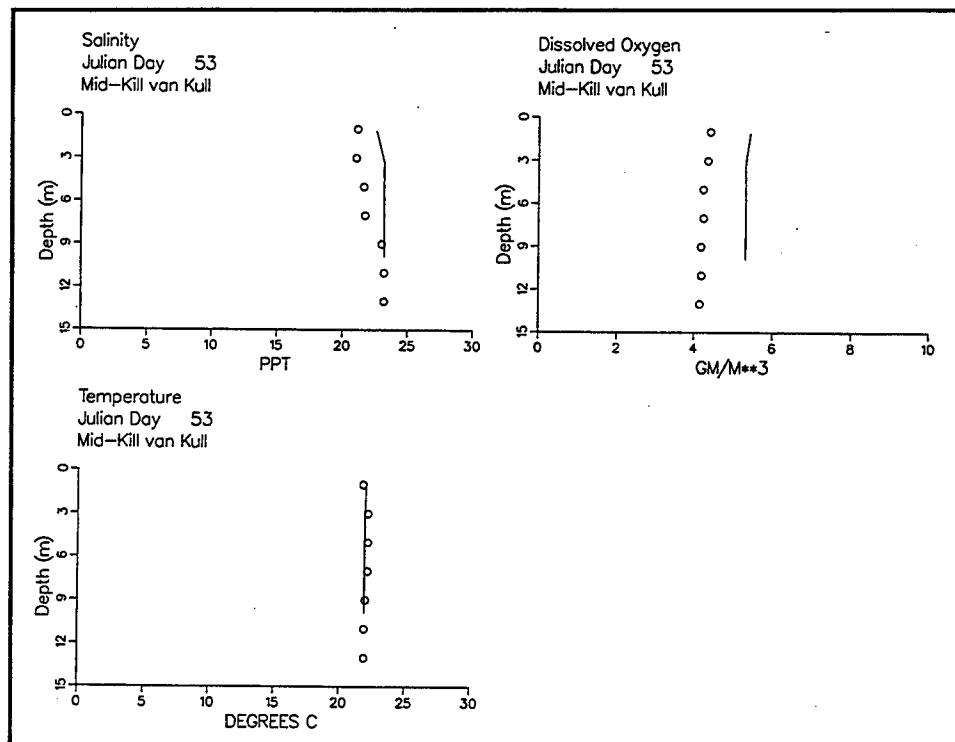
Figure 64. Computed and observed vertical profiles of salinity, dissolved oxygen, and temperature in mid-Kill van Kull, August 22-23, 1994
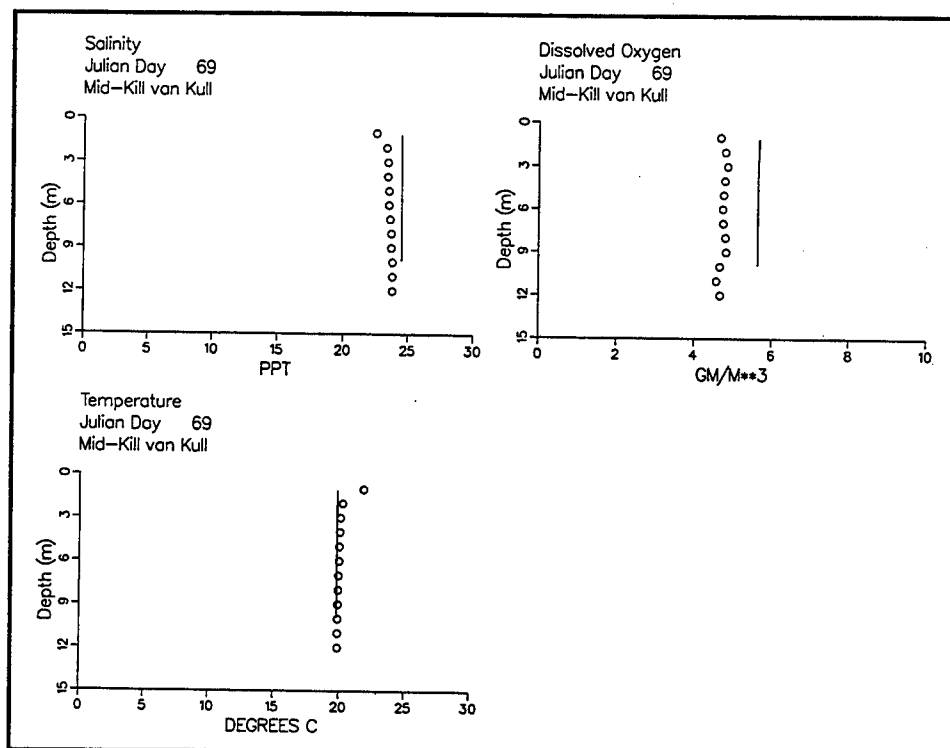
Figure 65.   Computed and observed vertical profiles of salinity, dissolved oxygen, and temperature in mid-Kill van Kull, September 7-8, 1994

also (e.g., Figures 55 and 57). Discrepancies between computed and observed vertical profiles usually represent differences uniformly distributed throughout the water column rather than differences in the surface-to-bottom distribution of parameters of interest (e.g., Figures 51 and 60).

An observation worth noting is that observed dissolved oxygen in surface waters of upper and mid-Newark Bay is occasionally less than bottom-water dissolved oxygen (Figures 51 and 54). These observations indicate water of low dissolved-oxygen concentration and low salinity exiting the Passaic River and floating on Newark Bay water of higher dissolved-oxygen concentration and salinity.

Statistical Summary of Calibration

The graphical comparisons presented in the previous sections provide useful, qualitative evaluation of model performance. Experienced viewers can examine the figures and instinctively judge the status of the calibration. Quantitative summaries and statistical evaluations of model performance can also be completed. These summaries provide numerical reinforcement to qualitative descriptives such as "excellent" or "adequate." The summaries can also provide insights that are not apparent from the graphical comparisons.

An obstacle to widespread employment of performance statistics is that no generally accepted suite of performance statistics exists. Neither are standards for acceptance or rejection of model results available. One reason for the absence of universal performance statistics is the variability of data sets and model applications. Statistical comparisons suitable for steady-state models are not necessarily applicable to time-varying models. Comparisons of model results to grab-sample data are expected to differ from comparisons to ensemble-average data. The modeler must adapt or create summary statistics that are appropriate to the observations, to the model formulation, and to the purpose of the model application.

Observations were collected for this study at the period of slack-before-ebb tidal current. Observations collected at this interval usually represent extreme conditions in the water column, e.g., maximum salinity. The time of slack water is only approximately known, however, and is based on astronomical tides. Meteorological and other factors can alter timing of slack currents in an unpredictable fashion. Moreover, practical considerations often prevent samples from being collected exactly at scheduled times. Owing to strong longitudinal gradients in some substances (e.g., BOD in Figure 41), small discrepancies between the occurrence of slack water and sample collection can lead to large discrepancies between observed and actual extreme concentrations.

The model provides computations on a 5-min basis. This interval is forced by the stability requirements of the finite-difference solution to the conservation of mass equation (1). Computations do not represent water quality on a 5-min basis because forcing functions are not resolved at such short time scales. Nevertheless, computations do represent variability in water quality on an intratidal time scale.

In view of the nature of the observations and model application, the following statistical summary was devised. Vertically averaged observations were compared with the range of vertically averaged computations corresponding to the day on which observations were collected. If the mean observation fell within the range of computations, the computation was judged "successful." This comparison was equivalent to judging if the observation was within the range of computations between high and low slack water. If the observation exceeded the maximum model computation, the computation was judged "low." If the observation was less than the minimum model computation, the computation was judged "high." Summaries were prepared by region for salinity (Table 12), dissolved oxygen (Table 13), temperature (Table 14), and BOD (Table 15) in each Stevens survey.

An overall summary (Table 16) indicates the model was successful in representing 65 to 82 percent of the observations. At no time did the model overestimate salinity. Roughly one-third of the salinity computations were low. This trend in computations versus observations is partially due to the nature of the observations. They were intended to be collected at the time of maximum salinity. More careful inspection of salinity results (Table 12) indicates the greater fraction of low computations were in the Passaic River, the Hackensack River, and the Arthur Kill. These are narrow channels that receive substantial nonpoint-source flows. Salinity computations were more successful in Newark Bay and in New York Bay.

Table 12
Summary of Salinity Computations

		July	August	September	Percent
Passaic River	High	0	0	0	0
	Successful	2	0	0	40
	Low	1	1	1	60
Hackensack River	High	0	0	0	0
	Successful	0	0	0	0
	Low	3	3	2	100
Newark Bay	High	0	0	0	0
	Successful	3	3	3	75
	Low	1	1	1	25
Arthur Kill	High	0	0	0	0
	Successful	2	2	1	45
	Low	2	2	2	55
Kill van Kull	High	0	0	0	0
	Successful	2	2	2	100
	Low	0	0	0	0
New York Bay	High	0	0	0	0
	Successful	5	5	5	100
	Low	0	0	0	0
Percent	High	0	0	0	0
	Successful	67	63	65	65
	Low	33	37	35	35

Table 13
Summary of Dissolved Oxygen Computations

		July	August	September	Percent
Passaic River	High	2	1	0	60
	Successful	2	0	0	40
	Low	0	0	0	0
Hackensack River	High	3	0	0	38
	Successful	0	3	2	63
	Low	0	0	0	0
Newark Bay	High	2	1	1	33
	Successful	2	3	3	67
	Low	0	0	0	0
Arthur Kill	High	2	1	2	45
	Successful	1	2	2	45
	Low	0	1	0	9
Kill van Kull	High	0	1	1	33
	Successful	2	1	1	67
	Low	0	0	0	0
New York Bay	High	0	1	0	7
	Successful	5	4	5	93
	Low	0	0	0	0
Percent	High	43	26	24	32
	Successful	57	68	76	67
	Low	0	5	0	2

Table 14
Summary of Temperature Computations

		July	August	September	Percent
Passaic River	High	0	1	0	10
	Successful	4	1	83	80
	Low	0	0	1	10
Hackensack River	High	1	1	0	17
	Successful	4	2	2	67
	Low	0	0	2	17
Newark Bay	High	0	1	0	8
	Successful	4	3	4	92
	Low	0	0	0	0
Arthur Kill	High	0	0	0	0
	Successful	1	2	3	55
	Low	2	2	1	45
Kill van Kull	High	0	0	0	0
	Successful	2	2	2	100
	Low	0	0	0	0
New York Bay	High	0	0	0	0
	Successful	5	5	5	100
	Low	0	0	0	0
Percent	High	4	15	0	6
	Successful	87	75	83	82
	Low	9	10	17	12

Table 15
Summary of BOD Computations

		July	August	September	Percent
Passaic River	High	0	1	1	18
	Successful	3	2	0	45
	Low	1	0	3	36
Hackensack River	High	1	1	1	21
	Successful	2	4	2	57
	Low	1	0	2	21
Newark Bay	High	0	0	0	0
	Successful	1	4	4	75
	Low	3	0	0	25
Arthur Kill	High	0	0	0	0
	Successful	4	4	1	75
	Low	0	0	3	25
Kill van Kull	High	0	0	0	0
	Successful	2	2	2	100
	Low	0	0	0	0
New York Bay	High	0	0	0	0
	Successful	3	5	4	80
	Low	2	0	1	20
Percent	High	4	9	8	7
	Successful	65	91	54	70
	Low	30	0	38	23

Table 16
Summary of All Computations

	Salinity	Dissolved Oxygen	Temperature	BOD
Percent High	0	32	6	7
Percent Successful	65	67	82	70
Percent Low	35	2	12	23

These are large bodies with lesser nonpoint-source flows. The summary indicates the nonpoint-source flows computed with runoff coefficients (Equation 13) are too high. Exact computation of salinity requires adjustment of the coefficients or, preferably, employment of a more sophisticated watershed model.

Dissolved oxygen computations that are not successful are almost exclusively high (Table 16). This trend reflects statistical summaries (Cerco and Cole 1994) that indicate mathematical models tend to overpredict rather than underpredict dissolved oxygen. Improved dissolved-oxygen statistics require improved information on loading. Observations in the Passaic and Hackensack, especially, indicate the presence of transients and sags that cannot be reproduced with monthly average or permit loads.

Temperature computations are the most successful of all (Table 16). Moreover, no bias towards overprediction or underprediction is evident. The successful predictions indicate the accuracy with which the major temperature source/sink, surface heat transfer, can be computed. Additional accuracy could be gained by supplying to the model detailed information on waste heat discharge to the system.

BOD computations are also largely successful (Table 16). A small bias towards underprediction is evident. Potential improvements require more detailed information on point-source loading and a more sophisticated model of nonpoint-source loading.

7   Tunnel Scenarios

Once the calibration was complete, the model was available for examination of tunnel impacts. A key question centered on maintenance of the tunnel between storm events. Due to the inverted siphon, stormwater may remain in the below-sea-level portion of the tunnel. The remaining water would be subject to degradation in the lengthy periods (circa 2 years) between discharge events. As an alternative, the tunnel could be pumped dry following storm events. The two options, water storage between events versus water removal, were referred to as "wet" and "dry" tunnel conditions. Scenarios were designed to examine the impact of discharges from a wet and dry tunnel versus "base" conditions with no tunnel in operation.

Scenario Design

The impact of the tunnel could be examined under an infinite range of conditions. The design process consisted of specification of scenario conditions that would examine the full range of responses to tunnel operation while limiting the number of model runs to a practical quantity.

A matrix of scenarios (Table 17) was constructed to examine the impact of tunnel discharge on receiving waters. Base scenarios specified future conditions without the tunnel. Future conditions resembled existing conditions except for a 15-cm (0.5-ft) increase in sea level. Wet-tunnel scenarios examined future conditions with the tunnel in operation and with floodwater remaining in the tunnel between flood events. Dry-tunnel scenarios examined future conditions with the tunnel in operation and with the tunnel pumped dry between flood events. Duration of each scenario

Table 17
Matrix of Scenario Runs

	Base		Wet Tunnel		Dry Tunnel	
2-Year Storm	July	February	July	February	July	February
25-Year Storm	July	February	July	February	July	February
100-Year Storm	July	February	July	February	July	February

was 27 days. The first 13 days were a "spin-up" period to allow predicted conditions to equilibrate with specified loads, temperature, and boundary conditions. The spin-up period was followed by a 14-day storm simulation.

Three flood conditions were considered: 2-year storm; 25-year storm; and 100-year storm. The 2-year storm is the minimum storm that will cause operation of the diversion tunnel. Storm flows in the Passaic and Hackensack basins for all scenarios were supplied by the U.S. Army Engineer District, New York, the project sponsor. These were generated through use of the UNET hydrological model (U.S. Army Corps of Engineers Hydrologic Engineering Center 1995). Remaining fall-line flows for the 2-year storm were set at long-term average values, as determined from USGS records. Fall-line flows for the 25-year and 100-year storms were based on observations recorded during a 25-year storm that occurred in April 1984. The New York District also supplied the daily rainfall values (Table 18) used to generate the storm flows in the Passaic and Hackensack basins. These were employed in relationships derived from the Section 208 study (Hazen and Sawyer 1978) to generate nonpoint-source flows in the remaining basins.

Table 18
Scenario Rainfall

Day	2-Year Storm, cm	25-Year Storm, cm	100-Year Storm, cm
1	0.91	1.57	1.96
2	1.73	3.00	3.73
3	8.56	14.86	18.54
4	1.17	2.03	2.54
5	0.76	1.30	1.63
6	0.66	1.12	1.40
7	0.58	0.99	1.24
8	0.51	0.89	1.12
9	0.48	0.81	1.02
10	0.43	0.76	0.94
11	0.41	0.71	0.86
12	0.38	0.66	0.81
13	0.36	0.61	0.76
14	0.33	0.58	0.74
15	0.30	0.56	0.69
Total	17.58	30.45	37.97

Scenarios were completed for February and July conditions. These are the months in which the coldest (1 °C) and warmest (28 °C) temperatures are observed in Newark Bay receiving waters. The conditions were selected to provide worst-case conditions for examination of temperature shock on living resources of water stored in the tunnel. Tunnel water temperature, 12.8 °C, was specified by the New York District.

Fall-line BOD loads were computed from scenario fall-line flows and present BOD concentrations. Existing point-source loads were employed. Nonpoint-source BOD loads were computed from scenario rainfall via Equation 14. Dissolved oxygen and salinity boundary conditions for the July scenarios were adapted from conditions observed in July 1994. Dissolved oxygen and salinity boundary conditions for the February scenarios were adapted from STORET and NMFS databases.

At initiation of each scenario, temperature of receiving water was specified as the equilibrium value. Temperature boundary conditions were also set at equilibrium values. These conditions were specified to isolate the impact of the tunnel. Receiving water initially at equilibrium with the atmosphere and boundary waters should remain at equilibrium except for tunnel water discharged at a different temperature. The equilibrium temperatures (Table 19) and surface heat exchange coefficients (KT in Equation 2) were specified based on monthly mean meteorological conditions at Newark Airport.

Table 19
Scenario Equilibrium Temperature and Heat Exchange Coefficients

Month	TE, °C	KT, watt m^{-2} °C^{-1}
February	2.2	23.7
July	26.3	41.7

Tunnel Water Quality

One concern regarding the impact of the tunnel diversion is the water that may be stored in the tunnel between flood events. The expected interval between events is 2 years or more. During this period the water may undergo significant deterioration. If the oxygen demand of biodegradable material greatly exceeds the available dissolved oxygen, anoxic degradation may occur. The anoxic degradation results in the production of reduced iron, sulfide, and methane. These materials may produce structural damage and will severely impact the dissolved-oxygen concentration of the receiving waters when the tunnel eventually discharges.

Initial indications of the effect of storage on tunnel water were obtained from examination of data retrieved from the STORET database. Observations from the Passaic River at Little Falls, downstream of the proposed

tunnel inlet, were summarized. At flows sufficient to operate the diversion tunnel (57 m^3 sec^{-1}), dissolved oxygen concentration (Figure 66) equaled or exceeded ultimate biochemical oxygen demand (Figure 67). Mean DO for flow >57 m^3 sec^{-1} was 10.1 mg/L; mean BODu was 7.1 mg/L. The data indicated the supply of biodegradable material in floodwater, isolated in the tunnel, will be consumed before dissolved oxygen is depleted. Consequently, anaerobic degradation should not occur, and production of reduced end products such as sulfide or methane is not expected.

Two incubation experiments were conducted to investigate the hypothesis formed from examination of the STORET data. In each experiment, storm water was collected in the vicinity of the tunnel inlet and incubated for 6 months. Storm water was incubated in three 25-L reactors, sealed against introduction of atmospheric oxygen. One reactor was set up to measure the volume of gas production. The other two were set up to allow samples of water to be withdrawn. Samples were withdrawn monthly for 5 months and analyzed for the following:

    a. Dissolved oxygen.

    b. Immediate oxygen demand.

    c. BOD.

    d. COD.

    e. Total sulfide.

    f. Reduced iron.

    g. Reduced manganese.

At the end of 6 months, a final measure of gas evolution was conducted.

Samples for the first incubation were collected during a storm event July 29, 1994. Flow during this event peaked at 28 m^3 sec^{-1}, roughly half the flow that will cause the diversion to operate. No substantial difference existed between dissolved oxygen and BOD during sample collection and conditions expected at higher flows, however (Figures 66 and 67). Samples for the second incubation were collected during a storm event November 15, 1995. Flow on this date was 133 m^3 sec^{-1}, well above the minimum flow required for the diversion to operate.

Monthly samples from the first incubation were analyzed for 5-day and 60-day (ultimate) BOD. Monthly samples from the second incubation were analyzed for 5-day BOD only. Results were scaled up to ultimate BOD using the median BOD60:BOD5 ratio, 1.6, from the first incubation.

Dissolved oxygen concentrations (8 to 9 mg/L) and BODu concentrations (6 to 9 mg/L) at initiation of the incubations were consistent with the values expected from analysis of the STORET data. Dissolved oxygen diminished rapidly to roughly 2 mg/L over a period of 60 days then diminished slowly through the remainder of the incubations (Figure 68). In neither incubation did completely anoxic conditions occur. No gas evolution occurred nor were detectable quantities of immediate oxygen demand, COD, sulfide, iron, or manganese observed.
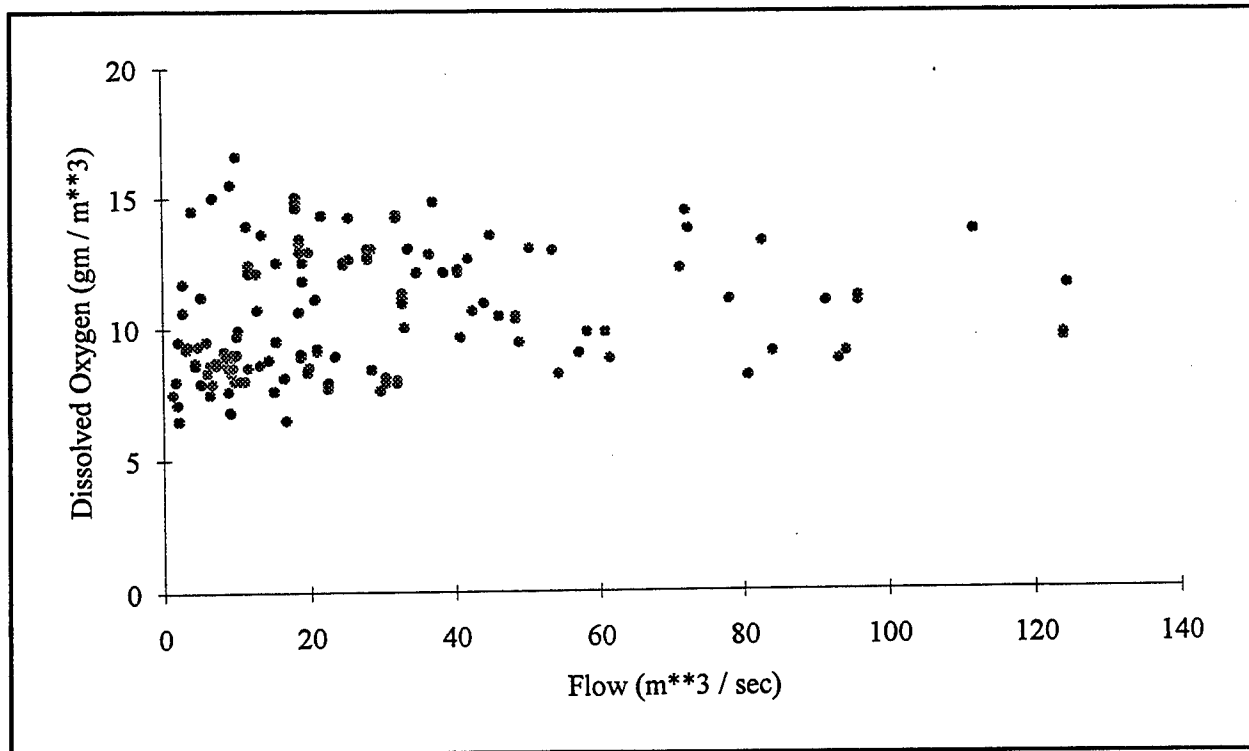
Figure 66.   Dissolved oxygen and flow at Little Falls
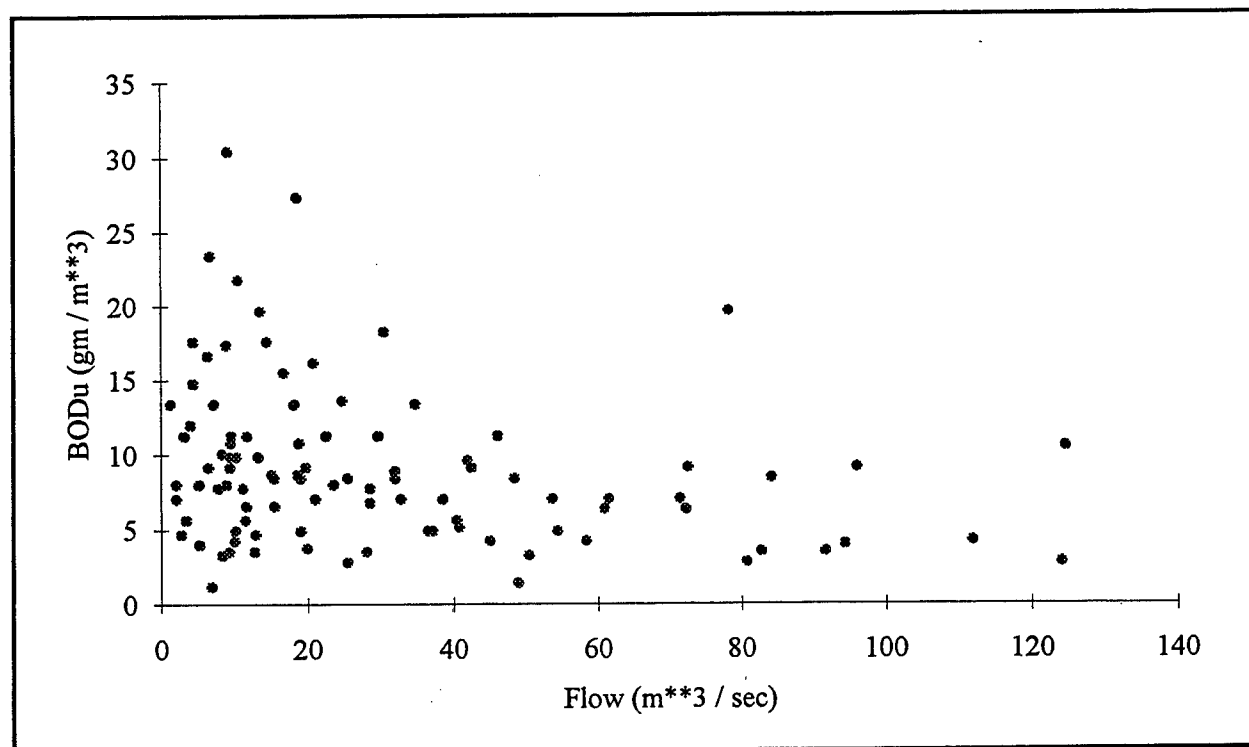
Figure 67.   BODu and flow at Little Falls
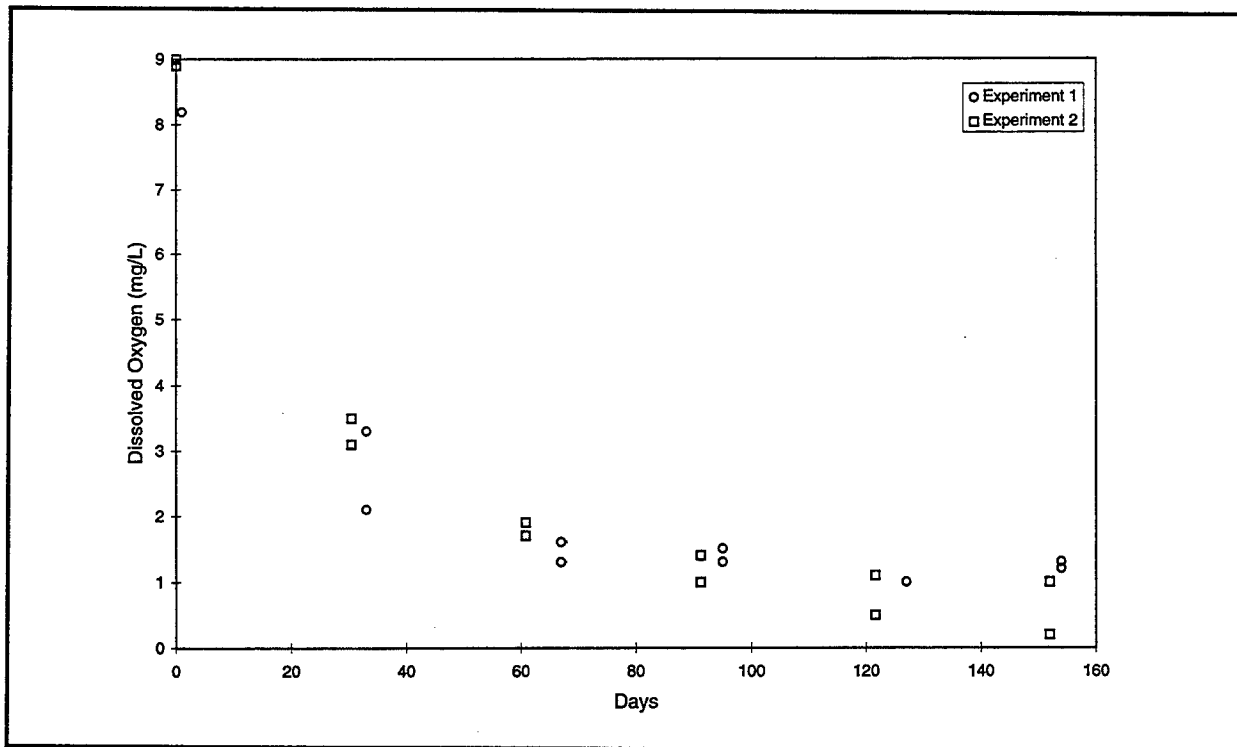
Figure 68. Dissolved oxygen in experimental reactors

BODu in the first incubation diminished rapidly, in rough proportion to dissolved-oxygen depletion, for 60 days then leveled off and showed no trend (Figure 69). BODu in the second incubation diminished slightly for 60 days then showed no trend. BOD consumption in the second experiment was not consistent with dissolved-oxygen depletion. The lack of accuracy inherent in the BOD analysis coupled with the BOD60:BOD5 scaling apparently disguised any interpretable BOD behavior.

The experiment largely confirmed expectations based on the data. Interpretation of the data and experiment for use in the model remained to be accomplished. Over the course of the experiment, not all of the organic matter (BOD) was degraded nor was all of the oxygen consumed. In the isolated reactors, a community adapted to the low DO conditions did not develop. A community adapted to low DO is expected to develop in the tunnel, however. Tunnel retention time is longer than the experimental incubation, and the tunnel is exposed to organisms in seepage from groundwater and in bay water leaking through the tunnel gates. A worst-case assumption was employed in the model. The assumption was that all organic matter in stored tunnel water will be degraded during which all oxygen will be consumed. No production of anaerobic end products will occur in the tunnel, however.
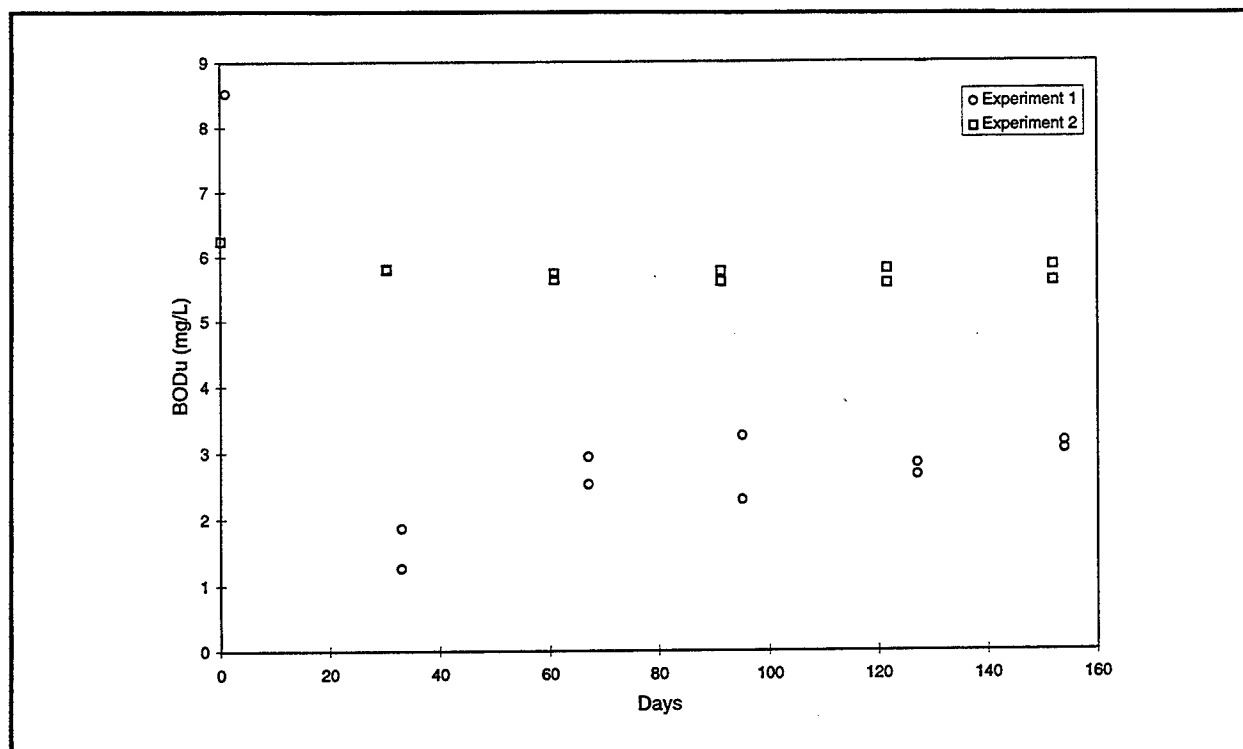
Figure 69. BODu in experimental reactors

Scenario Results

Scenario results were initially examined in the same fashion as the model calibration. Longitudinal plots were produced along major axes (Figures 34 and 35) and time series were produced at eight locations (Figure 36). The local impact of the tunnel was obscured in the examination over the extent of the grid, however. Results are presented here as time series immediately downstream of the tunnel discharge and as longitudinal plots along the axis of Newark Bay alone (Figure 70).

Time series are presented for dissolved oxygen, temperature, salinity, and BODu. Time series start 3 days before commencement of the scenario storm and continue for 14 days. Time zero is the time of storm commencement so that time preceding the storm is negative.

On the longitudinal plots, distance is measured downstream from the tunnel outlet. The small distance upstream of the outlet, between the tunnel and Kearny Point, has negative coordinates. Longitudinal plots show the minimum dissolved oxygen that occurs at any time along the Newark Bay axis and the time of occurrence, relative to storm commencement.
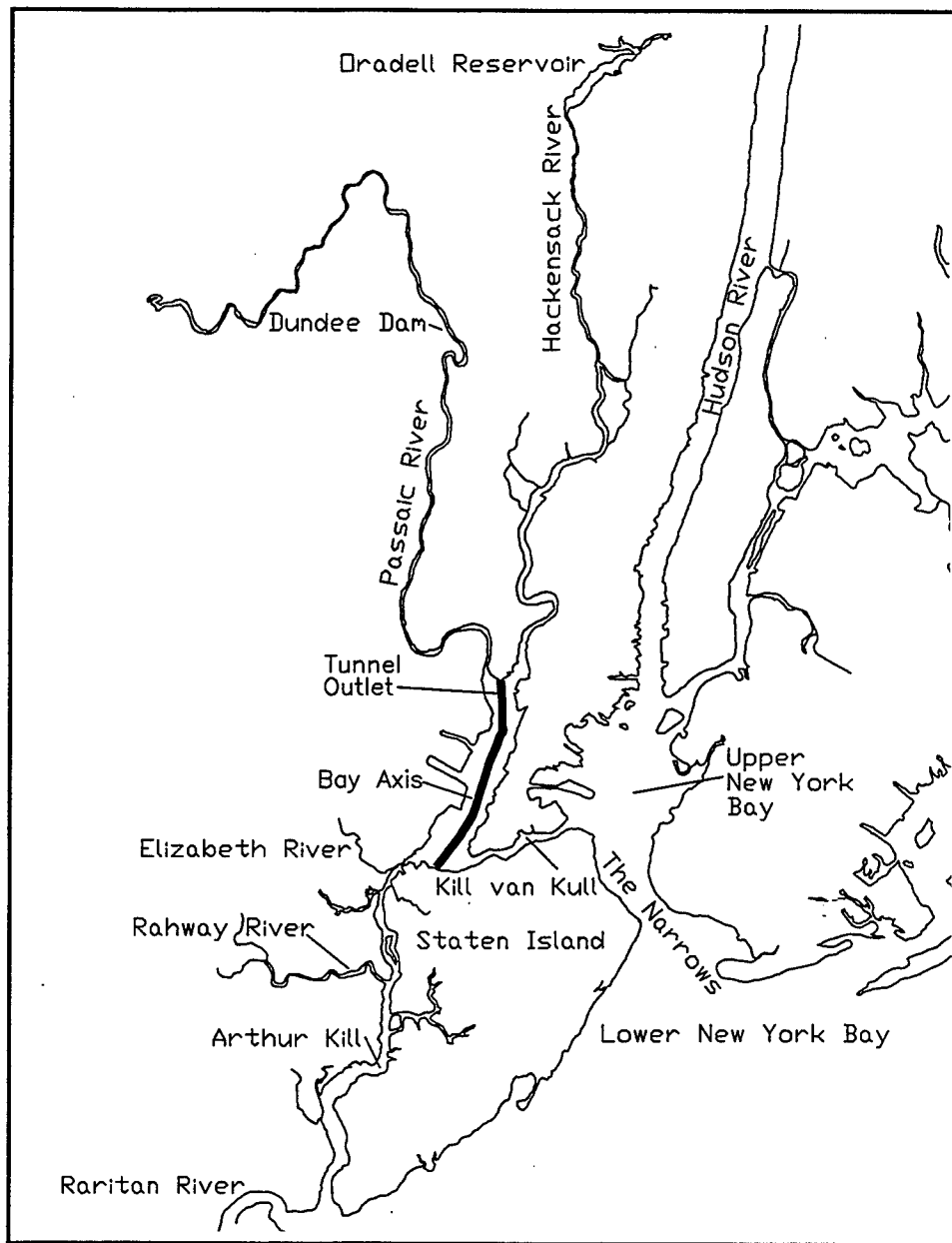
Figure 70. Tunnel discharge location and Newark Bay axis

Wet-Tunnel Operation

July conditions

The scenario matrix (Table 17) presents opportunity for multifaceted analyses: wet tunnel versus dry tunnel versus base conditions; 2-year versus 25-year versus 100-year storm; winter versus summer; etc. An issue of primary concern is the discharge of anoxic water stored in the tunnel at temperature substantially different from the receiving water. Two processes

are expected to be dominant in determining tunnel impacts. The first is the time to empty the tunnel: 12.3 hr for the 2-year storm; 4.7 hr for the 25-year storm; 4.6 hr for the 100-year storm. Shorter emptying times (larger storms) are expected to have effects of greater magnitude but lesser duration than longer emptying times (smaller storms). The second dominant process is the volume of storm water flowing down the Passaic and Hackensack rivers. Larger volumes of water are expected to have a dilutional effect that will mitigate the impact of stored tunnel water to a greater extent than flows from lesser storms.

Time series results (Figures 71, 73, 75) indicate the dissolved oxygen impact, in terms of minimum concentration, is greatest for the 25-year storm. Dissolved oxygen is depressed about 2 mg/L below the value that would occur without the tunnel discharge. For the 2-year and 100-year storms, dissolved-oxygen depression is little more than would occur in the storm in any event. The depression arrives earlier with the tunnel than it would without the tunnel, however. The depression caused by the tunnel is short-lived in any storm event. Following the emptying of the stored water, the tunnel has positive impact on dissolved oxygen. The positive influence occurs when water saturated in dissolved oxygen is routed directly to Newark Bay without undergoing degradation from SOD and other factors while flowing down the Passaic channel.

The longitudinal plots (Figures 72, 74, 76) indicate the dissolved-oxygen depression is not only short-lived, it is of limited spatial extent, roughly half kilometer downstream of the tunnel. Beyond the immediate vicinity of the tunnel outlet, minimum dissolved oxygen is greater with the tunnel than without it, due to the above-mentioned routing of water directly from the fall line to the bay.

The 25-year storm has the greatest temperature impact, roughly 10 $^\circ$C, followed by the 100-year storm and the 2-year storm (Figures 71, 73, 75). The sequencing indicates that the flows from the 100-year storm dilute the impact of the tunnel discharge more than the flows from the 25-year storm. For the 2-year storm, lesser dilution is offset by longer discharge time. As with dissolved oxygen, temperature impacts tend to be short-lived.

The tunnel has no discernable impact on salinity (Figures 71, 73, 75). Salinity in the vicinity of the tunnel outlet descends to zero roughly 3 days after commencement of any size storm, with or without the tunnel.

February Conditions

As with July conditions, dissolved-oxygen impact induced by discharge from the wet tunnel in February is maximum for the 25-year storm (Figures 77, 79, 81). Under these conditions, the impact of the rapid emptying of the tunnel is offset to a lesser degree than it is during a 100-year storm. Impact of the 100-year and 2-year storms is roughly equivalent although the duration of the 2-year impact is longer due to the slower emptying time. Dissolved-oxygen departure from ambient conditions is larger in February than in July, no doubt due to the much higher concentration in the February receiving waters.

Figure 71. Time series downstream of tunnel outlet for 2-year storm, wet tunnel, July conditions

Figure 72. Minimum dissolved oxygen and time of occurrence along Newark Bay axis for 2-year storm, wet tunnel, July conditions

Figure 73. Time series downstream of tunnel outlet for 25-year storm, wet tunnel, July conditions

Figure 74. Minimum dissolved oxygen and time of occurrence along Newark Bay axis for 25-year storm, wet tunnel, July conditions

Figure 75. Time series downstream of tunnel outlet for 100-year storm, wet tunnel, July conditions

Figure 76. Minimum dissolved oxygen and time of occurrence along Newark Bay axis for 100-year storm, wet tunnel, July conditions

Figure 77. Time series downstream of tunnel outlet for 2-year storm, wet tunnel, February conditions

Figure 78. Minimum dissolved oxygen and time of occurrence along Newark Bay axis for 2-year storm, wet tunnel, February conditions
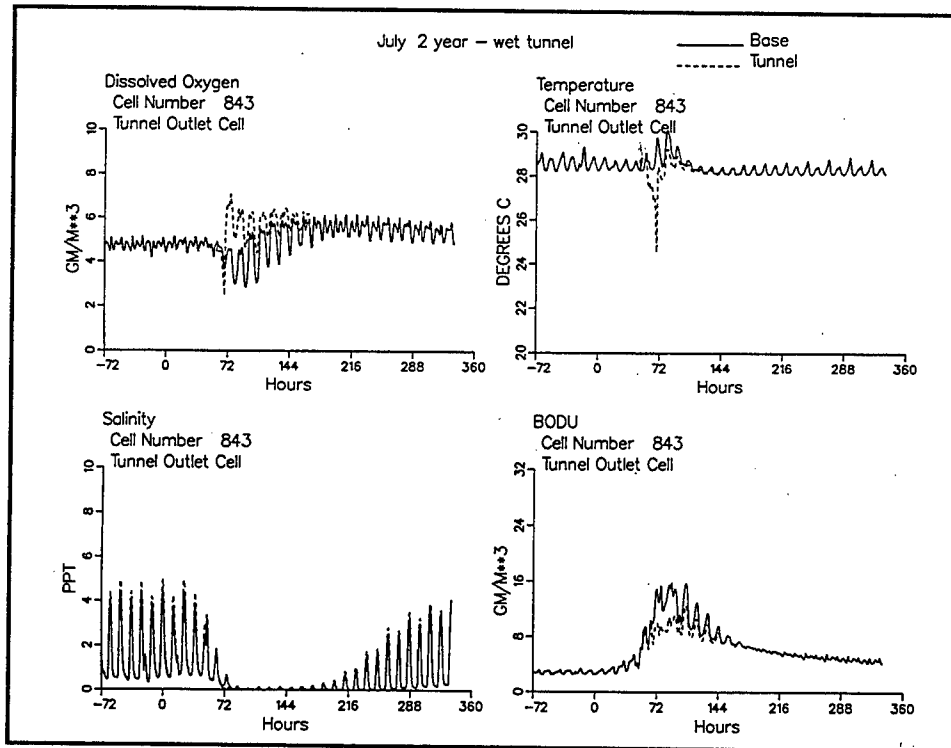
Figure 79.   Time series downstream of tunnel outlet for 25-year storm, wet tunnel, February conditions
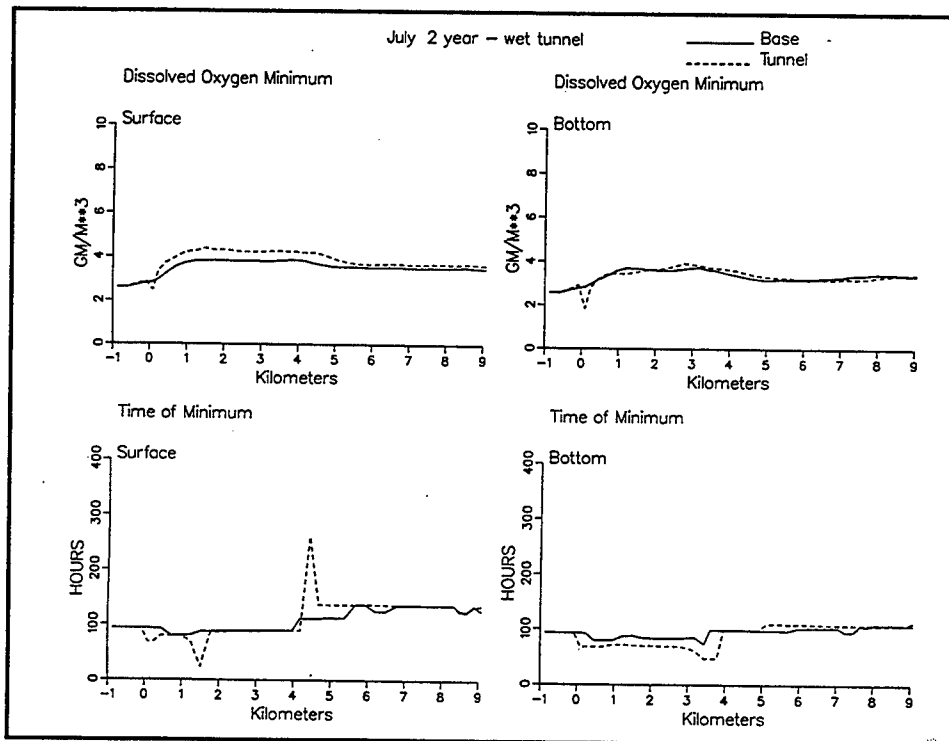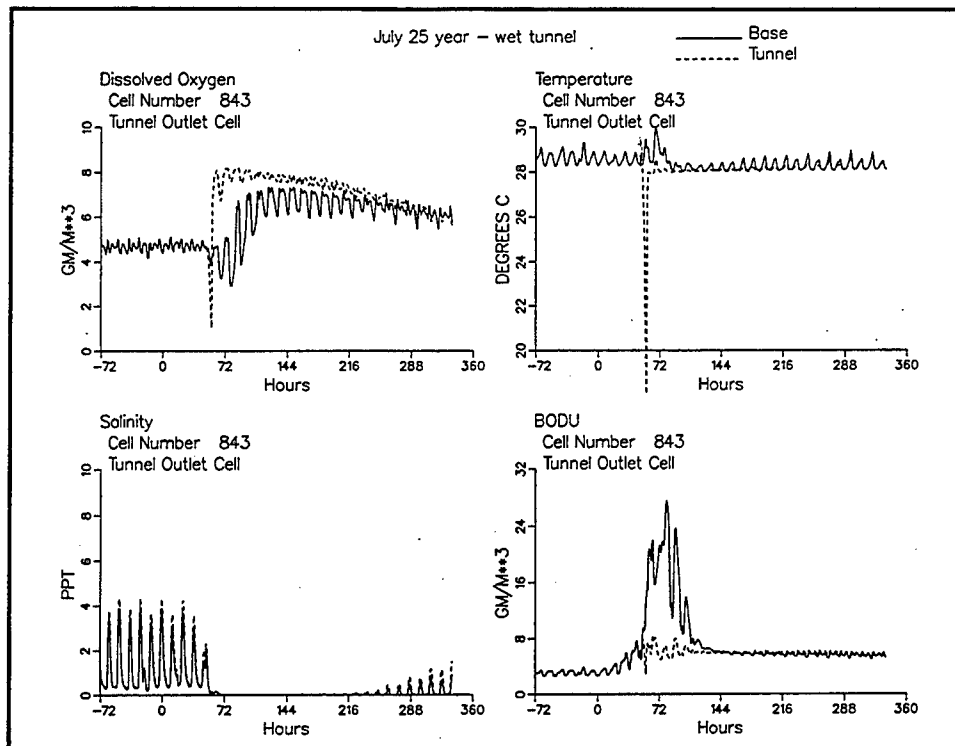

Figure 80.   Minimum dissolved oxygen and time of occurrence along Newark Bay axis for 25-year storm, wet tunnel, February conditions

Figure 81. Time series downstream of tunnel outlet for 100-year storm, wet tunnel, February conditions

Although the impact of the winter discharge is short-lived, the spatial extent is greater in February than in July (Figures 78, 80, 82) and the beneficial effect downstream of the tunnel mouth is largely absent. The larger spatial impact is due to the larger difference in oxygen between anoxic tunnel water and receiving water. No beneficial effect occurs because the receiving waters are already saturated with dissolved oxygen. Direct discharge of water from the fall line to the bay provides no additional oxygen.

Relative temperature impacts of the winter discharge from the wet tunnel are the same as for the summer discharge except the tunnel water is warmer than the receiving water (Figures 77, 79, 81). Impact is greatest for the 25-year storm, less for the 100-year storm, least for the 2-year storm. No significant difference exists in the magnitude of the temperature impact in summer versus winter. Impacts are short-lived in winter as well as summer.

Salinity conditions are virtually identical in winter and summer (Figures 77, 79, 81). No discernable impact of the tunnel occurs.

Figure 82. Minimum dissolved oxygen and time of occurrence along Newark
Bay axis for 100-year storm, wet tunnel, February conditions

Dry-Tunnel Operation

July conditions

Dissolved oxygen effects with the tunnel in operation and pumped dry
between storm events are solely beneficial during summer conditions (Figures 83-88). The beneficial effect occurs because dissolved-oxygen saturated water is routed directly from the fall line to Newark Bay without
undergoing degradation while flowing down the Passaic channel.

A slight temperature depression occurs for roughly 24 hr when the tunnel is in operation (Figures 83, 85, 87). The depression is no less than
would occur without the tunnel; the depression simply occurs sooner with
the tunnel in operation. With or without the tunnel, the depression is due
to displacement of warm water flowing down the Hackensack River with
cooler storm water flowing down the Passaic. Since the tunnel rapidly
routes storm water from the fall line to Newark Bay, the depression occurs
sooner than it would if the water arrive via the Passaic channel.

Operation of the dry tunnel has no discernable effect on salinity (Figures 83, 85, 87). Low-salinity water at the head of Newark Bay transitions to
freshwater roughly 72 hr after commencement of the storm with or without the tunnel in operation.

Figure 83. Time series downstream of tunnel outlet for 2-year storm, dry tunnel, July conditions
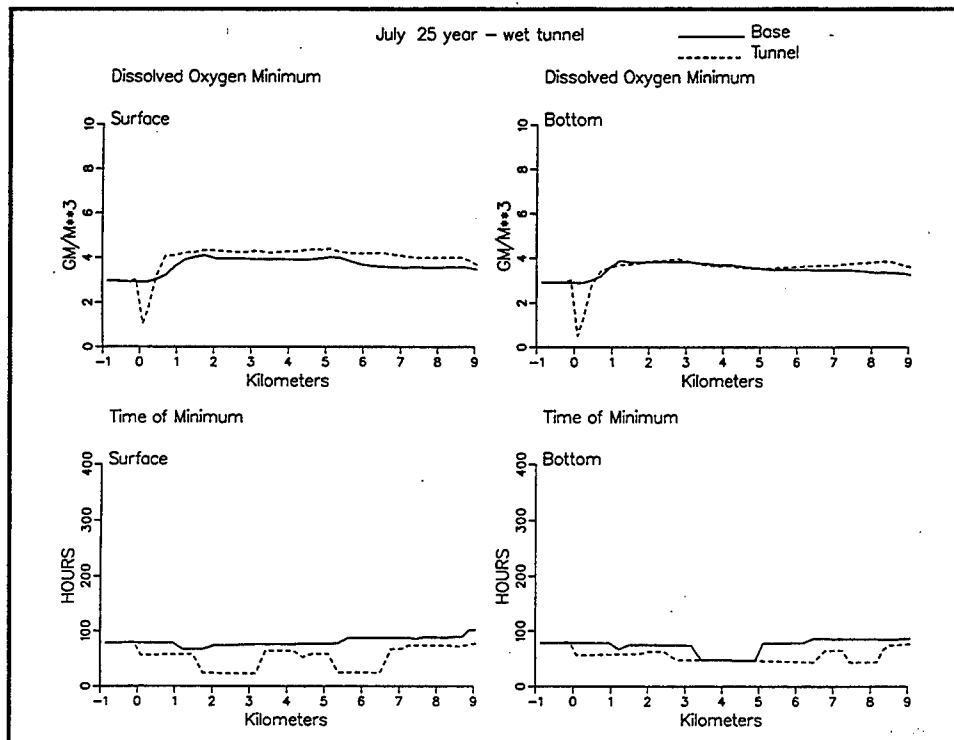

Figure 84. Minimum dissolved oxygen and time of occurrence along Newark Bay axis for 2-year storm, dry tunnel, July conditions
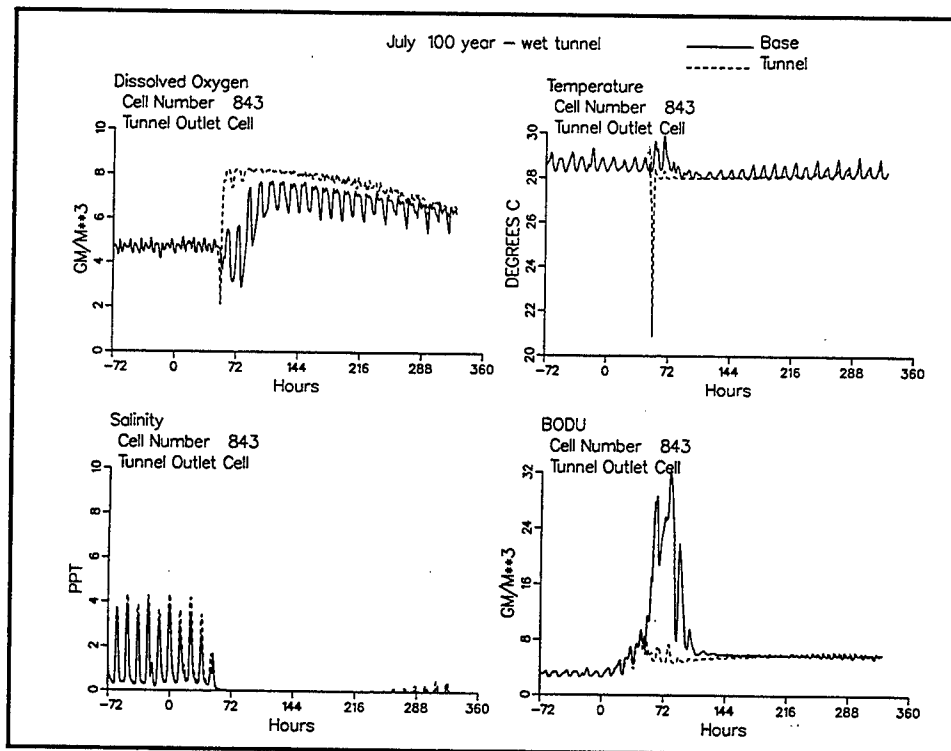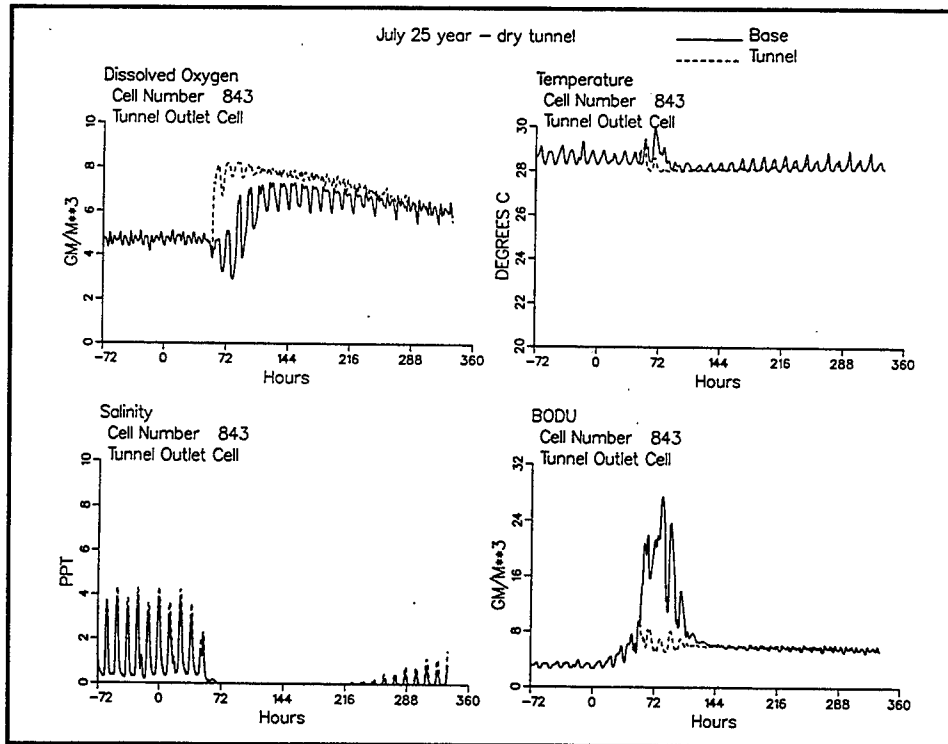
Figure 85. Time series downstream of tunnel outlet for 25-year storm, dry tunnel, July conditions
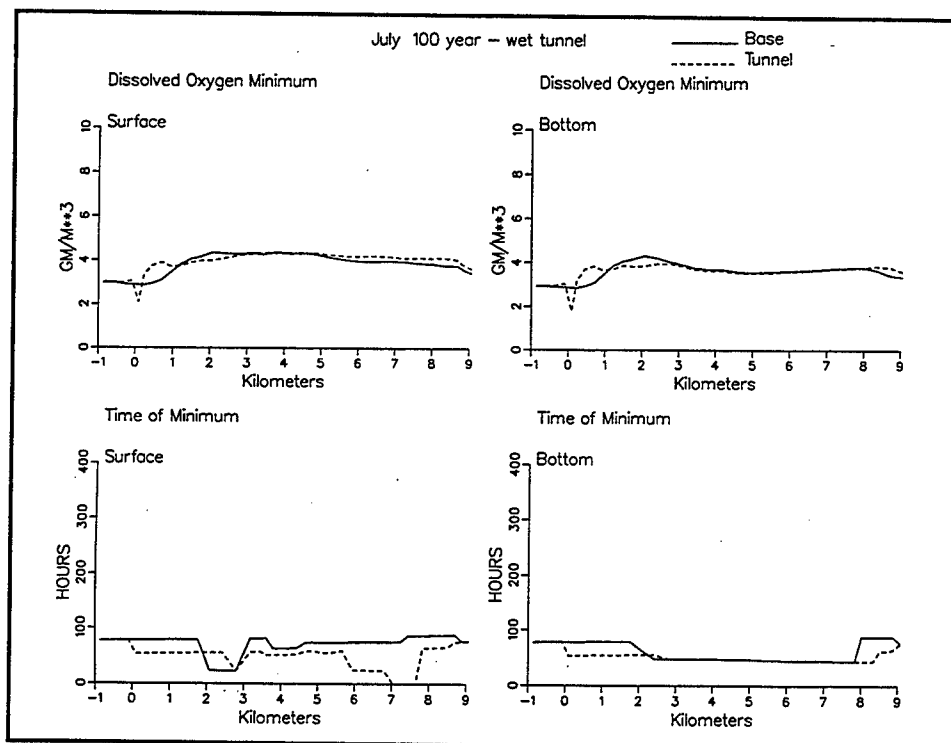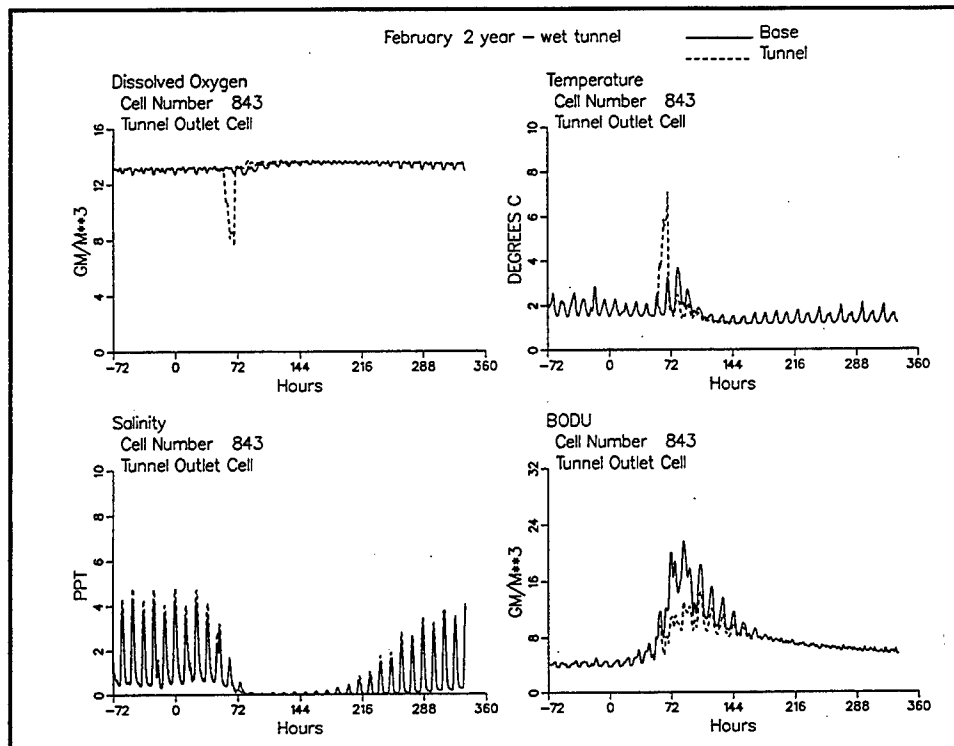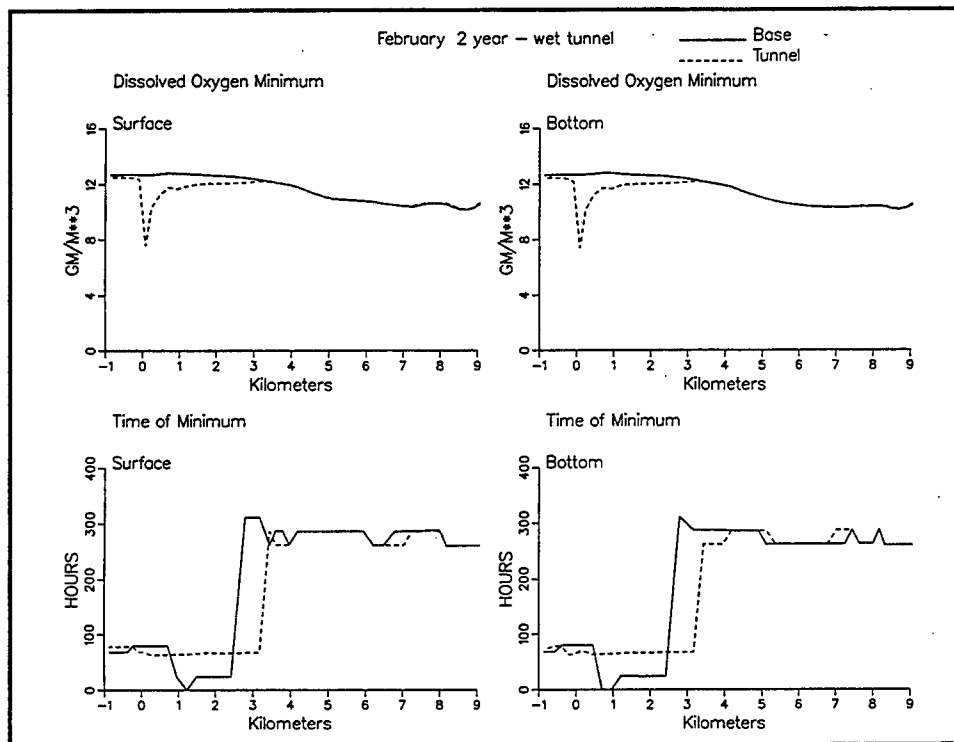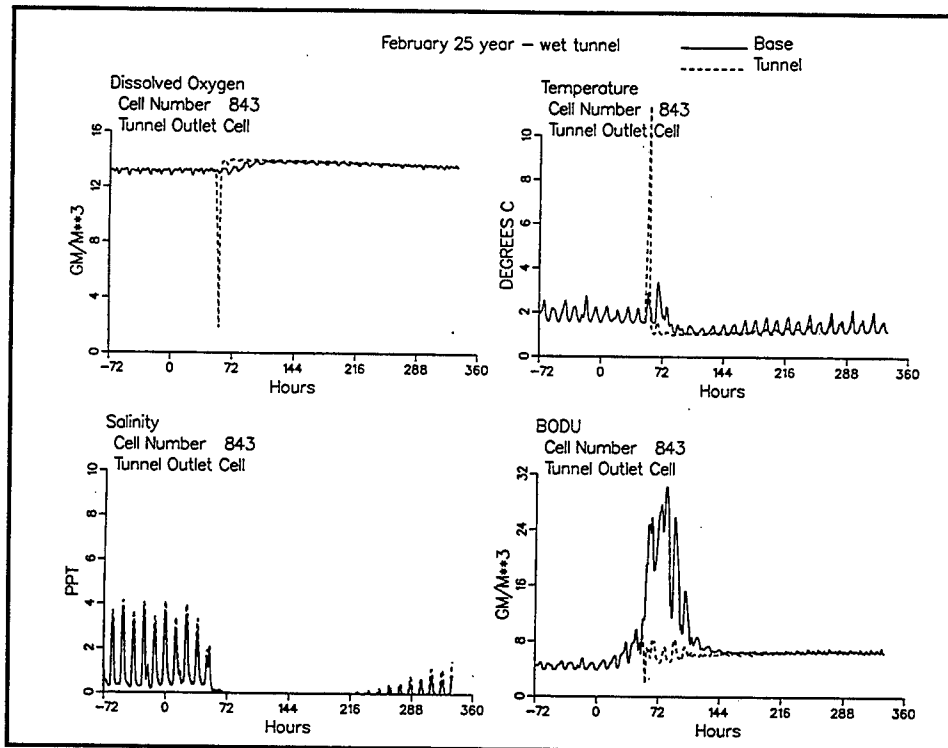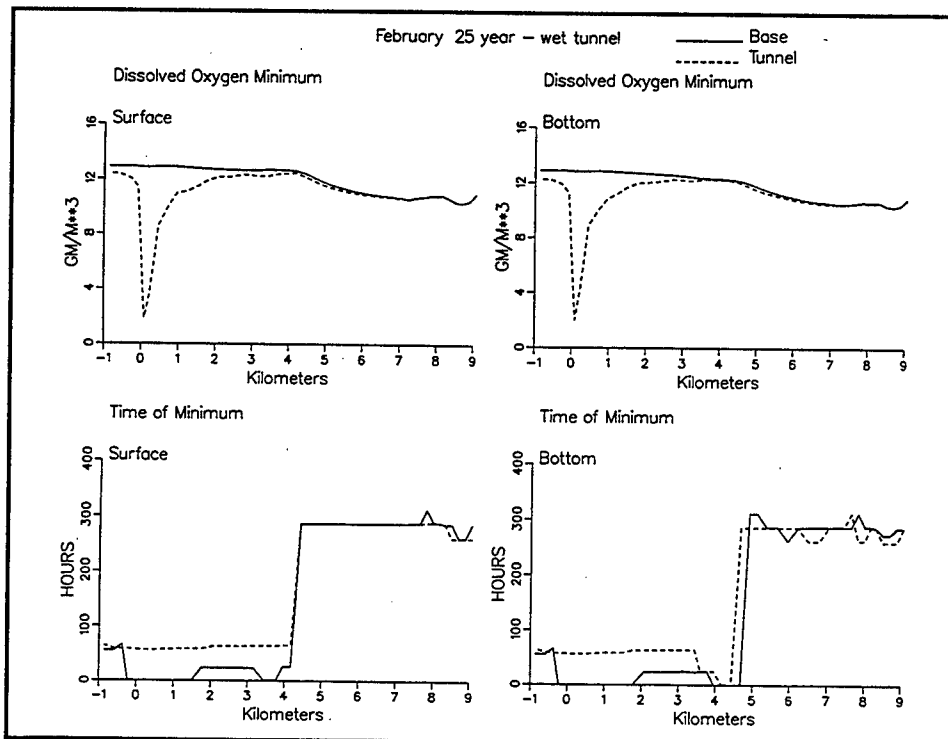

Figure 86. Minimum dissolved oxygen and time of occurrence along Newark Bay axis for 25-year storm, dry tunnel, July conditions
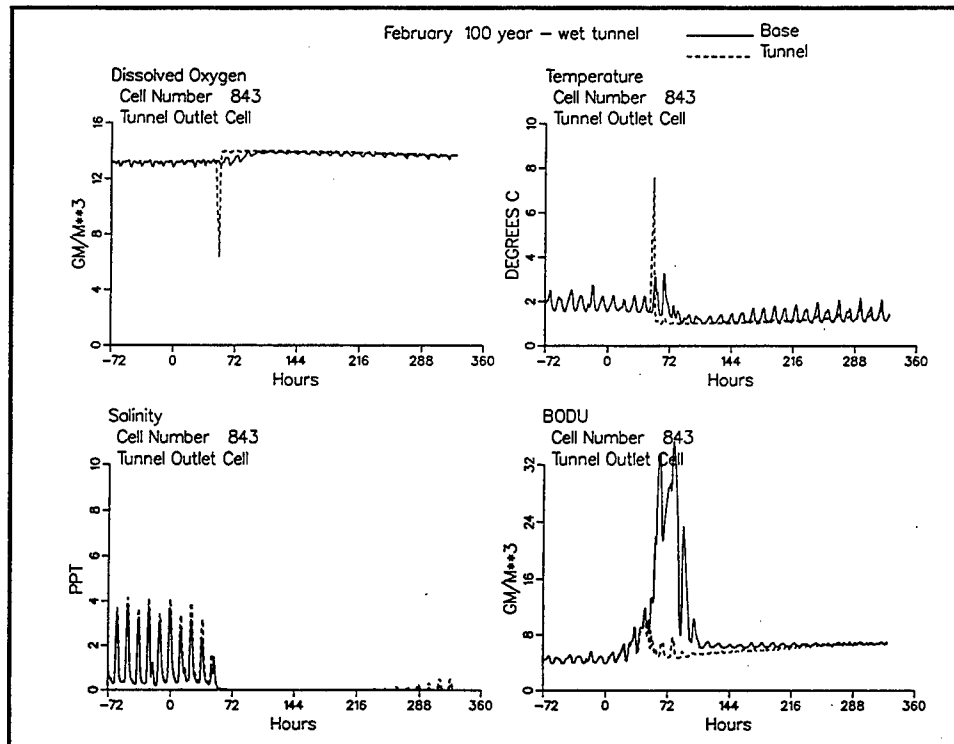
Figure 87. Time series downstream of tunnel outlet for 100-year storm, dry
tunnel, July conditions

Figure 88. Minimum dissolved oxygen and time of occurrence along Newark
Bay axis for 100-year storm, dry tunnel, July conditions

February conditions

Operation of the dry tunnel under winter conditions has only barely discernable effect on dissolved oxygen (Figures 89-94). To the extent that an effect exists, it is beneficial. As with previous scenarios, the beneficial effect occurs because dissolved-oxygen saturated water is routed directly from the fall line to Newark Bay. The water flowing down the Passaic under winter conditions undergoes little degradation, however; and the receiving waters of Newark Bay are nearly saturated with oxygen, so the beneficial effect of routing water from the fall line to Newark Bay is minimal.

Temperature effects of dry-tunnel operation in winter are identical to summer: a slight temperature depression occurs for roughly 24 hr when the tunnel is in operation (Figures 89, 91, 93). The depression is no less than would occur without the tunnel; the depression simply occurs sooner with the tunnel in operation. With or without the tunnel, the depression is due to displacement of warm water flowing down the Hackensack River with cooler storm water flowing down the Passaic. Since the tunnel rapidly routes storm water from the fall line to Newark Bay, the depression occurs sooner than it would if the water arrived via the Passaic channel.

Operation of the dry tunnel in winter has no discernable effect on salinity (Figures 89, 91, 93). Low-salinity water at the head of Newark Bay transitions to fresh water roughly 72 hr after commencement of the storm with or without the tunnel in operation.
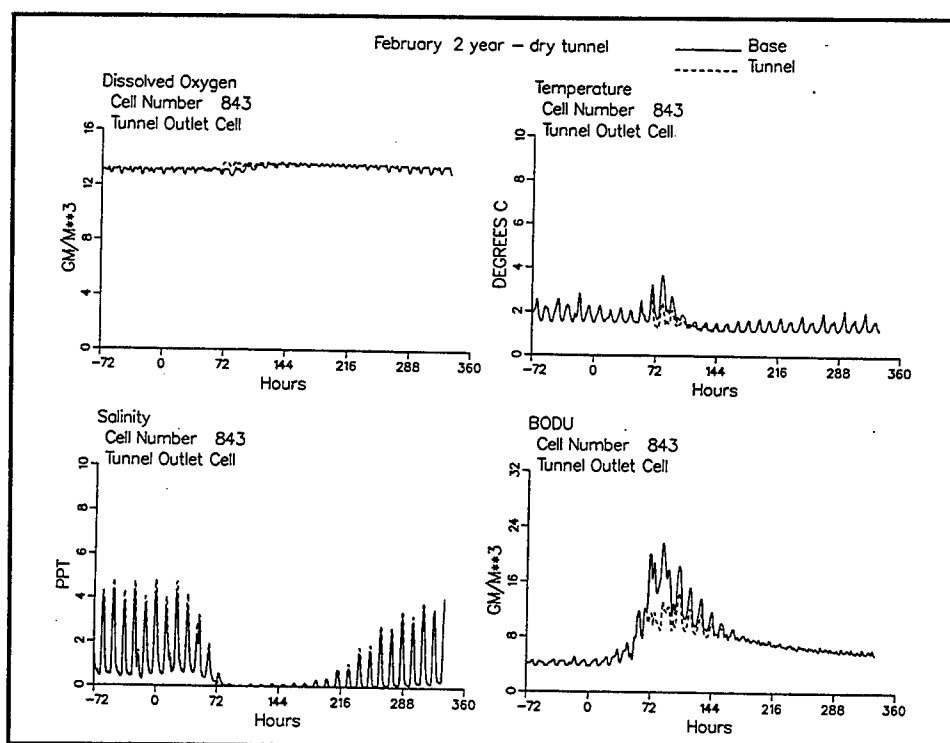
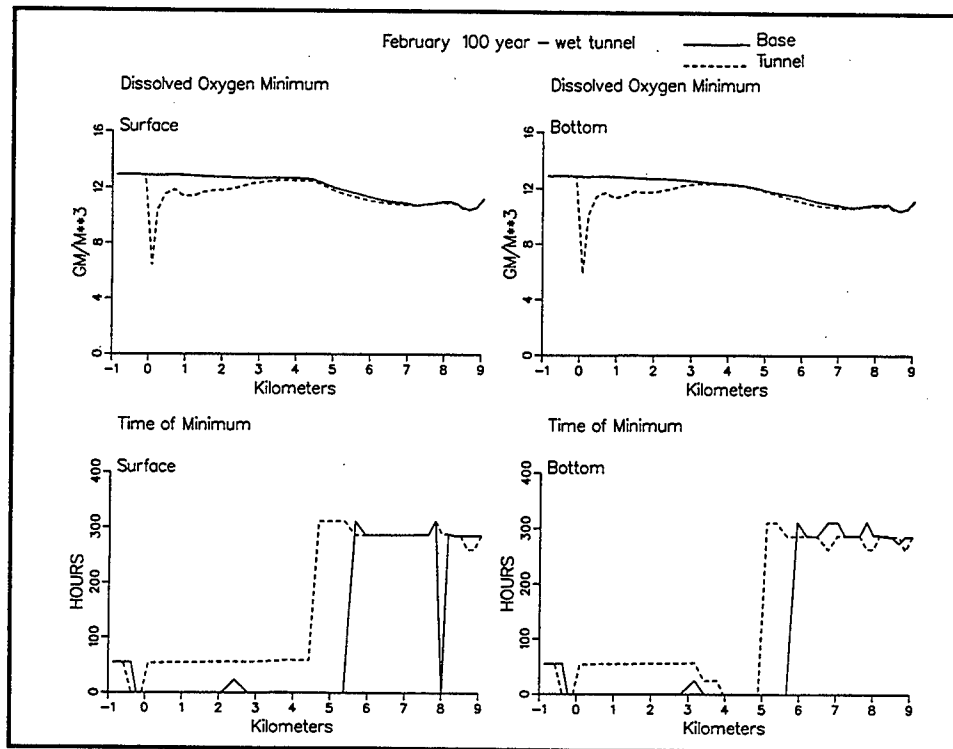Figure 89. Time series downstream of tunnel outlet for 2-year storm, dry tunnel, February conditions
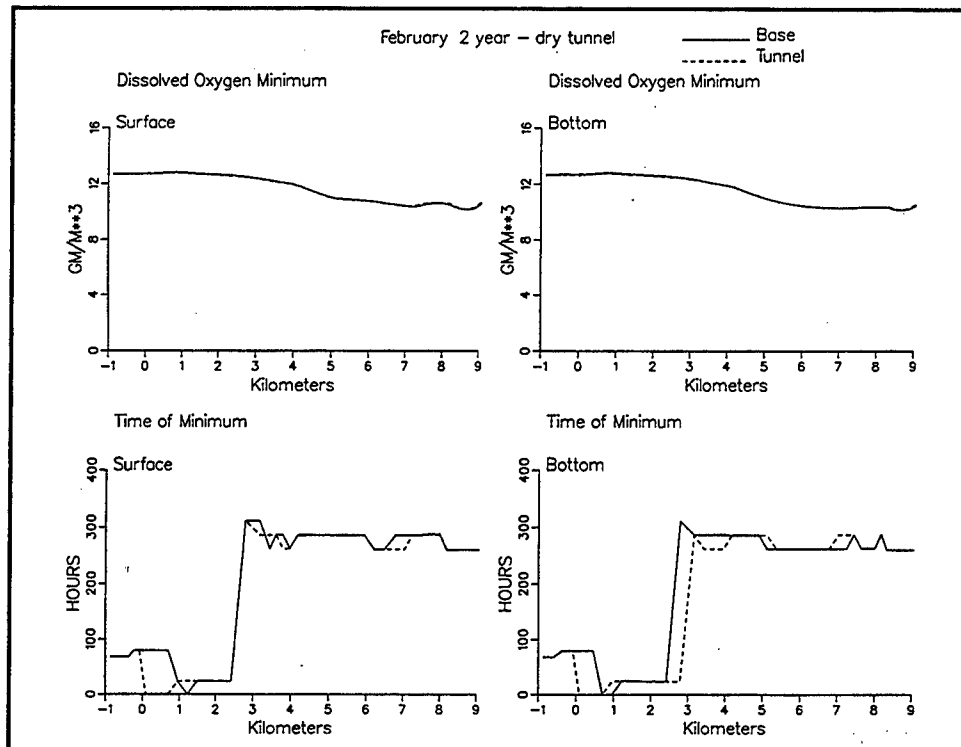
Figure 90.   Minimum dissolved oxygen and time of occurrence along Newark
             Bay axis for 2-year storm, dry tunnel, February conditions
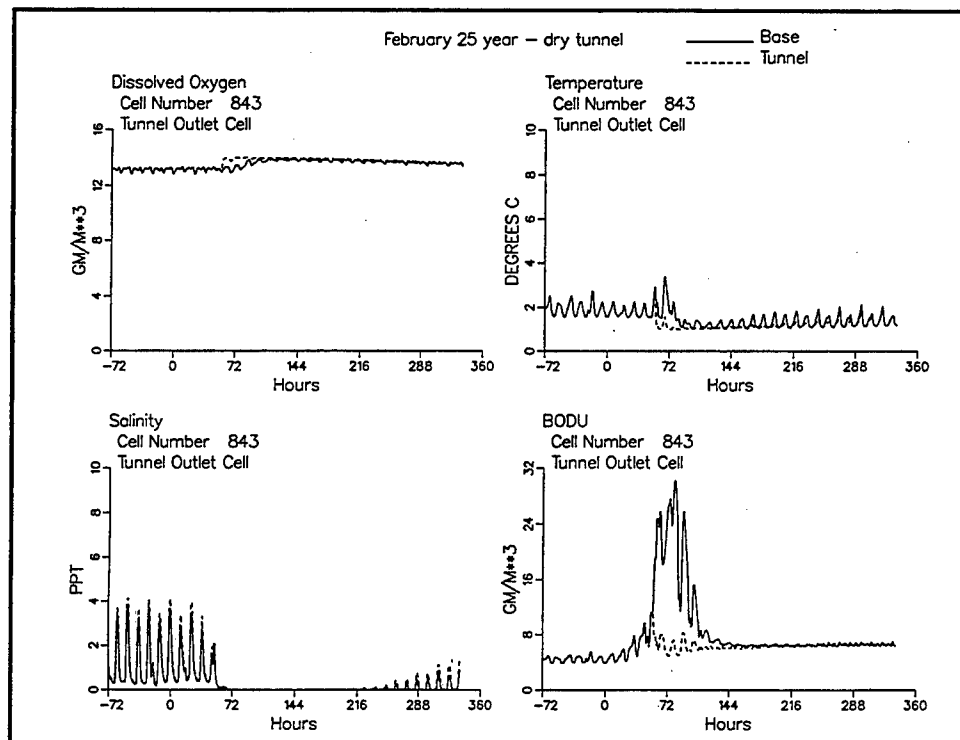
Figure 91.   Time series downstream of tunnel outlet for 25-year storm, dry
             tunnel, February conditions
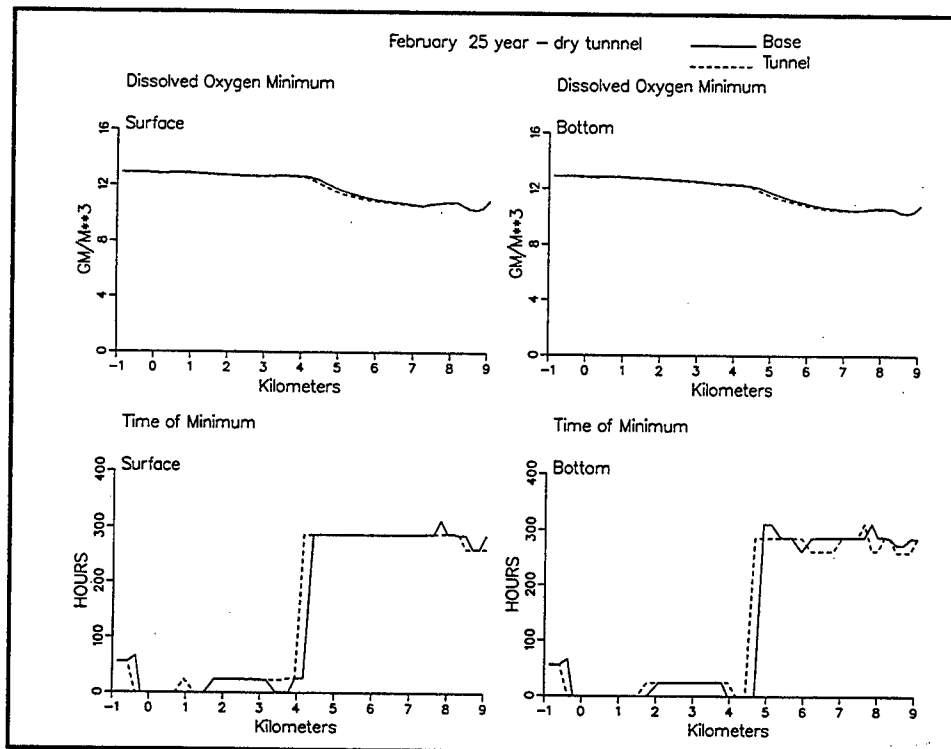
Figure 92. Minimum dissolved oxygen and time of occurrence along Newark
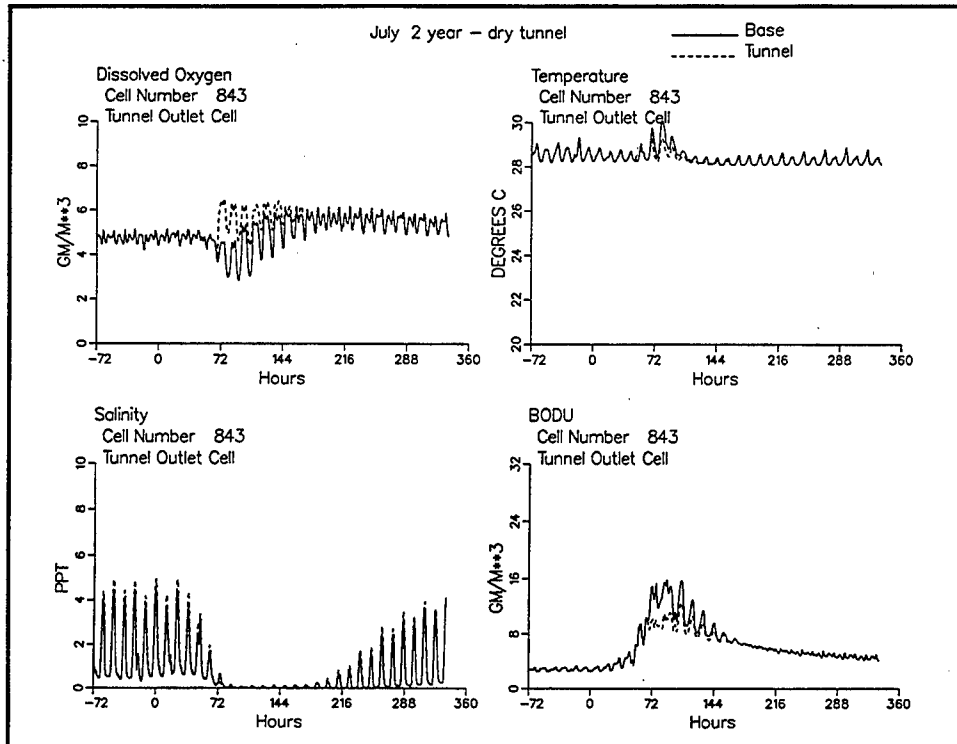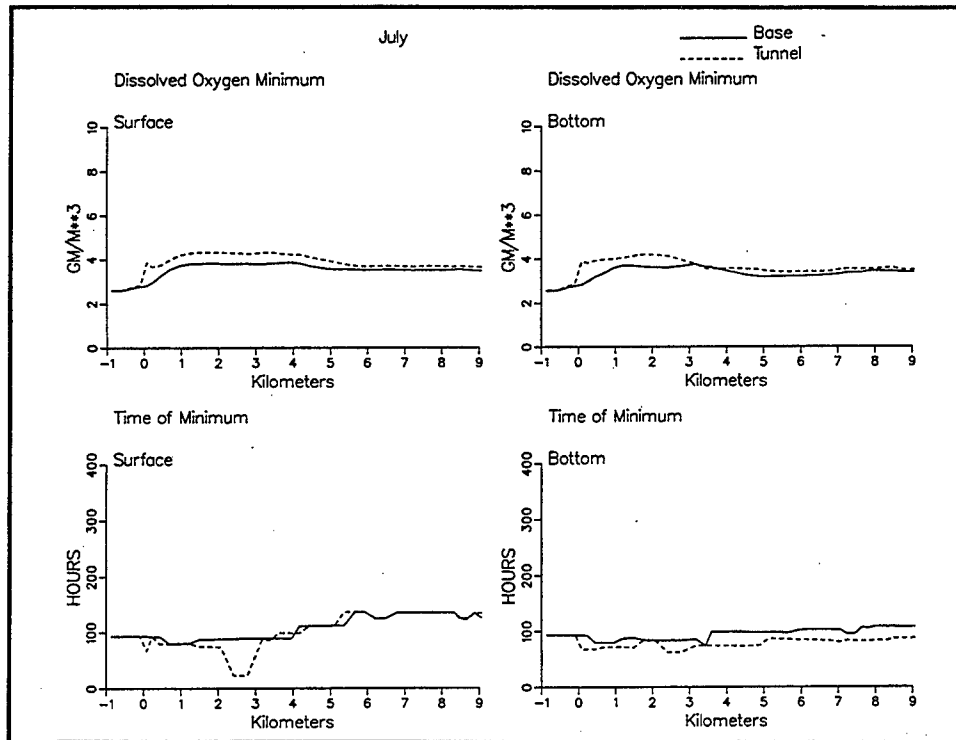Bay axis for 25-year storm, dry tunnel, February conditions
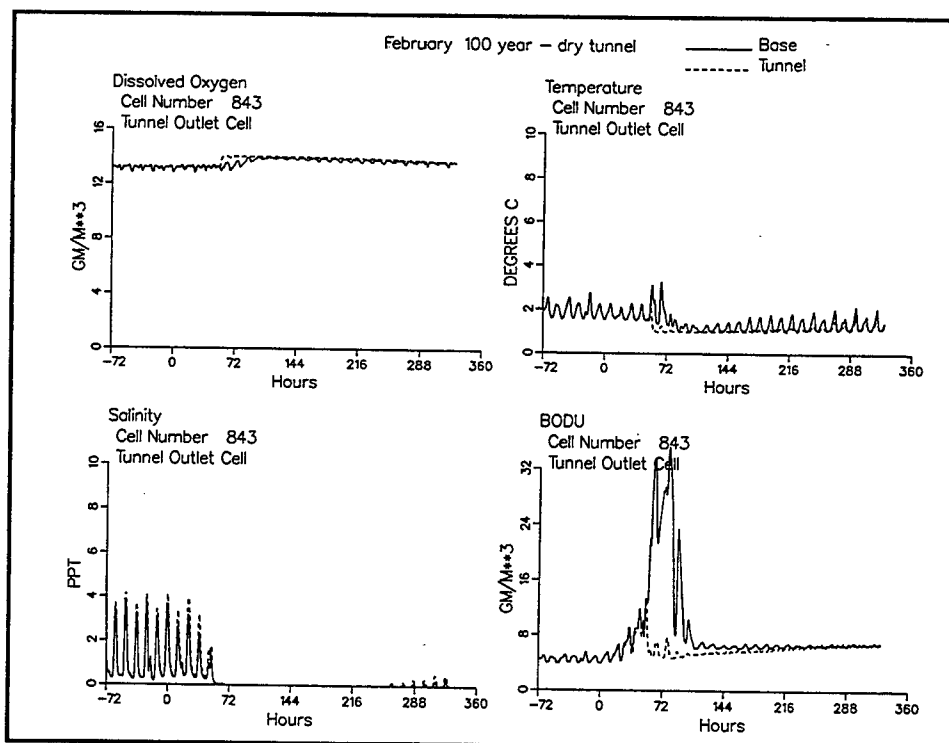
Figure 93. Time series downstream of tunnel outlet for 100-year storm, dry
tunnel, February conditions
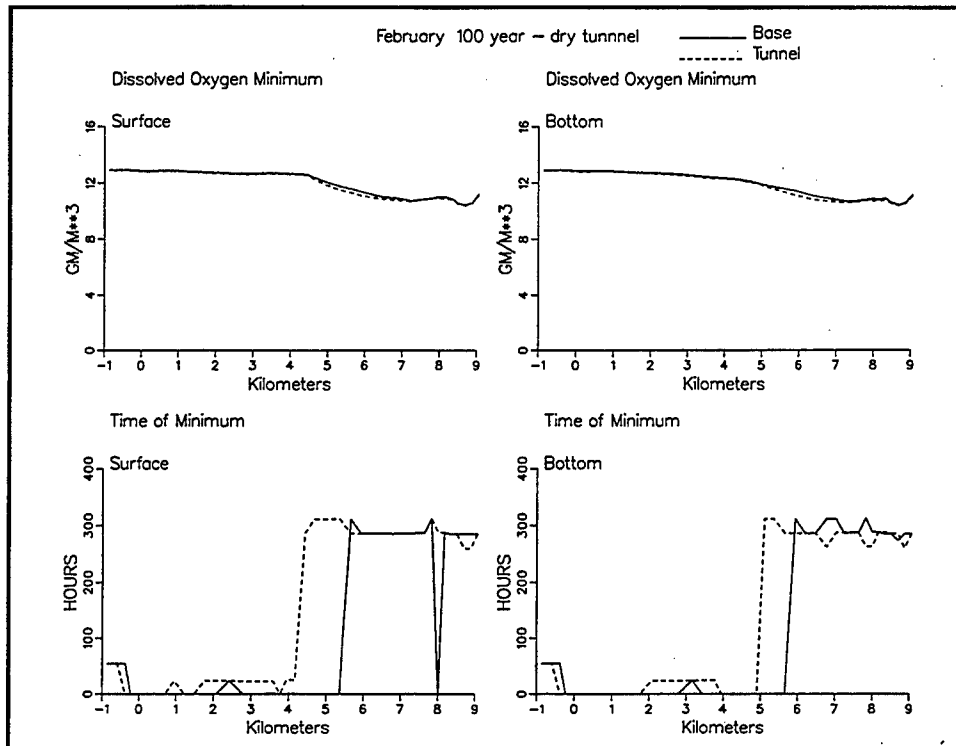
Figure 94.   Minimum dissolved oxygen and time of occurrence along Newark
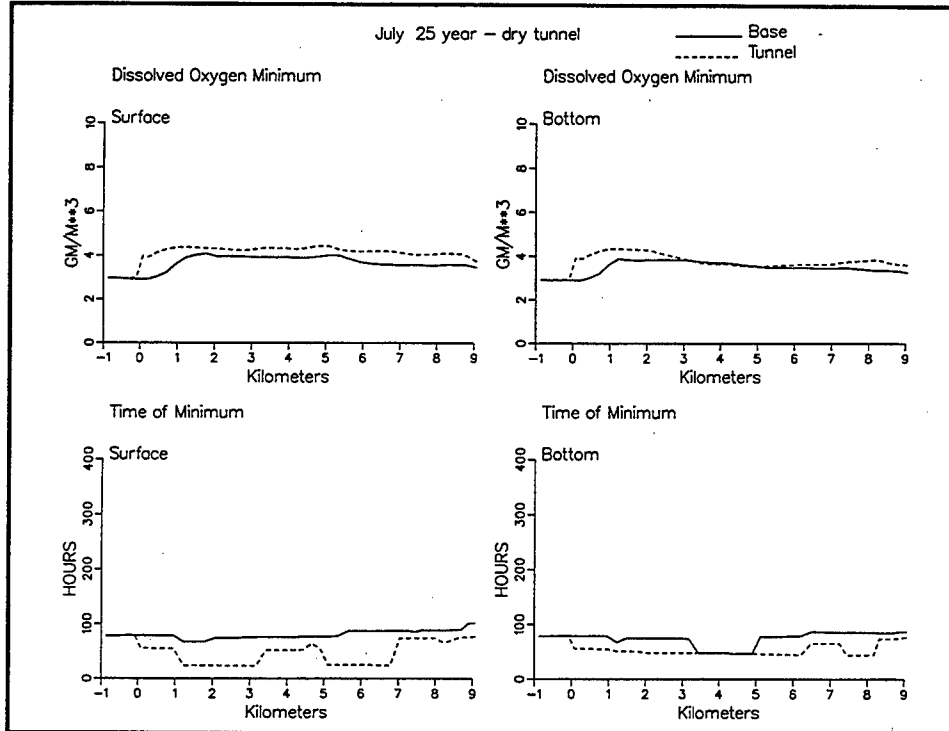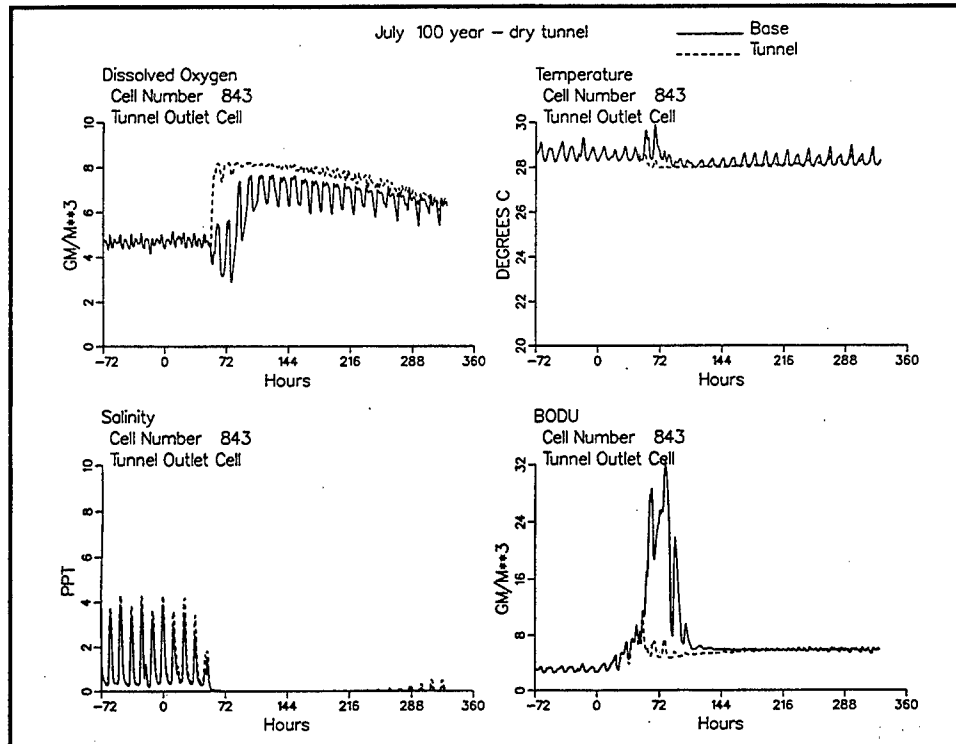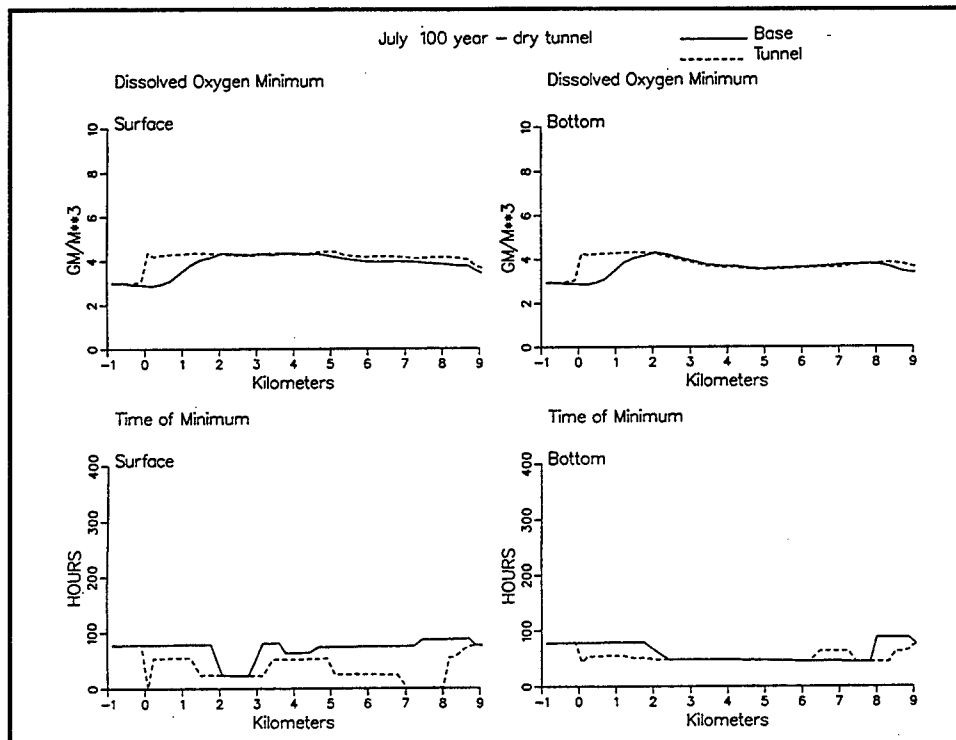Bay axis for 100-year storm, dry tunnel, February conditions

8   Summary and Conclusions

The Passaic River and Newark Bay form part of the complex New York-New Jersey harbor system (Figure 1). The upper portion of the Passaic River basin is subject to destructive flooding during storm events. A diversion tunnel is proposed to alleviate the flooding. The tunnel will divert flow from the headwaters of the Passaic directly to the upper end of Newark Bay (Figure 2).

The objective of the study is to provide information required to evaluate the effect of the diversion tunnel on living resources, primarily shellfish and finfish, in the vicinity of the tunnel outlet. Following consultation with the National Marine Fisheries Service, three living-resource parameters were selected for examination: salinity, water temperature, and dissolved-oxygen concentration.

Newark Bay

The proposed tunnel discharge is at the upper end of Newark Bay. The bay is normally saline throughout its extent although winter and spring freshets can drive fresh water into the bay under extreme conditions (Figure 3). Temperature (Figure 6) and dissolved oxygen (Figure 7) in the bay both undergo annual cycles. Maximum temperatures occur in July while annual minima, near freezing, occur in January and February. Minimum dissolved oxygen occurs in July and August, coincident with high temperatures. Maximum dissolved oxygen occurs in March, the result of cold temperature and wind-driven reaeration. Monthly minimum dissolved oxygen is ≈ 4 g m^{-3} and observations below 3 g m^{-3} seldom occur.

Hydrodynamic Model

Modeling impact of the proposed tunnel required two models. Transport processes were modeled by the CH3D-WES three-dimensional hydrodynamic model. Details of the model formulation and application are found in a companion report to this volume (Letter et al., in preparation). Transport information from the hydrodynamic model was processed and stored on magnetic media for subsequent use by the water quality model.

Water Quality Model

The CE-QUAL-ICM model applied in the Passaic River study was a modified version of a model developed for Chesapeake Bay (Cerco and Cole 1994). Modifications consisted of reducing the number of state variables to a suite appropriate for the problem of interest. The suite consisted of five state variables: salinity, temperature, dissolved oxygen, ultimate biochemical oxygen demand, and chemical oxygen demand.

Application of Water Quality Model

Field surveys and sample analyses for calibration of the water quality model were conducted by the Stevens Institute of Technology, Hoboken, NJ. Three surveys were conducted, at roughly 1-month intervals, from July 1994 to September 1994. Thirty stations were sampled (Figure 17). Surveys were conducted during daylight close to the period of slack-before-ebb tide. Water quality sampling included salinity, temperature, dissolved oxygen, BOD5, and BODu (60-day). Additional databases obtained from the New York Department of Environmental Protection, National Marine Fisheries Service, and STORET were also used to aid in model calibration.

Performance of the model was evaluated through graphical and numerical comparison of model computations with field observations. Graphical comparisons included spatial comparisons along two longitudinal axes, time-series comparisons at eight locations, and spatial comparisons along vertical axes at eight locations. Quantitative summaries (Table 16) indicated the model was successful in representing 65 to 82 percent of the observations. Overall, the model was most successful at computing temperature, followed by BOD, dissolved oxygen, and salinity.

Tunnel Scenario Design

A matrix of scenarios (Table 17) was constructed to examine the impact of tunnel discharge on receiving waters. Base scenarios specified future conditions without the tunnel. Wet-tunnel scenarios examined future conditions with the tunnel in operation and with floodwater remaining in the tunnel between flood events. Dry-tunnel scenarios examined future conditions with the tunnel in operation and with the tunnel pumped dry between flood events. Three flood conditions were considered: 2-year storm; 25-year storm; and 100-year storm. Duration of each scenario was 27 days. The first 13 days were a "spin-up" period to allow predicted conditions to equilibrate with specified loads, temperature, and boundary conditions. The spin-up period was followed by a 14-day storm simulation.

One concern regarding the impact of the tunnel diversion was the water that may be stored in the tunnel between flood events. The expected

interval between events is 2 years or more. During this period the water may undergo significant deterioration. Initial indications of the effect of storage on tunnel water were obtained from examination of data retrieved from the STORET database. Observations from the Passaic River at Little Falls, downstream of the proposed tunnel inlet, were summarized. At flows sufficient to operate the diversion tunnel, dissolved-oxygen concentration (Figure 66) equaled or exceeded ultimate biochemical oxygen demand (Figure 67). The data indicated the supply of biodegradable material in floodwater, isolated in the tunnel, will be consumed before dissolved oxygen is depleted. Consequently, anaerobic degradation should not occur, and production of reduced end products such as sulfide or methane is not expected.

Two incubation experiments were conducted to investigate the hypothesis formed from examination of the STORET data. Storm water was incubated in three 25-L reactors, sealed against introduction of atmospheric oxygen. One reactor was set up to measure the volume of gas production. The other two were set up to allow samples of water to be withdrawn. Samples were withdrawn monthly for 5 months and analyzed for dissolved oxygen, immediate oxygen demand, BOD, COD, total sulfide, reduced iron, and reduced manganese. At the end of 6 months, a final measure of gas evolution was conducted.

The experiment largely confirmed expectations based on the data. No gas evolution occurred, nor were detectable quantities of immediate oxygen demand, COD, sulfide, iron, or manganese observed.

Not all BOD and dissolved oxygen were consumed in the 6-month incubation. Since the expected interval between flood events is much longer, ≈2 years, a worst case was assumed for scenarios. The assumption was that organic matter in stored tunnel water will be degraded during which all oxygen will be consumed. No production of anaerobic end products will occur in the tunnel, however.

Wet-Tunnel Operation—July Conditions

Time series results (Figures 71, 73, 75) indicate the dissolved-oxygen impact, in terms of minimum concentration, is greatest for the 25-year storm. Dissolved oxygen is depressed about 2 mg/L below the value that would occur without the tunnel discharge. For the 2-year and 100-year storms, dissolved-oxygen depression is little more than would occur in the storm without the tunnel. The depression caused by the tunnel is short-lived in any storm event. Following the emptying of the stored water, the tunnel has positive impact on dissolved oxygen. The positive influence occurs when water saturated in dissolved oxygen is routed directly to Newark Bay without undergoing degradation from SOD and other factors while flowing down the Passaic channel.

The longitudinal plots (Figures 72, 74, 76) indicate the dissolved oxygen depression is not only short-lived, it is of limited spatial extent, roughly half kilometer downstream of the tunnel. Beyond the immediate vicinity

of the tunnel outlet, minimum dissolved oxygen is greater with the tunnel than without it, due to the above-mentioned routing of water directly from the fall line to the bay.

The 25-year storm has the greatest temperature impact, roughly 10 $^{\circ}$C, followed by the 100-year storm and the 2-year storm (Figures 71, 73, 75). As with dissolved oxygen, temperature impacts tend to be short-lived. The tunnel has no discernable impact on salinity (Figures 71, 73, 75).

Wet-Tunnel Operation—February Conditions

As with July conditions, dissolved-oxygen impact induced by discharge from the wet tunnel in February is maximum for the 25-year storm (Figures 77, 79, 81). Dissolved-oxygen departure from ambient conditions is larger in February than in July, no doubt due to the much higher concentration in the February receiving waters. As with summer, the impact of the winter discharge is short-lived, but the spatial extent is greater in February than in July (Figures 78, 80, 82). The larger spatial impact is due to the larger difference in oxygen between anoxic tunnel water and receiving water.

Relative temperature impacts of the winter discharge from the wet tunnel are the same as for the summer discharge except the tunnel water is warmer than the receiving water (Figures 77, 79, 81). Impact is greatest for the 25-year storm, less for the 100-year storm, least for the 2-year storm. No significant difference exists in the magnitude of the temperature impact in summer versus winter. Impacts are short-lived in winter as well as summer. Salinity conditions are virtually identical in winter and summer (Figures 77, 79, 81). No discernable impact of the tunnel occurs.

Dry-Tunnel Operation—July Conditions

Dissolved-oxygen effects with the tunnel in operation and pumped dry between storm events are solely beneficial during summer conditions (Figures 83, 85, 87). The beneficial effect occurs because dissolved-oxygen saturated water is routed directly from the fall line to Newark Bay without undergoing degradation while flowing down the Passaic channel.

A slight temperature depression occurs for roughly 24 hr when the tunnel is in operation (Figures 83, 85, 87). The depression is no less than would occur without the tunnel; the depression simply occurs sooner with the tunnel in operation. With or without the tunnel, the depression is due to displacement of warm water flowing down the Hackensack River with cooler storm water flowing down the Passaic. Since the tunnel rapidly routes storm water from the fall line to Newark Bay, the depression occurs sooner than it would if the water arrived via the Passaic channel. Operation of the dry tunnel has no discernable effect on salinity (Figures 83, 85, 87).

Dry Tunnel Operation—February Conditions

Operation of the dry tunnel under winter conditions has only barely discernable effect on dissolved oxygen (Figures 89, 91, 93). To the extent that an effect exists, it is beneficial. Temperature effects of dry-tunnel operation in winter are identical to summer: a slight temperature depression occurs for roughly 24 hr when the tunnel is in operation (Figures 89, 91, 93). Operation of the dry tunnel in winter has no discernable effect on salinity (Figures 89, 91, 93).

Conclusions

Scenarios were designed to illustrate the worst-case impact of the discharge tunnel on salinity, temperature, and dissolved oxygen. Under worst-case conditions, impacts of the tunnel on dissolved oxygen and temperature were minimal in magnitude, short-lived, and of limited spatial extent. Impact of the tunnel on salinity was indiscernible.

References

American Public Health Association. (1985). "Standard methods for the examination of water and wastewater," 16th ed., Washington, DC.

American Society of Civil Engineers. (1961). "Effect of water temperature on stream reaeration," *Journal of the Sanitary Engineering Division* 87(SA6), 59-71.

Cerco, C. F., and Cole, T. (1994). "Three-dimensional eutrophication model of Chesapeake Bay," Technical Report EL-94-4, U.S. Army Engineer Waterways Experiment Station, Vicksburg, MS.

Edinger, J., Brady, D., and Geyer, J. (1974). "Heat exchange and transport in the environment," Report 14, Department of Geography and Environmental Engineering, Johns Hopkins University, Baltimore, MD.

Genet, L., Smith, D., and Sonnen, M. (1974). "Computer program documentation for the Dynamic Estuary Model," U.S. Environmental Protection Agency, Systems Development Branch, Washington, DC.

Hansen, D., and Rattray, M. (1966). "New dimensions in estuary classification," *Limnology and Oceanography* 11(3), 319-326.

Hazen and Sawyer. (1978). "Areawide rainfall-runoff model," Task Report 225, Prepared by Hydroscience, Inc., Westwood, NJ, for Hazen and Sawyer, New York.

Hires, R., and Thomas, S. (1996). "Dye release experiments in the Kill van Kull-Newark Bay-Arthur Kill subsystem of the Hudson-Raritan estuary," Report prepared for U.S. Army Corps of Engineers under contract DACW39-94-K-0033, Department of Civil, Environmental and Ocean Engineering, Stevens Institute of Technology, Hoboken, NJ.

HydroQual. (1991). "Task 7.1 assessment of pollutant loadings to New York-New Jersey Harbor," HydroQual, Inc., Mahwah, NJ.

Letter, J. et al. (in preparation). "Passaic River tunnel diversion model study; Report 4, Three-dimensional estuarine hydrodynamic modeling for water quality," Technical Report HL-96-2, U.S. Army Engineer Waterways Experiment Station, Vicksburg, MS.

O'Connor, D. (1983). "Wind effects on gas-liquid transfer coefficients," *Journal of the Environmental Engineering Division* 190, 731-752.

Sheng, Y. (1986). "A three-dimensional mathematical model of coastal, estuarine and lake currents using boundary fitted grid," Report 585, ARAP Group of Titan Systems, Princeton, NJ.

Thomas, S. (1993). "Wind, tide and buoyancy induced residual circulation in a tidal straight," Ph.D. diss., Stevens Institute of Technology, Hoboken, NJ.

U.S. Army Corps of Engineers Hydrologic Engineering Center. (1995). "UNET one-dimensional unsteady flow through a full network of open channels," CPD-66, Davis CA.

Weand, B., and Grizzard, T. (1985). "James River water quality monitoring program water quality review 1985," Draft Report, Virginia Tech Department of Civil Engineering, Blacksburg, VA.

Wen, C., Kao, J., Wang, L., and Liaw, C. (1984). "Effect of salinity on reaeration coefficient of receiving waters," *Water Science and Technology* 16, 139-154.

REPORT DOCUMENTATION PAGE

Public reporting burden for this collection of information is estimated to average 1 hour per response, including the time for reviewing instructions, searching existing data sources, gathering and maintaining the data needed, and completing and reviewing the collection of information. Send comments regarding this burden estimate or any other aspect of this collection of information, including suggestions for reducing this burden, to Washington Headquarters Services, Directorate for Information Operations and Reports, 1215 Jefferson Davis Highway, Suite 1204, Arlington, VA 22202-4302, and to the Office of Management and Budget, Paperwork Reduction Project (0704-0188), Washington, DC 20503.

1. AGENCY USE ONLY *(Leave blank)*	2. REPORT DATE February 1997	3. REPORT TYPE AND DATES COVERED Report 5 of a series

4. TITLE AND SUBTITLE
Passaic River Tunnel Diversion Model Study; Report 5, Water Quality Modeling

5. FUNDING NUMBERS

6. AUTHOR(S)
Carl F. Cerco, Barry Bunch

7. PERFORMING ORGANIZATION NAME(S) AND ADDRESS(ES)
U.S. Army Engineer Waterways Experiment Station
3909 Halls Ferry Road
Vicksburg, MS 39180-6199

8. PERFORMING ORGANIZATION REPORT NUMBER
Technical Report HL-96-2

9. SPONSORING/MONITORING AGENCY NAME(S) AND ADDRESS(ES)
U.S. Army Engineer District, New York
Jacob K. Javits Federal Building
New york, NY 10278-0090

10. SPONSORING/MONITORING AGENCY REPORT NUMBER

11. SUPPLEMENTARY NOTES
Available from National Technical Information Service, 5285 Port Royal Road, Springfield, VA 22161.

12a. DISTRIBUTION/AVAILABILITY STATEMENT
Approved for public release; distribution is unlimited.

12b. DISTRIBUTION CODE

13. ABSTRACT *(Maximum 200 words)*

The Passaic River and Newark Bay form part of the complex New York-New Jersey harbor system. A diversion tunnel has been proposed to alleviate flooding in the upper portion of the Passaic River basin. The tunnel will divert flow from the headwaters of the Passaic directly to the upper end of Newark Bay. The objective of the study is to provide information required to evaluate the effect of the diversion tunnel on living resources in the vicinity of the tunnel outlet. Three living-resource parameters were selected for examination: salinity, water temperature, and dissolved-oxygen concentration.

Impacts were examined through use of the CE-QUAL-ICM water quality model. State variables in the model included salinity, temperature, dissolved oxygen, ultimate biochemical oxygen demand, and chemical oxygen demand. The model was calibrated to field data collected from July to September 1994. Hydrodynamics for the water quality model were supplied by the CH3D hydrodynamic model.

A matrix of scenarios was constructed to examine the impact of tunnel discharge on receiving waters. Base scenarios specified future conditions without the tunnel. Wet-tunnel scenarios examined future conditions with the tunnel in operation and with floodwater remaining in the tunnel between flood events. Dry-tunnel scenarios examined future conditions with the

(Continued)

14. SUBJECT TERMS

Dissolved oxygen	New York Harbor
Floods	Newark Bay
Models	Passaic River

15. NUMBER OF PAGES
120

16. PRICE CODE

17. SECURITY CLASSIFICATION OF REPORT UNCLASSIFIED	18. SECURITY CLASSIFICATION OF THIS PAGE UNCLASSIFIED	19. SECURITY CLASSIFICATION OF ABSTRACT	20. LIMITATION OF ABSTRACT

NSN 7540-01-280-5500

13. (Concluded).

tunnel in operation and with the tunnel pumped dry between flood events. Three flood conditions were considered: 2-year storm, 25-year storm, and 100-year storm.

Scenarios were designed to illustrate the worst-case impact of the discharge tunnel on salinity, temperature, and dissolved oxygen. Under worst-case conditions, impact of the tunnel on dissolved oxygen and temperature was minimal in magnitude, short-lived, and of limited spatial extent. Impact of the tunnel on salinity was indiscernible.